



SECOND INTERNATIONAL WORKSHOP  
**MODERN  
NANOTECHNOLOGIES**

RUSSIA, EKATERINBURG, AUGUST, 27-29

**ABSTRACT BOOK**

## IWMN-2016 organizers

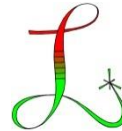
Institute of Natural Sciences  
Ural Federal University named  
after the first President of Russia  
B.N.Yeltsin (INS UrFU)  
<http://www.urfu.ru>



Ural Center for Shared Use  
“Modern Nanotechnology” UrFU  
<http://nanocenter.urfu.ru>



Labfer Ltd.  
<http://www.labfer.com>



Ferroelectric Laboratory  
INS UrFU  
<http://labfer.ins.urfu.ru>



Laboratory for Nanoscale  
Ferroelectric Materials  
INS UrFU



### Workshop Chairman

Prof. Vladimir Shur

### Local Organizing Committee

Prof. Vladimir Shur  
Mrs. Elena Pelegova  
Dr. Dmitry Pelegov  
Mrs. Alevtina Shur  
Ms. Tatiana Klyukina  
Ms. Victoria Pryakhina

## IWMN-2016 sponsors

Taylor and Francis Group  
<http://www.taylorandfrancis.com>



Russian Foundation for Basic Research  
<http://www.rfbr.ru/>



SPECS Surface Nano Analysis GmbH  
<http://www.specs.de/>



OPTEC  
<http://www.optecgroup.com/>



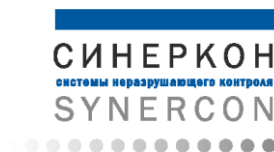
INTERTECH Corporation  
<http://www.intertech-corp.ru/>



NT-MDT Company  
<http://www.ntmdt.com>

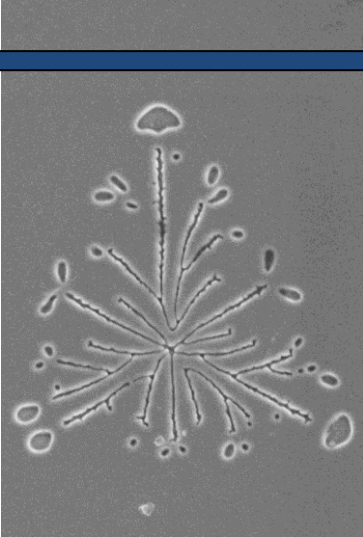


SYNERCON  
<http://www.synercon.ru/>



“KD Systems and Instruments”  
<http://kdsi.ru>





**INVITED  
PRESENTATIONS**

## Ural Center for Shared Use “Modern Nanotechnologies”. Achievements and horizons

V. Ya. Shur<sup>1,2</sup>

<sup>1</sup>*Ferroelectric Laboratory, Institute of Natural Sciences, Ural Federal University, 620000, Ekaterinburg, Russia  
vladimir.shur@urfu.ru*

<sup>2</sup>*Ural Center for Shared Use “Modern Nanotechnology”, Ural Federal University 620000, Ekaterinburg, Russia*

The Ural Center for Shared Use “Modern Nanotechnologies” of Ural Federal University (UCSU MN UrFU) was founded in 2007.

The current objectives of UCSU MN UrFU: (i) Fundamental and applied research in material science related to nanotechnology; (ii) Development of advanced material and device technologies based on nanotechnology; (iii) Effective use of UCSU equipment to execute orders of regional enterprises, companies and institutions; (iv) Exchange of experience, information, and educational programs with foreign partners; (v) Providing the best conditions for invited researchers from Russia and abroad.

UCSU MN UrFU became the key part of the Center of Excellence UrFU named “Research and development of functional nanomaterials for electronic and biomedicine application” with the main investigation areas: (i) Waveguide structures in nonlinear-optical crystals for photonic applications; (ii) New materials for supercapacitors and power sources; (iii) Domain walls and phase boundaries; (iv) Size effects and domain structure in ferroelectric nanocrystals; (v) Magnetoelectrics and multiferroics; (vi) Nanotoxicology and nanomaterial application in biomedicine; (vii) Ferroelectric-graphene structures for capacitors and memory devices; (viii) Functional visualization by scanning force microscopy; (ix) Modern methods of electron, optical and scanning probe microscopy for investigation of the advanced functional materials.

Recently we became Russian leader of the Network Centre for Materials Science and Nanotechnologies of the BRICS countries (CMSN BRICS) with the following key objectives: (i) arrange for the international cooperation in teaching and research activities; (ii) draft proposals for joint international research projects; (iii) raise resources for the development of research and technology; (iv) coordinate the activities of the Shared Scientific Equipment Centres; (v) promote the integration of science by arranging international conferences, workshops and videoconferences; (vi) arrange for joint training and supervision to PhD students; (vii) engage the new members from leading universities of BRICS countries.

Our dream is to establish a world-class University in the heart of Eurasia.

## **Modern aspects of technologies of atomic force microscopy and scanning spectroscopy for nano-materials and nano-structures investigations and characterizations**

V.A. Bykov<sup>1</sup>, A. Kalinin<sup>2</sup>

<sup>1</sup>*Research Institute of Physical Problems & NT-MDT Companies Group  
www.ntmdt.com, spm@ntmdt.ru*

<sup>2</sup>*Moscow Institute of Physics and Technology & NT-MDT Companies Group*

During last years the development of Scanning Probe Microscopy (SPM) technology was transformed to the side of specialization. The application field was increased very wide – from one side micro- and nanoelectronics with extra high-level the metrology requirements and up to material science, biology, ecology with requirements to the side of simplification in operation procedures, possibility of the materials and molecules recognitions.

SPM gives an opportunity to carry out studies of spatial, physical and chemical properties of objects with the typical dimensions of less than a few nanometers. Owing to its multifunctionality, availability and simplicity, Atomic Force Microscope (AFM) has become one of the most prevailing “tools for nanotechnology” nowadays. NTEGRA platform has been designed as the special base for the constantly developing options of SPM that combines them with various other modern research methods. Integration of SPM and confocal microscopy/luminescence/Raman spectroscopy/Infrared Apertureless Nearfield Spectroscopy and Microscopy. Owing to the effect of giant amplification of Raman scattering (Tip Enhances Raman Scattering -TERS) it allows carrying out spectroscopy studies and obtaining images with 10 nm resolution.

New generation of AFM control electronics now allows a real-time cantilever deflection tracking and analyzing. Based on a fast force-distance measurement we developed a new group of non-resonant AFM methods of scanning probe spectroscopy - Hybrid mode. This mode is the most proposal since it summarizes all advantages of amplitude modulation and contact modes allowing simultaneously: free of share force topography measurement with direct tip-sample interaction control, real-time quantitative nanomechanical measurements [1], conductivity [2], piezoresponse and electrostatic imaging with conventional scanning speed. Hybrid mode is very helpful for liquid measurements as it utilizes the issue with cantilever eigenfrequency detection.

Progress in micromechanics manufacturing resulted in significant increase of the cantilever yield rate (to practically 100%) with repeatability of resonant characteristics at 10% level, thus preconditioning implementation of the concept of multi-probe cartridges for AFM. Such cartridge is a multi-probe contour-type sensor with 38 cantilevers which can be the same type or "colored" with predefined coverings and rigidities. Depending on AFM system type the cartridge rotation to select working cantilever can be manual or software-

controlled and takes a few seconds. The cartridge can be exchanged manually by simple procedure without the risk to damage cantilevers. The cartridges operate in dedicated measuring heads, which are designed for integration in the latest instruments by the Company (Titanium, NEXT, SOLVER-NANO, NANOEDUCATOR-II).

The new Revolution Cartridge with multi-probe technology for automated replacement of cantilevers makes a breakthrough in AFM usability: • 38 tips on Cartridge • Fast tip exchange • Fully automated operation

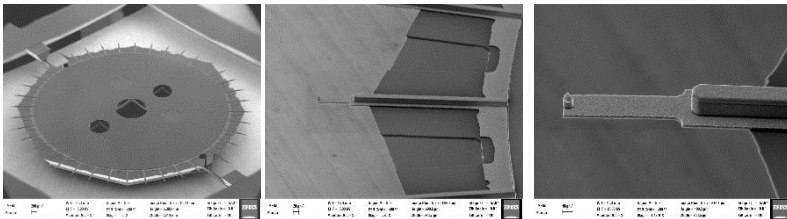


Figure 1. Part of multi-probe cartridge and SPM head with multi-probe cartridge for scanning probe microscope NEXT&TITANIUM.

For fully software-controlled AFMs Titanium and NEXT the cantilever setup procedure was motorized and automated including: precise cartridge rotation to the user-selected cantilever, optical beam deflection (OBD) system adjustment, lock-in amplifier tuning and sample positioning. This approaches us to the concept of ease-of-use AFM where routine system adjustment before scanning is preceded automatically in a few tens of seconds.

Ease-of-use is not the only feature of automated multi-probe cartridge. One of the most demanding applications of modern AFM is routine and repeatable atomic and molecular resolution. This requires extra-low tip-sample thermal drift assumed us [3] lower than  $1 \text{ \AA}/\text{min}$ . Development of thermally stabilized cabinet with  $0.01^\circ\text{C}$  temperature control accuracy and drift-minimized mechanical design of Titanium AFM helped us to achieve mentioned parameters [3]. But conventional cantilever exchange procedure requires opening the cabinet and manipulating with AFM thus destabilizing perfect temperature conditions. So the concept of automated multi-probe cartridge with active thermal stabilization and drift-minimized mechanical design can be a perfect tool for routine high-resolution AFM imaging.

AFM can solve some of “Metrology Difficult Challenges” proposed by The International Technology Roadmap for Semiconductors like: “Structural and elemental analysis at device dimensions and measurements for beyond CMOS”, “Nondestructive, production worthy wafer and mask-level microscopy for

critical dimension measurement for 3D structures, overlay, defect detection, and analysis". A rapid development of polymer [4] and single-molecular electronics [5] also requires AFM to measure and control the topography, conductivity, temperature and other properties at the nanoscale.

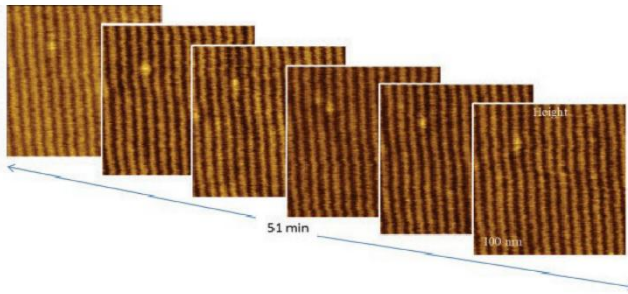


Figure 2. Height images of semi-fluorinated alkanes on graphite collected in sequential scans with 1 Hz scanning rate (measured by Titanium AFM in thermally stabilized room).

To summarize, future electronics development and manufacturing can be a wide field for AFM application, especially for large-sample AFMs. But the biggest drawback of AFM technology to overcome is low throughput.

Throughput of AFM is limited by: system adjustment time before scanning (OBD system and lock-in adjustment, area of interest searching time etc.), scanning parameters adjustment time, scanning speed and amount of data gathered after one scanning session. So to develop the next-generation AFM all these limits should be overcome.

To minimize system adjustment and scanning parameters tuning time we develop and improve new software algorithms allowing fully automated topography imaging. New high-speed control electronics together with Hybrid mode allow more data points and different properties to be recorded per one scanning session. We also develop new AFM-scanner control algorithms to increase a topography imaging speed noticeably. These developments implemented to the fully motorized large-sample AFM is a promising tool for nanotechnology industry. AFM-cluster technology in the portable SPM, such as Solver-NANO, can open the road for using of this unit right on the Space Stations for material quality control in the Space and Space Station conditions.

Development of modes for scanning spectroscopy combined with SPM in the instruments NTEGRA-SPECTRA and SPECTRUM provides new options of confocal laser luminescence spectroscopy and Raman spectroscopy as well as higher reliability of detection for TERS and high-resolution magnetic resonance probe-optical spectroscopy. Probes with diamond nanocrystals containing N-V defects are capable to detect microscopic magnetic states and single spins being promising for studies of surface catalytic activity and for detection of free radicals, including applications in biology and medicine.



1. S. Magonov, S. Belikov, M. Surtchev, S. Leesment, I. Malovichko, *Microscopy and Microanalysis* **21**, 2183 (2015).
2. J. Montenegro, C. Vazquez-Vazquez, A. Kalinin, K.E. Geckeler, J.R. Granja, J. Am. Chem. Soc. (2014).
3. J. Alexander, S. Magonov, *NT-MDT Application note* **88** (2015).  
[http://www.ntmdt.com/data/media/files/products/general/high-resolution\\_imaging\\_in\\_afm\\_an088\\_a4\\_full.pdf](http://www.ntmdt.com/data/media/files/products/general/high-resolution_imaging_in_afm_an088_a4_full.pdf)
4. Y. Karpov, T. Erdmann, I. Raguzin, M. Al-Hussein, M. Binner, et al., *Adv. Mater.* **28**, 6003 (2016).
5. Electronics: From Concept to Function. *Chemical Reviews*, acs.chemrev.5b00680.  
<http://doi.org/10.1021/acs.chemrev.5b00680>

## Structural and magnetic phase transitions in multiferroic rare-earth tetraborate crystals

A.S. Krylov, E.M. Moshkina, I.A. Gudim, V.L. Temerov, A.N. Vtyurin

*L.V. Kirensky Institute of Physics SB RAS, 660036, Krasnoyarsk, Russia  
shusy@iph.krasn.ru, www.kirensky.ru*

Crystals of the  $\text{RFe}_3(\text{BO}_3)_4$  family (R is rare earth ion) were reported to possess multiferroic features, demonstrating both structural and magnetic phase transitions [1 – 3], where transition points may be varied by rare earth composition. In this work we study  $\text{Ho}_{1-x}\text{Nd}_x\text{Fe}_3(\text{BO}_3)_4$  ( $x = 0, 0.25, 0.5, 0.75$ ) and  $\text{Sm}_{1-y}\text{La}_y\text{Fe}_3(\text{BO}_3)_4$  single crystals ( $y = 0, 0.75$ ).

Temperature measurements were performed in the temperature range 10–400 K. The aim of this study is to investigate possible existence of a soft mode related to structural order parameter and effects of magnetic transitions on Raman spectra. Structural transitions manifest clearly by soft mode restoration and new Raman lines appearance below 366 K and 203 K for  $x = 0$  и  $x = 0.25$ . In Nd-doped crystals significant modification of Raman scattering was induced by magnetic ordering below the Neel temperature (about 40 K), that include both magnon scattering and strong intensity redistribution of high frequency lattice modes. Analysis of vibrational spectra and its numerical simulation demonstrate that bigger cell volume of Nd-containing solid solutions provides bigger displacements of oxygen ions in a  $\text{BO}_3$  groups below the Neel temperature that results in stronger magnetoelastic interactions.

Raman spectra of Sm–La system has no changes associated with structural phase transition in the entire temperature range. Raman spectra changes at low temperatures including the area of the magnetic phase transition has been analyzed. Anomalies corresponding to the phase transition of the second order has been detected at temperatures  $T_N = 32$  K ( $y = 0$ ), and  $T_N = 31$  K ( $x = 0.75$ ) in the spectra. These temperatures correspond to temperatures of magnetic phase transitions and are consistent with previously reported results of a study of the magnetization. A number of anomalies in the temperature dependences of the spectral lines associated with the occurrence of magnetic order. In the spectrum of low-frequency range there is a mode corresponding to two-magnon scattering. But otherwise, the nature of the changes relevant to the phase transition for crystals with different quantity Sm and La is different. There, as the offset lines below the temperature of the magnetic phase transition similar to that previously observed in the solid solutions  $(\text{Nd}_{1-x}\text{Ho}_x)\text{Fe}_3(\text{BO}_3)_4$ .

1. A.K. Zvezdin, S.S. Krotov, A.M. Kadomtseva, G.P. Vorob'ev, Yu.F. Popov, et al. *JETP Lett.* **81**, 272 (2005).
2. D. Fausti, A.N. Nugroho, Paul H.M. van Loosdrecht *Phys. Rev. B* **74**, 024403 (2006).
3. A.S. Krylov, S.N. Sofronova, I.A. Gudim, A.N. Vtyurin, *Solid State Commun.* **174**, 26 (2013).

## Polar nanoregions in paraelectric phase in $\text{Sr}_{0.61}\text{Ba}_{0.39}\text{Nb}_2\text{O}_6$ crystal probed by second harmonic generation

A.M. Pugachev<sup>1</sup>, I.V. Zaytseva<sup>1,2</sup>, V.K. Malinovsky<sup>1</sup>, N.V. Surovtsev<sup>1</sup>,  
L.I. Ivleva<sup>3</sup>, P.A. Lykov<sup>3</sup>

<sup>1</sup>*Institute of Automation and Electrometry RAS, 630090, Novosibirsk, Russia*  
apg@iae.nsk.su

<sup>2</sup>*Novosibirsk State University, 630090, Novosibirsk, Russia*

<sup>3</sup>*Prokhorov General Physics Institute, RAS, 119991, Moscow, Russia*

One of unique feature of relaxors is the formation of nanoscaled polar regions (PNR) in paraelectric phase [1]. The assumption of the existence of local polar regions below the temperature  $T_d$  (Burns temperature) in the paraelectric phase has been used used for explaining different physical properties of ferroelectrics [1]. On the other hand, the second harmonic generation (SHG) is known as the reliable method used for detecting these regions in a centrosymmetric phase. In [2, 3] the temperature evolution of second harmonic signal was investigated in the paraelectric phase in crystal and powder of  $\text{BaTiO}_3$  and in  $\text{Pb}_3(\text{MgNb}_2)\text{O}_6$  crystal.

The present work is devoted to investigation of the polar nanoregions in  $\text{Sr}_{0.61}\text{Ba}_{0.39}\text{Nb}_2\text{O}_6$  (SBN 61) crystal, which exhibits a diffuse phase transition [4]. The temperature dependence of the SHG demonstrates that in the paraelectric phase the formation of the PNR appears below  $T = 300\text{K}$ , which is known as the Burns temperature in SBN 61 [4]. SHG signal continually increases until  $T \approx 355\text{ K}$ . Below this temperature the intensity of SHG increases abruptly, indicating that the phase transition in the polar phase occurs. Critical temperatures obtained from SHG measurements, coincide with temperatures obtained from the measurements of relaxation response (central peak in Raman scattering [5]) and from dielectric spectroscopy [6].

This work was supported by Russian Foundation for Basic Research (Grants N 15-02-04950 and N 14-02-00189).

1. A.A. Bokov, Z.-G. Ye, *J. Mater. Sci.* **41**, 31 (2006)
2. A.M. Pugachev, V.I. Kovalevskii, N.V. Surovtsev, S. Kojima, S.A. Prosandeev, I.P. Raevskii, S.I. Raevskaya, *Phys. Rev. Lett.* **108**, 247601 (2012)
3. A.M. Pugachev, V.I. Kovalevskii, V.K. Malinovskii, M.A. Malitskaya, S.I. Raevskaya, I.P. Raevskii, N.V. Surovtsev, *Physics of the Solid State* **57**, 472 (2015)
4. L.E. Gross, *Ferroelectrics* **76**, 241 (1987)
5. V.K. Malinovsky, A.M. Pugachev, N.V. Surovtsev, *Bulletin of the Russian Academy of Sciences: Physics* **74**, 1231 (2010).
6. D.V. Isakov, T.R. Volk, L.I. Ivleva, *Phys Sol Stat* **51**, 2334 (2009)

## The effect of magnetic and non-magnetic trivalent ions substitutions for Fe in $\text{Pb}(\text{Fe}_{1/2}\text{Nb}_{1/2})\text{O}_3$ on its magnetic phase transition temperature

I.P. Raevski<sup>1</sup>, S.P. Kubrin<sup>1</sup>, A.V. Pushkarev<sup>2</sup>, N.M. Olekhnovich<sup>2</sup>, C.-C. Chou<sup>3</sup>, Yu.V. Radyush<sup>2</sup>, S.I. Raevskaya<sup>1</sup>, H. Chen<sup>4</sup>, V.V. Titov<sup>1</sup>, M.A. Malitskaya<sup>1</sup>, S.A. Prosandeev<sup>1</sup>, A.V. Blazhevich<sup>1</sup>, D.A. Sarychev<sup>1</sup>, I.N. Zakharchenko<sup>1</sup>

<sup>1</sup>Research Institute of Physics and Faculty of Physics, Southern Federal University, 344090, Rostov-on-Don, Russia  
igorraevsky@gmail.com

<sup>2</sup>Scientific-Practical Materials Research Centre of the National Academy of Sciences of Belarus, 220072, Minsk, Belarus.

<sup>3</sup>National Taiwan University of Science and Technology, 106, Taipei, Taiwan, China.

<sup>4</sup>Institute of Applied Physics and Materials Engineering, Faculty of Science and Technology, University of Macau, 999078, Macau, China

Multiferroics are of great interest as promising multifunctional materials. An important task is the search for the routes of changing the temperatures of their ferroelectric and magnetic phase transitions. The scope of the present work was the study of the effect of magnetic (Mn, Cr) and non-magnetic (In, Sc) trivalent ions substitutions for Fe in PFN on its magnetic phase transition temperature,  $T_M$ . Ceramic samples of  $(1-x)\text{PbFe}_{1/2}\text{Nb}_{1/2}\text{O}_3-x\text{PbM}_{1/2}\text{Nb}_{1/2}\text{O}_3$  (M- Mn, Cr, In, Sc) solid solution compositions with  $0 \leq x \leq 0.2$  were fabricated by a usual solid state synthesis route. The  $T_M$  value was determined by studying Mossbauer spectra at different temperatures. Addition of all the ions studied leads to lowering of  $T_M$ . However above a certain compositional threshold ( $x \approx 0.05$ ) fast lowering of  $T_M$  stops and a new magnetic state with comparatively high ( $\sim 50$  K) transition temperature becomes stable in a rather wide compositional range. Similar  $T_M(x)$  dependences were observed previously for the PFN solid solutions with  $\text{PbTiO}_3$  and  $\text{PbZrO}_3$  [1]. However the threshold value for the latter systems was about  $x \approx 0.10$ . This difference seems to be due to the fact that in contrast to Mn, Cr, In, Sc, which substitute only Fe ions, Ti and Zr substitute both Fe and Nb ions. Anomalies of  $T_M(x)$  dependence at  $x \approx 0.05-0.1$  are supposed to be due to the percolation phase transition.

This work was partially supported by RFBR (grant 16-52-00072\_Bel\_a), Ministry of Education and Science of the Russian Federation (research project 2132) and Research Committee of the University of Macau (Research & Development Grant for Chair Professor No RDG007/FST-CHD/2012).

1. I. P. Raevski, S.P. Kubrin, V.V. Laguta, M. Marysko, H. Chen, S.I. Raevskaya, V.V. Titov, C.-C. Chou, A.V. Blazhevich, E.I. Sitalo, D.A. Sarychev, T.A. Minasyan, A.G. Lutokhin, Yu.N. Zakharov, L.A. Pustovaya, I.N. Zakharchenko, M.A. Malitskaya, *Ferroelectrics*, **475**, 20 (2015).

## Magnetolectricity of domain walls of rare-earth iron garnets

A.I. Popov<sup>1</sup>, Z.V. Gareeva<sup>2</sup>, A.K. Zvezdin<sup>3</sup>, A.P. Pyatakov<sup>4</sup>, A.S. Sergeev<sup>4</sup>

<sup>1</sup>National Research University of Electronic Technology, Zelenograd, 124498, Moscow, Russia

<sup>2</sup>Institute of Molecule and Crystal Physics, 450075, Ufa, Russia

<sup>3</sup>A.M. Prokhorov General Physics Institute, Russian Academy of Sciences, 119991, Moscow, Russia

<sup>4</sup>Moscow State University, 119991, Moscow, Russia

Magnetolectricity being a highly developing area of research offers attractive opportunities for cross-control of electric and magnetic ordering promising for spintronic applications. Recent breakthroughs in magnetolectricity are related to the discovery of multiferroic properties of cubic magnets (rare earth iron garnets and orthoferrites) [1-3].

We report a new mechanism of magnetolectric effect in rare earth iron garnets related to low symmetry rare earth ions environment and the presence of domain walls of the iron subsystem. The lack of space inversion in the dodecahedral rare-earth ion environments allows ferroelectric ordering in these materials. In iron garnets exchange interaction between rare – earth ( $f$ ) and iron ( $d$ ) magnetic sublattices induces the electric-dipole structure<sup>4</sup>. In single-domain samples the electric-dipole structure appear to be antiferroelectric and as a result electric polarization is absent. We show that the magnetic domain walls of the iron subsystem generate an effective inhomogeneous magnetic field arising from the rare-earth - iron exchange interaction, which leads to emergence of electric polarization (Fig. 1). Peculiarities of polarization at domain walls with various magnetic configurations are considered.

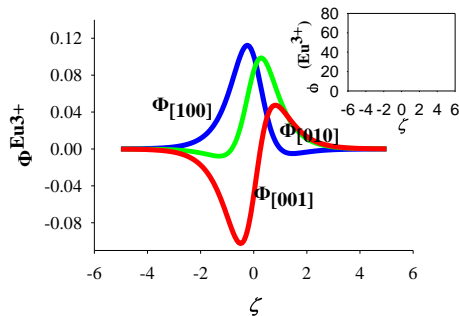


Figure 1. Distribution of projections of reduced polarization vector across 710 Bloch domain wall in EIG. Profile of the 710 Bloch domain wall is shown in insert.

1. X. Wang, et al. *Phys. Rev. Lett.* **115**, 087601 (2015).
2. A.K. Zvezdin, A.A. Mukhin, *JETP Lett.* **88**, 505 (2008).
3. A.I. Popov, D.I. Plokhov, A.K. Zvezdin, *Phys. Rev. B* **90**, 214427 (2014).

**Phase separation and locally induced states in manganites**R.F. Mamin<sup>1</sup>, D.A. Bizyaev<sup>1</sup>, R.V. Yusupov<sup>2</sup>, A.A. Bukharaev<sup>1,2</sup><sup>1</sup>Zavoisky Physical-Technical Institute of RAS, 420029, Kazan, Russia  
mamin@kfti.knc.ru<sup>2</sup>Kazan Federal University, 420000, Kazan, Russia

The complicated interplay among charge, spin and lattice degrees of freedom in doped manganites lead to the unexpected phenomena such as phase separation with charge segregation [1]. The possibility of the ferroelectricity and multiferroic behaviour due to charge ordering were discussed [2]. The problem of spatially inhomogeneous states in the charged systems frustrated by the Coulomb interactions is constantly under debate for different systems. In this work we discuss the possibility of polar states and multifunctional behaviour due to magnetic phase separation with charge segregation phenomenon in pre-percolation regime in manganites. It is expected that pronounced changes of the electric properties might occur if the concentration of doped carriers is locally varied in a controllable way. The properties of the local states induced by electric field in  $\text{La}_{0.9}\text{Sr}_{0.1}\text{MnO}_3$  and  $\text{La}_{0.89}\text{Sr}_{0.11}\text{MnO}_3$  single crystals [3,4] can be also associated with this phenomenon. We have performed the induction of the local states at the surface of the  $\text{La}_{0.89}\text{Sr}_{0.11}\text{MnO}_3$  and  $\text{La}_{0.875}\text{Sr}_{0.125}\text{MnO}_3$  single crystal by applying a bias via the AFM tip. The long-lived distinct contrast of the electric field induced polar states was observed. We find out the influence of the external magnetic field on the writing of electric-field-induced polar states. These results show that the dependence of the surface potential of induced area on the writing time a similar as for ferroelectrics. These phenomena are discussed in the framework of the model supposed the phase separation with charge segregation. The magnetic properties and colossal magnetocapacitance effect at  $\text{La}_{1-x}\text{Sr}_x\text{MnO}_3$  single crystals [5] was discussed in framework of that approach.

The work is performed according to the Russian Government Program of Competitive Growth of Kazan Federal University. The reported study was partially supported by RFBR, research project No. 14-02-01154 a.

1. E. Dagotto, T. Hotta, A. Moreo, *Physics Report* **344**, 1 (2001).
2. J. van den Brink, D. I. Khomskii, *J. Phys.: Condens. Matter* **20**, 434217 (2008).
3. R.F. Mamin, I.K. Bdikin, A.L. Kholkin, *Appl. Phys. Lett.* **94**, 222901, (2009).
4. R.F. Mamin, D.A. Bizyaev, A.A. Bukharaev, *Bull. of Russ. Acad. Sci.: Phys.* **75**, 5 (2011).
5. R.F. Mamin, T. Egami, Z. Marton, S.A. Migachev, *Phys. Rev. B* **75**, 115129 (2007).

**Piezoelectric calcium phosphates**S.A.M. Tofail

*Department of Physics and Energy and Materials & Surface Science Institute, University of Limerick, V94 T9PX, Limerick, Ireland*  
*E-mail: tofail.syed@ul.ie*

Starting from an historical oversight, hydroxyapatite, the synthetic analogue of the mineral in bone and teeth, has emerged to be used in piezoelectric energy harvesting. While nanocrystalline apatites in bone are yet to be conclusively found as piezoelectric, piezoelectricity in bone collagen is known for over six decades. Bone apatite is a highly substituted calcium phosphate. There arises the question as regards to the piezoelectricity of substituted apatites. We show some of the theoretical and crystallographic considerations for piezoelectricity to occur in substituted apatites. We also provide new experimental evidence of piezoelectricity in tricalcium phosphates, chlorapatite and their respective mixed phases with hydroxyapatite.

1. T. Nishigaki, S. Hontsu, *Key Engineering Materials*, **631**, 253 (2015).
2. S.A.M. Tofail, J. Bauer (Eds.), *Electrically Active Materials for Medical Devices*, (Imperial College Press), in press (2016).
3. A.A. Gandhi, M. Wojtas, S.B. Lang, A.L. Kholkin, S.A.M. Tofail, *J. Am. Ceram. Soc.*, **97**, 2867 (2014).
4. S.A.M. Tofail, A.A. Gandhi, M. Gregor, J. Bauer, *Pure and Applied Chemistry*, **87**, 221 (2015).
5. S.A.M. Tofail, D.P. Haverty, K.T. Stanton, J.B. McMonagle, *Ferroelectrics*, **319**, 117 (2005).
6. D.P. Haverty, S.A.M. Tofail, K.T. Stanton, J.B. McMonagle, *Phys. Rev. B*, **71**, 941031 (2005).
7. S.B. Lang, S.A.M., Tofail, A.A. Gandhi, M. Gregor, C. Wolf-Brandstetter, J. Kost, S. Bauer, M. Krause, *Applied Physics Letters*, **98**, 123703 (2011).
8. S.B. Lang, S.A.M. Tofail, A.L. Kholkin, M. Wojtas, M. Gregor, A.A. Gandhi, Y. Wang, S. Bauer, M. Krause, A. Plecenik, *Scientific Reports*, **3**, 22151 (2013).

**Electrically active biomaterials**

J. Bauer<sup>1</sup>, S.A.M Tofail<sup>2</sup>

<sup>1</sup>*Department of Biomedical Engineering, Wroclaw University of Science and Technology, 50-370, Wroclaw, Poland  
joanna.bauer@pwr.edu.pl*

<sup>2</sup>*Department of Physics and Energy and Materials & Surface Science Institute, University of Limerick, V94 T9PX, Limerick, Ireland  
tofail.syed@ul.ie*

The electrical properties such as local electrostatic charge distribution at biomaterial surfaces are well known to play a significant role in defining interactions with biological surroundings. The exact nature of such interactions is still not well-defined, however. Presently available biomaterials used in medical sector do not explicitly address the interfacial phenomena. That's why the interactions between biomaterial surface and tissues need a deepened attention - both from the scientific and applicable point of view. An understanding of the interface between the biomaterial' surface and the biological environment is critical to learn how to trigger or suppress a targeted biological response and which of surface' properties should be modified to achieve a therapeutic outcome.

In the literature as the most crucial surface properties are usually mentioned: chemical composition, crystallinity, roughness, wettability, surface charge, surface diffusion, heterogeneity and modulus to biological reactions. These properties can be highly interrelated. Moreover, there is no a priori understanding in regard to which surface property is the most important as a number of them can be simultaneously influencing biological interactions at the same time.

We will outline these issues to shed more light on the biological interface with biomaterials which can also be relevant for understanding nano-bio interactions. Furthermore, in this presentation we will give examples of the application of electrically modified biomaterials surfaces for minimally invasive and non-invasive medical applications.

1. S.A.M. Tofail, J. Bauer, *Advanced Materials* **28**, 5470 (2016).
2. S.A.M. Tofail, J. Bauer (Eds.), *Electrically Active Materials for Medical Devices*, (Imperial College Press), in press (2016)
3. A.A. Gandhi, M. Wojtas, S.B. Lang, A.L. Kholkin, S.A.M. Tofail, *J. Am. Ceram. Soc.*, **97**, 2867 (2014).
4. S.A.M. Tofail, A.A. Gandhi, M. Gregor, J. Bauer, *Pure and Applied Chemistry*, **87**, 221 (2015).
5. K. Kowal, P. Cronin, E. Dworniczek, J. Żegliński, P. Tiernan, W. Wawrzyńska, H. Podbielska, S.A.M. Tofail, *RSC Advances*, **4**, 19945 (2014).



## Terahertz imaging technique for cancer diagnostics using frequency conversion by gold nano-objects

K.A. Moldosanov<sup>1</sup>, A.V. Postnikov<sup>2</sup>, V.M. Lelevkin<sup>1</sup>, N.J. Kairyev<sup>1</sup>

<sup>1</sup>Kyrgyz-Russian Slavic University, 44 Kiyevskaya St., 720000, Bishkek, Kyrgyzstan  
altair1964@yandex.ru

<sup>2</sup>Université de Lorraine, LCP-A2MC, 1 Bd Arago, F-57078 Metz, France  
andrei.postnikov@univ-lorraine.fr

A technique is suggested (that includes the device's scheme and assessments of its feasibility) for imaging cancer cells in the biological tissue samples *in vitro* and in human skin *in vivo*, based on exposing these objects to 3.77 THz radiation. The interest for imaging in THz is explained by an enhanced absorption (or reflection) in this frequency range by water molecules, relatively abundant in cancer cells. The main parts of the device are: (i) a 3.77 THz radiation source whose working element is a system of gold nano-objects (nanobars or nanorings) irradiated by “standard” (domestic oven) microwaves at 2.45 GHz; (ii) a terahertz radiation sensor combining the THz-to-infrared (IR) converter with an IR sensitive camera. The conversion of THz radiation into heat employs, in its turn, the corresponding ability of gold nanoparticles which are the converter's essential element. The IR camera is conventional, able to yield two-dimensional images with sufficient resolution for examining the biological tissue sample (in the transition geometry) or the patient's skin and hypodermic tissue (in the reflection geometry). The bulk of presentation will be concentrated on the physics of GHz-to-THz and THz-to-IR conversion mediated by gold nano-objects, and the selectivity of the latter with respect to their optimal sizes and shapes.

1. A. Postnikov, K. Moldosanov, *Phonon-assisted radiofrequency absorption by gold nanoparticles resulting in hyperthermia*, Chapter 9 in: *Fundamental and Applied Nano-Electromagnetics, NATO Science for Peace and Security, Series B: Physics and Biophysics*; Eds.: A. Maffucci and S. Maksimenko (Springer Netherlands), (2016).
2. K. Moldosanov, A. Postnikov, *Beilstein J. Nanotechnol.* **7**, 983 (2016).
3. K.A. Moldosanov, N.J. Kairyev, V.M. Lelevkin, A.V. Postnikov, *Perspectives of terahertz imaging the human skin cancer with the help of the gold-nanoparticle-based terahertz-to-infrared converter* (2016, to be published).

## Surface modified hydroxyapatites with various functionalized nanostructures

V.S. Bystrov<sup>1</sup>, E.V. Paramonova<sup>1</sup>, Yu.D. Dekhtyar<sup>2</sup>, A.V. Bystrova<sup>2</sup>,  
R.C. Pullar<sup>3</sup>, S. Kopyl<sup>3</sup>, J. Coutinho<sup>4</sup>

<sup>1</sup>*Institute of Mathematical Problems of Biology RAS, 142290, Pushchino, Russia  
vsbys@mail.ru*

<sup>2</sup>*Biomedical Engineering and Nanotechnology Institute, Riga Technical University, Riga, Latvia*

<sup>3</sup>*Department of Engineering of Materials and Ceramics / CICECO – Aveiro Institute of Materials, University of Aveiro, Aveiro, Portugal*

<sup>4</sup>*Department of Physics and I3N, University of Aveiro, Aveiro, Portugal*

Hydroxyapatite ( $\text{Ca}_{10}(\text{PO}_4)_6(\text{OH})_2$ , HAP) the most important material for bone regeneration and implants. Its structural features define its basic physical properties, particularly the charge density and electric potential, which have especially important role at the surface, Modeling and computational study of the structure of the HAP and its possible changes during the formation of the various defects to determine the electric potential of the surface charge density (polarization) and their changes is a necessary task for the creating of new nanostructures HAP modifications for wide biomedical applications [1-3]. Studies have shown that the creation of such surface charges (polarization) increases the adhesion of the osteoblasts cells and to enhance their reproduction and growth. According to [4], it is especially noticeable on the *negatively charged HAP surfaces*. Therefore, the important aspect of the computer modeling of HAP is to build such models and structural modifications of HAP, which would allow explicitly creating and exploring such change in the charges structure of HAP and electrical potential at the HAP surface that could be mostly adhesive for living cells and therefore improve the implant quality. In this work we present a density functional modelling (DFT) study of HAP, as bulk as well with special HAP model of the *layered slab supercells units*, which included *vacuum spaces* between the layered slabs forming HAP surface, similar as described in [5]. To this end, first principle calculations of bulk and surface modified HAP were carried out using local basis (local density approximation LDA, AIMPRO) and plane-wave (generalized gradient approximation GGA, VASP) codes. Data of all structures and defects of surface modified HAP models are analyzed using both approaches. Study was supported by RFBR grant 15-01-04924.

1. V.S. Bystrov, et al., *J. Phys.: Condens. Matter*, **23**, 065302, (2011).
2. V.S. Bystrov et al., *J. Phys. D: Appl. Phys.* **48**, 195302, (2015).
3. A.V. Bystrova, et al., *Ferroelectrics* **475** (1), 135-147 (2015).
4. Yu. Dekhtyar, et al., *IFMBE Proceedings* **38**, 182, (2013).
5. A. Slepko, A. Demkov, *J. Chem Phys.*, **139**, 044714, (2013).

## Experimental investigation of wide aperture PPLN structures for optical parametric oscillator at MID-IR spectral region

D.B. Kolker<sup>1,2</sup>, A.A. Boyko<sup>1</sup>, A.N. Pronyushkina<sup>3</sup>, S.I. Trashkeev<sup>1,2</sup>,  
B.N. Nuyshkov<sup>1,2</sup>, N.Yu. Kostyukova<sup>1,3</sup>, I.V. Sherstov<sup>1,2</sup>

<sup>1</sup>Research Laboratory of Quantum Optics Technology, Novosibirsk State University, 630090, Novosibirsk, Russia  
dkolker@mail.ru, [http://www.nsu.ru/SAE\\_ru](http://www.nsu.ru/SAE_ru)

<sup>2</sup>Institute of Laser physics SB RAS, 630090, Novosibirsk, Russia

<sup>3</sup>Novosibirsk State Technical University, 630072, Novosibirsk, Russia

Optical parametric oscillator is attractive wide tunable device for medical, spectroscopic and special application. High energy OPO device is of a great interest for antiterrorism, for instance as an optical source for special equipment for monitoring explosive and poisoning gases in real atmosphere [1]. For OPO experiment LQ215 Solar Laser System was used as a pump source at 1.064 mm. First: measurements of the idler energy dependence across the aperture were made (Fig. 1b). The scanning step is the beam diameter or 400  $\mu\text{m}$  and the energy map of PPLN structure was recorded.

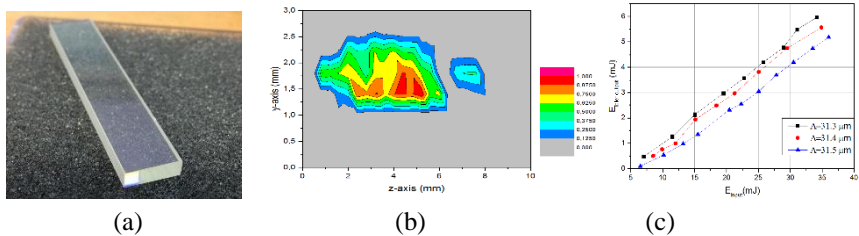


Figure 1. (a)  $3 \times 10$  aperture PPLN structure, (b) Energy diagram of  $3 \times 10$  mm aperture multi fan-out PPLN structure, (b) input- output.

Second: idler wave energy as a function of pump energy is presented on fig 1c for multi grating PPLN structure ( $3 \times 10 \times 10$  mm). 6 mJ idler output energy was shown in spectral region 3.2-3.4  $\mu\text{m}$ . The pump beam diameter was  $v=2.23$  mm on vertical coordinate and  $v=2.98$  mm on horizontal respectively.

We are proposing a novel method of high power OPO pumping by using a full aperture PPLN structure by high energy (20 Hz, 200 mJ, 5.5 ns) Nd:YAG Laser. We are expecting at least one order energy output improvement by using cylindrical dilator of pump beam for full PPLN crystal aperture pumping ( $3 \times 10$  and  $3 \times 20$  mm) without optical damaging of PPLN structures.

1. Y.V. Kistenev, D.B. Kolker, et al, *Journal of Biomedical Optics*. **20**, 6. (2015).

**Self-oscillatory motion of extended defects in solid**A. L. Korzhenevskii*Institute for Problems in Mechanical Engineering, RAS, St. Petersburg, Russia*

Starting from a bulk description of a phase-field type some methods of the derivation of the effective equations of motion of various extended defects in solid are discussed. It is demonstrated that in case the system dynamics has the gradient character using the energy-momentum tensor allows to derive the equations in a very elegant way.

The general idea of the method is elucidated by the example of a concerted propagation of a fast brittle crack with the process zone where a rearrangement of the solid structure takes place.

In case a system dynamics is described on a more macroscopic level that implies making use of phenomenological constitutive relations some pertinent approximations of Green's functions may be very useful.

As an example the interface dynamics in the explosive crystallization of amorphous solid is explicitly treated in this way.

1. A.L. Korzhenevskii, R.E. Rozas, J. Horbach, *J. Phys. Cond. Matter.* **28**, 035001 (2015)
2. A.L. Korzhenevskii, A. Boulbitch, *Europhys. Lett.* **112**, 16003 (2016).
3. A.L. Korzhenevskii, A. Boulbitch, *Phys. Rev. E.* **93**, 063001 (2016).

**Piezoelectric properties of 2D-materials: a case of graphene**

K. Romanyuk<sup>1,2</sup>, P.S. Zelenovskiy<sup>1</sup>, R. Vidyasagar<sup>2</sup>, D.O. Alikin<sup>1</sup>, S. Kopyl<sup>2</sup>, A.A. Esin<sup>1</sup>, V.Ya. Shur<sup>1</sup>, A. L. Kholkin<sup>1,2</sup>

<sup>1</sup>*Institute of Natural Sciences, Ural Federal University, Ekaterinburg 620026, Russia  
kholkin@gmail.com*

<sup>2</sup>*Physics Department & CICECO-Aveiro Institute of Materials, University of Aveiro,  
3810-193 Aveiro, Portugal*

Recent discovery of piezoelectricity in two-dimensional (2D) materials [1] opens up new opportunities for stretchable electronics sensors, actuators and other electronic components based on the direct and converse piezoelectric effects. Being a 2D monoatomic material with many unique properties, graphene (or graphene oxide) is one of the favorable candidates for these applications. In this work, we report a strong piezoelectric activity of a single-layer graphene (SLG) deposited on Si/SiO<sub>2</sub> calibration grating substrates [3]. The electric field induced strain was measured by Piezoresponse Force Microscopy (PFM) – a novel technique that can map small piezoelectric displacements with high lateral resolution [2]. The piezoelectric activity of graphene layers was mainly attributed to the chemical interaction of carbon atoms with underlying oxygen from SiO<sub>2</sub> substrate. Piezoelectric effect is sufficiently high ( $d_{33} \approx 1.4$  nm/V, that is, more than twice of the best piezoelectric ceramics such as modified lead zirconate titanate - PZT) and can be used in a variety of microelectromechanical systems based on graphene. The effect was linear in the range of applied voltages up to 2 V and was strongly amplified by the cantilever resonance. In addition, we found that the strong ability of graphene to form polar bonds can be also used to enhance the piezoelectric properties of other emergent materials such as peptide nanotubes [4]. We show that using piezoelectric activity of graphene a number of novel nanoelectromechanical devices can be created, such as high-frequency piezoelectric resonators, filters, and high authority actuators. The research was made possible in part by the Russian Foundation for Fundamental Research (grant 16-29-14050 ofr\_m).

1. K.A.N. Duerloo, M.T Ong, J. T. J. Reed, *Phys. Chem. Lett.* 3, 2871 (2012).
2. A. Gruverman, A. L. Kholkin, *Rep. Progr. Phys.* 69, 2443 (2006).
3. G. da Cunha et al, *Nat. Commun.* 6, 7572 (2015); *ibid* 7, 11571 (2016).
4. A. L. Kholkin et al, *ACS Nano* 4, 610 (2010).

**Physical properties and reentrant behavior in PLZT thin films**

M. Melo<sup>1</sup>, E.B. Araujo<sup>1</sup>, A.P. Turygin<sup>2</sup>, A.A. Esin<sup>2</sup>, V.Ya. Shur<sup>2</sup>, A.L. Kholkin<sup>3</sup>

<sup>1</sup>*Department of Physics and Chemistry, São Paulo State University, 15385-000 Ilha Solteira, SP, Brazil*  
*eudes@dfq.feis.unesp.br*

<sup>2</sup>*Institute of Natural Sciences, Ural Federal University, 620000 Ekaterinburg, Russia*

<sup>3</sup>*Physics Department & CICECO, University of Aveiro, 3810-193 Aveiro, Portugal*

The lead lanthanum zirconate titanate,  $\text{Pb}_{1-x}\text{La}_x(\text{Zr}_y\text{Ti}_{1-y})_{1-x/4}\text{O}_3$  (PLZT), is known to exhibit remarkable dielectric, piezoelectric and electro-optic properties. The composition  $\text{La}/\text{Zr}/\text{Ti} = 9/65/35$  mol% shows a relaxor behavior and is particularly important because most of its properties have potential for technological applications. As thin films, the great potential of the PLZT system has been demonstrated in the past years for applications in capacitors, nonvolatile ferroelectric random memories, waveguide and others. In the present work, polycrystalline PLZT 9/65/35 thin films have been prepared using a chemical polymeric method to study its structural, dielectric and local piezoelectric properties. The studied films are uniform, crack free with 540 nm in thickness and shows a random oriented orthorhombic phase (*Pmmm* space group) with cell parameters  $a = 4.090$  Å,  $b = 4.096$  Å and  $c = 4.086$  Å. The out-of-plane images recorded by piezoresponse force microscopy (PFM) reveals that the studied films are quite homogeneous in terms of piezoresponse. The active piezoregion in the film is discussed in terms of autocorrelation analysis on the PFM images. The effective  $d_{33}$  peak shift to positive values in the out-of-plane distributions suggests a local imprint behavior in our PLZT films due to an internal bias field so that domains are oriented towards free surface. The imprint behavior is confirmed by asymmetries observed on the slim P-E hysteresis loops of the PLZT film such as  $\Delta P_r = +0.7$   $\mu\text{C}/\text{cm}^2$  and  $\Delta E_c = -12.8$   $\text{kV}/\text{cm}$ . Hysteresis loops recorded on cooling, in the 180-300 K range, reveals that remanent polarization gradually increases at first and then decreases after reach a maximum value at around 223 K. This behavior suggests the occurrence of a reentrant phenomenon in the studied PLZT films such as observed in most spin glasses and relaxor ferroelectrics. Although the origin of the reentrant behavior remains unclear, we discuss the results in terms of competition between ferroelectric and antiferroelectric interactions and as well ferroelectric regions and surrounding dipole glassy region.

**Ferroelectric glass ceramics for energy storage application**

Y. Zhang, X.Z. Song, Y.Z. Chen, D.L. Yang

*Beijing Key Laboratory of Fine Ceramics, State Key Laboratory of New Ceramics and Fine Processing, Institute of Nuclear and New Energy Technology, Tsinghua University, Beijing 100084, P R China*  
*yzhang@tsinghua.edu.cn*

Ferroelectric glass-ceramics, containing major crystalline phases such as barium strontium titanate with perovskite structure, are considered to be the most attractive candidates for dielectric materials used in capacitors with high energy storage densities. A series of barium strontium titanate based glass-ceramics has been prepared via controlled crystallization in an aluminum silicate glass. Their phase evolution, crystallization kinetics, crystal morphology, dielectric properties and energy storage characteristics have been investigated as a function of silica/alumina ratio, barium/titanium ratio, as well as  $\text{La}_2\text{O}_3$ ,  $\text{AlF}_3$  and  $\text{MnO}_2$  additions. In addition, impedance spectroscopy (IS) and thermally stimulated depolarization current (TSDC) have been employed to study the dielectric relaxation processes in the glass-ceramics. The TSDC characteristics demonstrate that the degree of crystallinity in the glass-ceramics is a predominant factor in deciding the features of dielectric relaxation mechanisms.

## Finsler geometry modeling for elongation of flexible materials under external magnetic field

H. Koibuchi

National Institute of Technology, Ibaraki College, Japan

Magnetic/Electric strain phenomenon for flexible materials such as liquid crystal elastomer (LCE) is studied by using Finsler geometry (FG) model [1,2,3]. This FG model is defined in a 3D spherical body, which is discretized by tetrahedrons [3]. The Hamiltonian is defined on tetrahedrons, and it includes the Gaussian bond potential, which is obtained by extending the one for 1D linear chain [4]. On the vertices of tetrahedrons, we introduce the spin variable  $\sigma$ , which represents directional degrees of freedom of liquid crystal molecule in LCE. This  $\sigma$  is used to define the Finsler metric in the Gaussian bond potential. By applying an external magnetic/electric field, the spherical body deforms into oblong shape along the direction of the magnetic/electric field. The strain  $L/L_0$  vs. the external magnetic field  $B$ , and the magnetization  $M$  vs.  $B$  increase with increasing  $B$  (Fig.1(a) and 1(b)), where  $L$  is the maximal diameter and  $L_0$  is  $L$  for  $B=0$ , and  $M$  is the magnetization corresponding to  $\sigma$ .

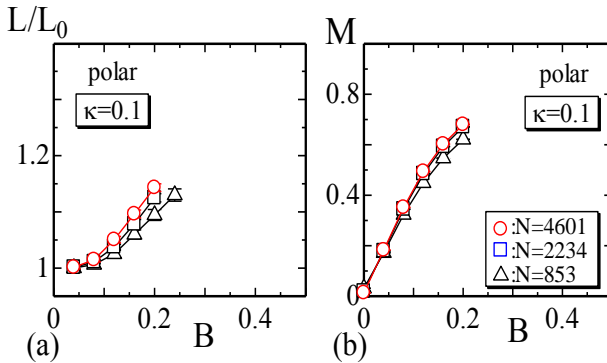
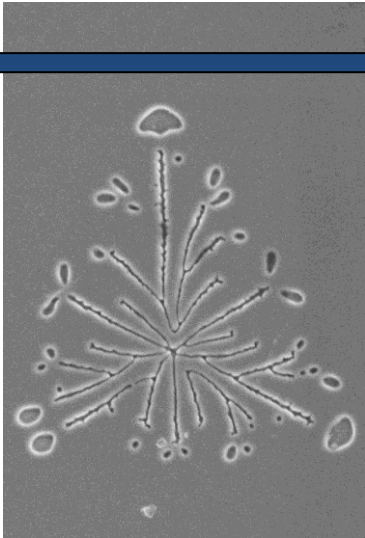


Figure 1. (a) The strain  $L/L_0$  vs.  $B$  and (b) the magnetization  $M$  vs.  $B$ .

1. H. Koibuchi and H. Sekino, *Physica A* **393**, 37 (2014).
2. S. Usui and H. Koibuchi, "Finsler geometry modeling of phase separation in multi-component membranes", (submitted).
3. K. Osari and H. Koibuchi, "Finsler geometry modeling and Monte Carlo study of 3D liquid crystal elastomer", (submitted).
4. M. Doi and S.F. Edwards, *The Theory of Polymer Dynamics*, (Oxford University Press), 1986.





# **ORAL PRESENTATIONS**

## Compositional imaging of surface properties using resonant and non-resonant AFM oscillatory modes

S.N. Magonov<sup>1</sup>, S.I. Leesment<sup>2</sup>, A.S. Kalinin<sup>2</sup>, V.V. Polyakov<sup>2</sup>

<sup>1</sup>*NT-MDT Development Inc., 85284, Tempe, AZ, USA*

<sup>2</sup>*NT-MDT, 124460, Moscow, Zelenograd, Russia*

*polyakov@ntmdt.ru, www.ntmdt.com*

A family of atomic force microscopy (AFM) techniques has recently been enriched by an addition of the HybriD Mode, in which a cantilever deflection during oscillatory non-resonant tip-sample force interactions is tracked with high sensitivity. Such operation, which becomes possible with an implementation of fast data acquisition and real-time signal processing, leads to new advanced applications. The recording of the deflection response in the different parts of the interaction cycle offers new capabilities for the feedback control and mapping of local mechanical and electromagnetic properties. The experimental data collected with the HybriD Mode on a variety of samples demonstrate the unique features of this mode and provide its rational comparison with the results of Amplitude Modulation technique, which is more broadly applied so far.

The set of oscillatory resonance AFM modes is expanded with frequency modulation (FM) mode and frequency imaging (FI) in amplitude modulation mode (Fig. 1). The backgrounds of these modes are discussed and their capabilities are compared on the practical examples. The data show how these techniques complement the amplitude modulation with phase imaging. The frequency imaging enhances the compositional mapping of heterogeneous samples. Frequency modulation mode provides a superior capability in imaging at low tip-sample forces.

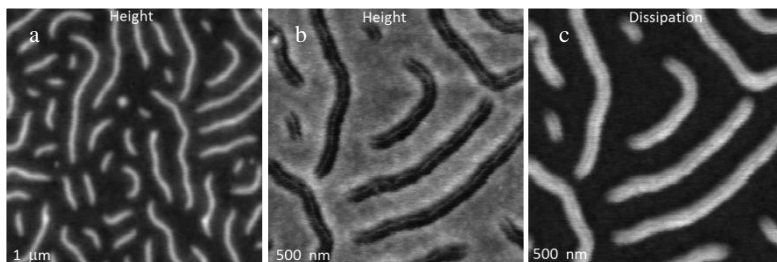


Figure 1. The height (a) - (b) and dissipation (c) images of brush-like macromolecules on mica in FM mode at  $\Delta\omega_{sp} = -24$  Hz at the large (a) and small (b)-(c) tip-sample distances. The height contrast in (a) - (b) is in the 0 – 8 nm range. The contrast in (c) is in the relative units.

**Advances in AFM application: Novel electric and combined techniques**V.S. Neudachina

*Intertech Corporation, Moscow representative office, 119333 Moscow, Russia  
vsn@intertech-corp.ru, www.intertech-corp.ru*

Electric measurements are among the most widespread AFM applications for various materials, including metals, semiconductors, and dielectrics. Recently, a number of novel or optimized existing approaches have been developed by Oxford Instruments Asylum Research, together with the corresponding tools and instruments that allow investigating the aforementioned properties in detail and with superb reproducibility.

One of the most interesting novel approaches is sMIM (Scanning Microwave Impedance Microscopy), a near-field technique that uses a microwave source coupled to a proprietary shielded AFM probe. As the tip scans the sample, local sample variations in permittivity ( $\epsilon$ ) and conductivity ( $\sigma$ ) affect the reflected microwaves. This is analyzed, distinguishing between changes in the measured capacitance (C) and resistance (R). A modulated bias can be applied to the sample to also measure the amplitude and phase of the dC/dV and dR/dV response. On semiconductor materials, the dC/dV signal is highly sensitive to doping, with the phase indicating dopant type and the amplitude proportional to dopant concentration. On thin films, the sMIM capacitance can be related to the film thickness and dielectric constant. More generally, sMIM is useful on a wide range of nanomaterials where variations in permittivity and conductivity might help distinguish materials that show no contrast in topography. The method can operate on a wide range of linear and non-linear materials including conductors, semiconductors, and insulators. It provides higher lateral resolution (<50nm) and superior signal-to-noise (>10X) while operating up to 80X faster and at lower power compared to competing technologies.

Other important electric techniques that have recently gained more attention of general public include NanoTBDD (Nanoscale Time Dependent Dielectric Breakdown), Piezoresponse Force Microscopy PFM and photoconductive AFM (pcAFM) will also be discussed with the appropriate examples. All of the aforementioned methods are available for the MFP-3D AFM systems with up to 220V voltage and for the Cypher AFM systems with up to 150V voltage.

**Digital microscopy as the new solution to go beyond the optical limit**

P. Belin<sup>1</sup>, A. Yusupov<sup>2</sup>

<sup>1</sup>*Leica Microsystems, F-92737 Nanterre, France  
Patrice.Belin@leica-microsystems.com*

<sup>2</sup>*Synercon, 117105 Moscow, Russia*

Leica Microsystems is a major actor of microscopy for more than 166 years, with a portfolio ranging from lenses/objectives to high end microscopes via cameras, sample preparation systems, binoculars, metallography microscopes and application software. Leica had taken the turn of digital microscopy with DMS, DVM6 & DCM8 microscopes up to now.

We will show you how the DCM8 is able to achieve 0.1 nm real vertical resolution and pixel sampling on the object down to 90 nm. Some applications in Surface Metrology will be presented then.

Moreover, some sample testing will be possible during the congress thanks to the presence on site of a DCM8.

## Carl Zeiss Delta SEM – first aberration corrected scanning electron microscope with atomic resolution

V.S. Vlasenko, A.A. Trifonov

“OPTEC” LLC, 105005, Moscow, Russia

trifonov@optecgroup.com , www.optecgroup.com

In one of the most cited lectures by Richard P. Feynman in late 1959 ‘There's plenty of room at the bottom’ he clearly addressed that Microscopy plays a key role in his considerations and formulated a basic challenge how to help scientists: Make the Electron Microscope 100 times better.

Huge progress has been made since that time in both scanning electron microscopy (SEM) and transmission electron microscopy (TEM) (see Fig.1) and currently it is clear that TEMs are very close to possible theoretical resolution limit, as well as conventional SEM. But with the recent advances in column and detectors design of SEMs as well as faster electronics enable construction of a new type “Aberration-corrected” SEM which provides interesting capabilities in contrast enhancement and going further in resolution down to as low as 2 Angstroms.

Working principles and first results obtained on such microscope are presented in this report.

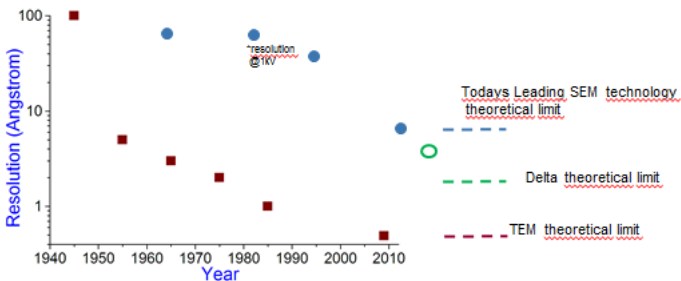


Figure 1. Practical resolution and theoretical limits of SEM, TEM and DeltaSEM.

1. J. Cazaux, "From the physics of secondary electron emission to image contrasts in scanning electron microscopy." *Journal of Electron Microscopy* **61**, 261 (2012).

## Scanning probe microscopy and spectroscopy of graphene on different metal substrates measured with SPM Aarhus - highest productivity in UHV SPM

Y. Alekseeva<sup>1</sup>, O. Schaff<sup>1</sup>, A. Thissen<sup>1</sup>, Y. Dedkov<sup>2</sup>, E. Voloshina<sup>3</sup>

<sup>1</sup>*SPECS Surface Nano Analysis GmbH, 13355 Berlin, Germany  
www.specs.com*

<sup>2</sup>*IHP GmbH -Innovations for High Performance Microelectronics/Leibniz-Institut für innovative Mikroelektronik, 15236 Frankfurt (Oder), Germany*

<sup>3</sup>*Humboldt Universität zu Berlin, Institut für Chemie – Quantenchemie der Festkörper/Katalyse, 12489 Berlin, Germany*

STM, ncAFM and KPFM results of graphene layers on different metal substrates are presented. With its stability and productivity the SPM Aarhus 150 is the ideal instrument for investigating lattice mismatched surfaces, like graphene/Ir(111). Microscopy experiments were performed in constant current / constant frequency shift (CC/CFS) and constant height (CH) modes, exploiting a combination of the STM and NC-AFM capabilities of the system. We found that in STM imaging the electronic contribution is prevailing compared to the topographic one and the inversion of the contrast can be assigned to the particular features in the electronic structure of graphene on Ir(111). Contrast changes observed in constant height AFM measurements are analyzed on the basis of the energy, force, and frequency shift curves, obtained in DFT calculations, reflecting the interaction of the W-tip with the surface and are attributed to the difference in the height and the different interaction strength for high-symmetry sites within the moiré unit cell of graphene on Ir(111). The presented findings are of general importance for the understanding of the properties of the lattice-mismatched graphene/metal systems especially with regard to possible applications as templates for molecules or clusters.

## Calorimetric studies of ferroelectric phase transition in KDP nanocrystals

V.A. Abalmassov<sup>1</sup>, A.M. Pugachev<sup>1</sup>, A.Yu. Milinskiy<sup>2</sup>, S.V. Baryshnikov<sup>2</sup>

<sup>1</sup>*Institute of Automation and Electrometry, 630090, Novosibirsk, Russia*  
 abalmassov@iae.nsk.su

<sup>2</sup>*Blagoveschensk State Pedagogical University, 675000, Blagoveschensk, Russia*

Ferroelectric properties of nanocrystals are of fundamental and practical interest. Previous dielectric [1] and calorimetric [2] studies of KDP nanocrystals confined in nanopores of different matrices claim the strong increase in the critical temperature  $T_c$  from 130 up to 250 K as the pore size decreases from 100 to 5 nm. Non-monotonic increase in  $T_c$  from 124 to 130 K was reported in [3] from dielectric measurements for the crystal size from 23 to 312 nm. The latter agrees with the results obtained in [4,5].

Recent dielectric studies of KDP in MCM-41 nanopores of 3.8 and 2.6 nm in size reveal only a very slight increase in  $T_c$ , no more than 1 K as to compare with the bulk value of 123 K, but a substantial broadening of the dielectric constant peak [6]. Our measurements of the thermal capacity with the same samples confirm a slight change in  $T_c$  and show the broadening of the heat capacity peak (Fig. 1). These effects are consistent with the finite size effects for the Ising model [7] on which the phase transition theory in KDP is based.

Dielectric and calorimetric study reveal no phase transition in the same samples with DKDP in the nanopores. Our Raman spectra of these samples at room temperature (Fig. 2) correspond to the monoclinic phase [8] in accordance with the neutron diffraction results [9].

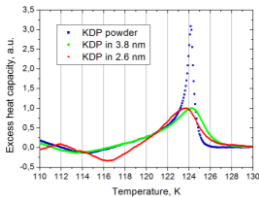


Figure 1. Heat capacity of KDP on heating

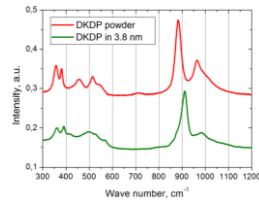


Figure 2. Raman spectra of DKDP

V.A.A. and A.M.P. acknowledge the support from the RFBR grants N 14-02-00189 and N 15-02-04950.

1. E.V. Colla, A.V. Fokin, Yu.A. Kumzerov, *Solid State Commun.* **103**, 127 (1997).
2. Yu.A. Kumzerov et al., *Phys. Solid State* **53**, 1099 (2011).
3. A. Cizman et al., *Phase Transition* **86**, 910 (2013).
4. V. Tarnavich et al., *Optica Applicata* **XL**, 305 (2010).
5. A. Sieradzki et al., *Journal of Advanced Dielectrics* **1**, 337 (2011).
6. A.Yu. Milinskiy, S.V. Baryshnikov, E.V. Charnaya, *Ferroelectrics* (submitted).
7. D.P. Landau, *Phys. Rev. B* **13**, 2997 (1976).
8. L. Zhang et al., *CrystEngComm* **17**, 4705 (2015).
9. B. Dorner et al., *Ferroelectrics* **286**, 213 (2003).

**Raman spectroscopy study of cryoprotectant distribution in frozen straws**

Yu. A. Karpegina<sup>1,3</sup>, K.A. Okotrub<sup>1</sup>, E.Yu. Brusentsev<sup>2</sup>, S.Ya. Amstislavsky<sup>2,3</sup>,  
N.V. Surovtsev<sup>1,3</sup>

<sup>1</sup>*Institute of Automation and Electrometry RAS, Novosibirsk, 630090, Russia*  
*lab21@iae.nsk.su*

<sup>2</sup>*Institute of Cytology and Genetics RAS, Novosibirsk 630090, Russia*

<sup>3</sup>*Novosibirsk State University, Novosibirsk, 630090, Russia*

Cryopreservation of biological cells and biomaterials plays a crucial role in biological studies, medicine and industry. Biological sample freezing is a very complicated process which is carried out in strict agreement with a specialized freezing protocol using specific cryoprotectant solution and a container. The most common container for sample freezing is a plastic straw which is widely used for freezing mammalian semen, oocytes and embryos. Although the straws are successfully used for freezing and cryopreservation purposes, there are still some unanswered questions. One of these questions is whether the distribution of the cryoprotectant solution and ice is uniform within the frozen straw. Answer for this question is important for development of freezing procedures and for comparison of different cryopreservation protocols.

In the present work we studied the distribution of cryoprotectant (10% glycerol) and ice along the frozen straw by the Raman scattering technique. Raman spectroscopy being a contactless, non-invasive tool was applied for the straws filled by the cryoprotectant solution and frozen by controlled rate programs commonly used for mammalian embryos freezing. Analysis of Raman spectra measured from different points along the straws reveals a non-uniform distribution of the cryoprotectant. The ratio between the non-crystalline solution and ice was found to be increased by several times at the bottom side of the solution column frozen by standard freezing program. The increase of the cryoprotectant fraction occurs in the area where cryopreserved embryos or oocytes are placed. The effects of the cooling rate and ice nucleation temperature on the glycerol distribution along the straw were studied. Cryoprotectant concentration at the bottom side slightly increases when the ice nucleation temperature increases. Our findings reveal an important phenomenon which should be taken into account for the further improvement the cryopreservation procedures, and highlight that the ice fraction around cryopreserved embryos or oocytes can differ significantly from the averaged one in the frozen plastic straws.



## Micro-Raman structural characterization of electrode materials for Li-ion batteries

D.V. Pelegov<sup>1</sup>, B.N. Slautin<sup>1</sup>, V.S. Gorshkov<sup>2</sup>, P.S. Zelenovskiy<sup>1</sup>, D.O. Alikin<sup>1</sup>, D.K. Kuznetsov<sup>1</sup>, A.A. Koshkina<sup>1</sup>, E.A. Kiselev<sup>1</sup>, A.L. Kholkin<sup>1,3</sup>, V.Ya. Shur<sup>1</sup>

<sup>1</sup>*Institute of Natural Sciences, Ural Federal University, 620000 Ekaterinburg, Russia  
dmitry.pelegov@urfu.ru*

<sup>2</sup>*JSC Eliont, 620137, Ekaterinburg, Russia*

<sup>3</sup>*Physics Department and CICECO – Materials Institute of Aveiro, University of Aveiro, 3810-193 Aveiro, Portugal*

Fast growth of battery market driven by electric vehicle (EV) and stationary energy storage system (ESS) segments has stimulated interest for lithium titanate  $\text{Li}_4\text{Ti}_5\text{O}_{12}$  (LTO) with its low cost, perfect cycleability and excellent safety. Whereas low electric conductivity ( $10^{-8} \div 10^{-13}$  S/cm) is the main drawback of LTO, it can be compensated by the grain size reducing down to sub-micron scales.

In this presentation we report our new results [1] about structural heterogeneity in solid-state synthesized LTO with sub-micron grain size can be described locally in terms of: (1) structural characterization of single particles (Fig. 1) and (2) “big-data” analysis using conventional micro-Raman Spectroscopy.

The equipment of the Ural Center for Shared Use “Modern nanotechnology” UrFU was used. Supported by Government of the Russian Federation (Act 211, Agreement 02.A03.21.0006).

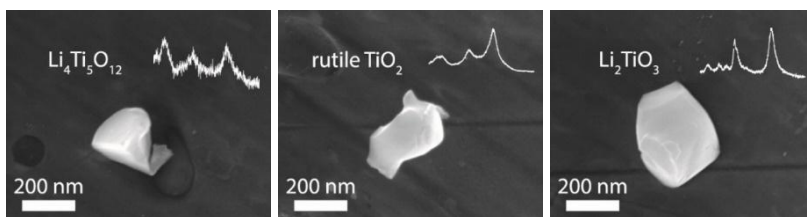


Figure 1. SEM images and corresponding Raman spectra of single particles of target phase  $\text{Li}_4\text{Ti}_5\text{O}_{12}$  and two nearest phases  $\text{Li}_2\text{TiO}_3$  and  $\text{TiO}_2$  (rutile). SEM images sizes are  $0.8 \times 1.0 \mu\text{m}$ .

1. D.V. Pelegov, B.N. Slautin, P.S. Zelenovskiy, D.K. Kuznetsov, E.A. Kiselev, D.O. Alikin, A.L. Kholkin, V.Ya. Shur, *Journal of Raman Spectroscopy* (in press) (2016), doi: 10.1002/jrs.4999.

## Temperature dependence of the relaxation time in nano-domain structures in relaxor ferroelectrics

A.V. Maksimov, O.G. Maksimova

*Institute of Information Technologies, Cherepovets State University, 162612, Cherepovets, Russian Federation*  
*a\_v\_maximov@mail.ru, www.chsu.ru*

To describe the evolution of nano-domain structures in relaxor ferroelectrics we use one- and two-component models [1, 2], consisting of flexible and rigid elements with anisotropic orientation interactions. The extension of flexible elements (FE) in the high-temperature region occurs with decreasing temperature up to the critical point at which the effect “critical slowdown” [3] manifests: relaxation times increase infinitely (in the FE-model without the fixation of mean-square length of FE).

In the critical point, the two-component FE-model with the fixation of mean-square length of FE is transformed into a one-component one (RE), because a “rigiding” of FE occurs, and the relaxation times are maximized. Therefore, in the high-temperature region it’s necessary to use the RE-model the relaxation times of which are practically independent of temperature (at energetic character of the constant of orientation interactions [4]) or decrease with decreasing temperature (at entropic character of the constant of orientation interactions [5]). Obtained both types of mobility behavior in the nano-domain structures are confirmed by experimental data by the study of the temperature dependence of the relaxation times in niobate barium strontium (SBN) [6] and zinc niobate-lead (PZN-PT) [7] relaxors respectively.

1. Yu.Ya. Gotlib, A.V. Maksimov, O.G. Maksimova, *Polymer Science* **A38**, 394(1996).
2. A.V. Maksimov, O.G. Maksimova, and D. S. Fedorov, *Polymer Science* **A48** (11), 751 (2006).
3. H.E. Stanley. *Introduction to Phase Transitions and critical Phenomena* (Clarendon Press), 333 (1971).
4. A.V. Maksimov, O.G. Maksimova, E.M. Egorova, Yu.Ya. Gotlib *Polymer Science* **A41**(7), 732 (1999).
5. A.V. Maksimov, G.M. Pavlov, *Polymer Science* **A** **49**, 828 (2007).
6. V.Ya. Shur, D.V. Pelegov, V.A. Shikhova et. al., *Ferroelectrics* **374**, 177 (2008).
7. V.A. Shikhova, V.Ya. Shur, D.V. Pelegov, et. al., *Ferroelectrics* **398**, 115 (2010).

## Studies of polarization hysteresis loops in the relaxor-like and non-relaxor Li-doped ceramics of $\text{Pb}(\text{Fe}_{1/2}\text{Ta}_{1/2})\text{O}_3$ multiferroic

S.I. Raevskaya<sup>1</sup>, M. Savinov<sup>2</sup>, P. Bednyakov<sup>2</sup>, A.A. Gusev<sup>3</sup>, V.P. Isupov<sup>3</sup>, S.P. Kubrin<sup>1</sup>, V.V. Titov<sup>1</sup>, C.-C. Chou<sup>4</sup>, V.Yu. Shonov<sup>1</sup>, I.P. Raevski<sup>1</sup>, H. Chen<sup>5</sup>, M.A. Malitskaya<sup>1</sup>, T.A. Minasyan<sup>1</sup>, E.I. Sitalo<sup>1</sup>, I.N. Zakharchenko<sup>1</sup>

<sup>1</sup>Research Institute of Physics and Faculty of Physics, Southern Federal University, 344090, Rostov-on-Don, Russia  
Sveta.Raevskaya@mail.ru

<sup>2</sup>Institute of Physics, AS CR, Prague, Czech Republic

<sup>3</sup>Institute of Solid State Chemistry and Mechanochemistry, Siberian Branch of the Russian Academy of Sciences, Novosibirsk, Russia

<sup>4</sup>National Taiwan University of Science and Technology, 106, Taipei, Taiwan, China

<sup>5</sup>Institute of Applied Physics and Materials Engineering, Faculty of Science and Technology, University of Macau, 999078, Macau, China

Lead iron tantalate  $\text{PbFe}_{1/2}\text{Ta}_{1/2}\text{O}_3$  (PFT) –based materials are among the promising multiferroics. On cooling PFT undergoes transitions from paraelectric cubic to ferroelectric tetragonal phase at  $\approx 270$  K and then to monoclinic ferroelectric phase at  $\approx 215$  K [1]. Since its discovery in 1959 PFT was believed to be a relaxor ferroelectric. However recently a non-relaxor PFT ceramics was obtained using high-energy mechanical activation technique [2]. Li-doping enabled us to obtain highly-resistive samples of both nonrelaxor and relaxor-like PFT ceramics which are capable to withstand the application of strong electric field. This gave us an opportunity to study the polarization hysteresis loops in a wide temperature range (100–280 K) including both tetragonal and monoclinic ferroelectric phases as well as antiferromagnetic phase transition. Ferroelectric-type polarization hysteresis loops have been observed in both tetragonal and monoclinic phases. Anomalies in the temperature dependences of remnant polarization and coercive field have been revealed in the vicinity of antiferromagnetic phase transition ( $\approx 150$  K).

This work was partially supported by Ministry of Education and Science of the Russian Federation (research project 2132) and Research Committee of the University of Macau (Research & Development Grant for Chair Professor No RDG007/FST-CHD/2012).

1. I.P. Raevski, M.S. Molokeev, S.V. Misyul, E.V. Eremin, A.V. Blazhevich, S.P. Kubrin, H. Chen, C.-C. Chou, S.I. Raevskaya, V.V. Titov, D.A. Sarychev, M.A. Malitskaya, *Ferroelectrics*. **475**, 52 (2015).
2. A.A. Gusev, S.I. Raevskaya, V.V. Titov, E.G. Avvakumov, V.P. Isupov, I.P. Raevski, H. Chen, C.-C. Chou, S.P. Kubrin, S.V. Titov, M.A. Malitskaya, A.V. Blazhevich, D.A. Sarychev, V.V. Stashenko, S.I. Shevtsova, *Ferroelectrics*. **475**, 41 (2015).

**Nanotoxicological research in UCSU “Modern Nanotechnology”**

V.Ya. Shur<sup>1</sup>, A.E. Tyurnina<sup>1,2</sup>, D.K. Kuznetsov<sup>1</sup>, A.P. Potapov<sup>1</sup>, I.V. Zubarev<sup>1</sup>, E.V. Shishkina<sup>1</sup>, D.S. Vasileva<sup>1</sup>, V.A. Vazhenin<sup>1</sup>, M.V. Morozova<sup>1</sup>

<sup>1</sup>*Institute of Natural Sciences, Ural Federal University, 620000 Ekaterinburg, Russia  
vladimir.shur@urfu.ru*

<sup>2</sup>*UNIM, 620000 Ekaterinburg, Russia*

The study of nanoparticle toxicity (nanotoxicology) needs production of the stable colloids of high concentration with model pure nanoparticles of given composition, sizes and shapes. The laser ablation in water gives the unique ability to produce the colloids of pure metals and metal oxides with required parameters. The colloids of Au, Ag, CuO, NiO, PbO, ZnO, Fe<sub>2</sub>O<sub>3</sub>, and Mn<sub>3</sub>O<sub>4</sub> nanoparticles with narrow distribution function and concentration up to 0.5 g/l with high enough stability have been produced to study the impact of the nanoparticles on the biological tissues and cells.

The pulsed Yb fiber laser (1064 nm, 100 ns, 21 kHz) has been used for ablation of pure metal target in deionized water and subsequent fragmentation of the suspension. The NPs synthesis was performed in several stages: surface treatment by focused laser beam scanning, ablation the target, separated additional fragmentation, drying to increase the concentration of the solution up to 0.5 g/l and heating for NP self-organization and reshape. The optimized technology allowed to produce the required colloids with stability over month of spherical NPs with averaged sizes from 10 to 60 nm. The size distribution function has been measured by particle size analyzer Zetasizer Nano ZS and by statistical analysis of the images obtained by scanning electron microscope Auriga CrossBeam. The composition has been analyzed by confocal Raman microscope Alpha 300 AR WiTec.

The total content of metals in the samples of liver, kidneys, spleen, and brain of the rats administered by NPs was obtained by atomic emission spectroscopy method using atomic emission spectrometer with inductively coupled plasma iCAP 6500 Duo. Samples of freeze-dried homogenized tissue were subjected to acid ignition with the help of a MARS 5 microwave accelerated reaction system. The content of NPs of paramagnetic metals has been revealed by electron paramagnetic resonance (EPR) method using electron paramagnetic resonance spectrometer EMX Plus Bruker.

The impact of nanoparticles on alveolar macrophages has been *in vivo* studied by atomic force and transmission electron microscopy. It was found that phagocytosis of NPs leads to nanoscale change of the cells surface morphology. The sizes of surface pits revealed by atomic force microscopy on the cells of rats administered by NPs are close to the NPs sizes. Such pits were absent on the surface of reference cell. The positions of NPs in the samples of rat's tissue and induced destructions have been revealed by scanning transmission electron microscopy.

## **A synthesis of the most important inferences from animal experiments assessing adverse health effects of metallic nanoparticles**

L.I. Privalova<sup>1</sup>, M.P. Sutunkova<sup>1</sup>, I.A. Minigalieva<sup>1</sup>, B.A. Katsnelson<sup>1</sup>, V.B. Gurvich<sup>1</sup>, V.Ya. Shur<sup>2</sup>, E.V. Shishkina<sup>2</sup>, O.H. Makeyev<sup>3</sup>, I.E. Valamina<sup>3</sup>

<sup>1</sup>*Medical Research Center for Prophylaxis and Health Protection in Industrial Workers, 620014 Ekaterinburg, Russia*

<sup>2</sup>*Institute of Natural Sciences, Ural Federal University, 620000 Ekaterinburg, Russia*

<sup>3</sup>*Ural State Medical University, 620109 Ekaterinburg, Russia*

Nanoparticles (NPs) of metals and their oxides are of special interest in the light of health risks assessment as along with engineered NPs there exists a substantial fraction of metallic NPs as fraction of condensation aerosols generated by arc-welding and metallurgical technologies. During 2009-2016 we carried out a number of toxicological experiments on rats exposed to single intratracheal instillation or repeated intraperitoneal injections of Ag, Au, Fe<sub>3</sub>O<sub>4</sub>, CuO, NiO, PbO, ZnO and Mn<sub>3</sub>O<sub>4</sub> NPs and microparticles (MPs) in stable water suspensions as well as a long-term inhalation experiments with Fe<sub>2</sub>O<sub>3</sub> NPs.

Based on obtained experimental results and some corroborating data of other researchers we maintain that metallic NPs (Me-NPs) are much more noxious on both cellular and systemic levels as compared with their one micrometer or even submicron counterparts. However, within the nanometer range the dependence of systemic toxicity on particle size is intricate and non-unique due to complex and often contra-directional relationships between the intrinsic biological aggressiveness of the specific Me-NPs and complex mechanisms that control their toxicokinetics. Among these mechanisms associated with more or less significant solubilization of Me-NPs in biological milieus proved very important, which fact is taken into consideration by a multicompartmental toxicokinetic model proposed and identified by us.

For certain size of the Me-NPs, both integral and specific adverse effects caused by them depend on the properties of particular metal, but toxic impact on liver, spleen and kidneys as well as systemic genotoxicity proved virtually obligatory. Of a special interest is a marked neuronal damage to the striatum and the hippocampus of rats subchronic exposed to NPs of CuO or Mn<sub>3</sub>O<sub>4</sub>.

Our data testify the high activity of the pulmonary phagocytosis of Me-NPs deposited in low airways. This fact suggests that safe levels of exposure to airborne NPs are possible in principle. For workroom air, such permissible levels of metallic NP can be proposed at this stage, even if tentatively, based on a sufficiently conservative approach of decreasing approximately tenfold the exposure limits officially established for respective MPs.

It was shown that against the background of adequately composed combinations of some bioactive agents the systemic toxicity and even genotoxicity of Me-NPs could be markedly attenuated.

## Growth kinetics, piezoelectric and pyroelectric properties of diphenylalanine microtubes

S.G. Vasilev<sup>1</sup>, A.S. Nuraeva<sup>1</sup>, D.S. Vasileva<sup>1</sup>, K.N. Romanyuk<sup>1,2</sup>,  
D.S. Chezganov<sup>1</sup>, A.A. Esin<sup>1</sup>, P.S. Zelenovskiy<sup>1</sup>, V.Ya. Shur<sup>1</sup>, A.L. Kholkin<sup>1,2</sup>

<sup>1</sup>*Institute of Natural Sciences, Ural Federal University, 620000 Ekaterinburg, Russia  
semen.vasilev@urfu.ru*

<sup>2</sup>*Physics Department & CICECO – Aveiro Institute of Materials, University of Aveiro,  
3810-193 Aveiro, Portugal*

In this work the growth kinetics, piezoelectric and pyroelectric properties of diphenylalanine microtubes were investigated in the context of their possible applications as sensors, actuators and energy harvesters.

Diphenylalanine (FF) is a model object for the investigation of organic molecules self-assembling and formation of micro- and nanotubes and rods [1]. Moreover, FF microtubes have attracted research interest in recent decade due to excellent piezoelectric properties [2] and possibility to developing biocompatible piezoelectric and pyroelectric elements for medical devices [3].

Usually peptide microstructures grow from pure organic solvents. In this work FF microtubes were grown from the mixture of methanol and water. It was shown that increasing of the water concentration led to change of the morphology from flat dendrite structures to tubes and rods.

High values of piezoelectric response were obtained for all configurations of microcrystals. It was revealed that the polar axis in FF microtubes is oriented along their long axis. It was shown that the microtubes grown from the common center have the same polarization direction, whereas independently grown microtubes can include areas with opposite sign of piezoresponse, similar to domains in ferroelectrics. Full matrix of piezoelectric coefficients has been measured and interpreted in terms of anisotropic structure of FF.

Pyroelectric properties of FF tubes were investigated as well. The evaluated pyroelectric coefficient exceeds  $10^{-6}$  C/(m<sup>2</sup> K). Notable piezoelectric and pyroelectric coefficients and their temperature behavior have been attributed to the aligned water molecules inside nanochannels.

The equipment of the Ural Center for Shared Use “Modern Nanotechnology”, Ural Federal University has been used. The research was made possible by the President of Russian Federation grant for young scientists (Contract 14.Y30.15.6554-MK).

- 1 E. Gazit, *The Royal Society of Chemistry* **36**, 1263 (2007).
- 2 A. Kholkin, N. Amdursky, I. Bdikin, et al. *ACS Nano* **4**, 610 (2010).
- 3 I. Coondoo, S. Kopyl, M. Ivanov, V.Ya. Shur, A.L. Kholkin, *Electrically Active Materials for Medical Devices* (Imperial College Press), 297 (2016).

## Subpicoliter droplets produced by pyroelectric field

E.A. Mingaliev, M.S. Kosobokov, A.V. Makaev, V.Ya. Shur

*Institute of Natural Sciences, Ural Federal University, 620000, Ekaterinburg, Russia  
ea.mingaliev@urfu.ru*

The dispensing of subpicoliter droplets under the action of the pyroelectric field created by heating or cooling of the lithium tantalate  $\text{LiTaO}_3$  (LT) plate was studied [1]. The reproducible deposition of the dielectric and conductive liquid droplets with the volume below picoliter was demonstrated and applied for deposition of metal nanoparticles and growth of organic microcrystals.

The electric field was produced during cyclic heating and cooling of LT plate with tailored domain structure. The drop reservoir of proper liquid was situated under the LT plate (Fig. 1). The temperature of LT plate was changed uniformly by thermoelectric cooler (TEC) with accuracy  $0.1^\circ\text{C}$  [2]. Droplets dispensed on the thin glass plates moved by motorized 2D motion driver. The fast camera with 10000 fps at resolution  $640 \times 480$  pixels was used for *in situ* recording of the droplet generation process and growth of microcrystals during drying of the deposited droplet. The shape of the initial drop was changed into the cone after plate heating. For pyroelectric field above the threshold value the fine microjet appeared on the cone top and small droplet dispensed to the substrate.

This technique allows generating the droplets of dielectric and conductive liquids with volume down to 0.3 picoliter with diameter about ten microns. The organic microcrystals of glycine and various patterns of metal nanoparticles have been produced by drying of droplets.

The small rings of Ag nanoparticles were used for realization of the Surface Enhanced Raman Scattering effect (SERS). The future application of proposed technique for 3D cell printing for tissue engineering will be presented.



Figure 1. Scheme and instantaneous images of the droplet generation process.

The equipment of the Ural Center for Shared Use “Modern Nanotechnology”, Ural Federal University has been used. The research was made possible in part by Government of the Russian Federation (Act 211, Agreement 02.A03.21.0006).

1. P. Ferraro, S. Coppola, S. Grilli, M. Paturzo, V. Vespini, *Nature Nanotechnology* **5**, 429 (2010).
2. E.A. Mingaliev, D.V. Zorikhin, M.S. Kosobokov, A.V. Makaev, V.Ya. Shur, *Ferroelectrics* **476**, 156 (2015).

## Investigation of domain kinetics in KTP single crystals for periodical poling applications

A.R. Akhmatkhanov<sup>1</sup>, E.V. Pelegova<sup>1</sup>, E.M. Vaskina<sup>1</sup>, M.A. Chuvakova<sup>1</sup>, V.Ya. Shur<sup>1</sup>, M. Ivanov<sup>2</sup>, A.L. Kholkin<sup>1,2</sup>

<sup>1</sup>*Institute of Natural Sciences, Ural Federal University, 620000, Ekaterinburg, Russia  
andrey.akhmatkhanov@urfu.ru*

<sup>2</sup>*Physics Department and CICECO-Aveiro Institute of Materials, 3810-193 Aveiro, Portugal*

The domain shape evolution and kinetics of the domain structure has been studied in potassium titanyl phosphate (KTiOPO<sub>4</sub>, KTP) single crystals using various complementary experimental methods. The studied KTP samples representing 2-mm-thick plates cut perpendicular to polar axis were grown by top-seeded solution method in the Crystals of Siberia Ltd. (Russia).

It was shown, that the optical microscopy without selective chemical etching could be used for visualization of statics and kinetics of domain structure. This effect was related to change of the refractive index in the vicinity of the domain wall caused by residual depolarization field due to electrooptic effect. The *in situ* visualization of the domain structure evolution during polarization reversal allowed revealing two types of the isolated domain shapes: stripe and rhombus, oriented along Y direction. Two types of the moving domain walls were distinguished. First, the walls of the rhombus domains deviated from Y-orientation for the angle below 10 degrees (Y<sub>+</sub> walls). Second, the walls deviated from X-orientation for the angle close to 30 degrees (X<sub>+30</sub> walls). It was shown that the X<sub>+30</sub> walls were essentially faster than Y<sub>+</sub> ones. The jump-like domain wall motion caused by domain merging was revealed. The domain shape stability effect representing the restoration of the rhombus shape after merging of small isolated rhombus was demonstrated.

The model of domain growth by generation and motion of elementary steps was presented. The effect of polarization reversal induced by chemical etching was revealed and related to the action of the low residual depolarization field appeared as a result of partial removing of the screening charge layer by etching.

The equipment of the Ural Center for Shared Use “Modern Nanotechnology”, Ural Federal University was used. The research was made possible by Russian Foundation for Basic Research (grant 16-02-00724-a). The work was supported by Government of the Russian Federation (act 211, agreement 02.A03.21.0006). VYS acknowledges financial support within the State Task from the Ministry of Education and Science of Russian Federation (Project No. 1366.2014/236). ALK acknowledges the CICECO-Aveiro Institute of Materials (Ref. FCT UID /CTM /50011/2013), financed by national funds through the FCT/MEC and when applicable co-financed by FEDER under the PT2020 Partnership Agreement.



## Electron beam domain engineering in optical waveguides in lithium niobate crystals

L.S. Kokhanchik<sup>1</sup>, R.V. Gainutdinov<sup>2</sup>, Ya.V. Bodnarchuk<sup>2</sup>, T.R. Volk<sup>2</sup>

<sup>1</sup>*Institute of Microelectronics Technology and High Purity Materials RAS, 142432, Chernogolovka, Russia*  
 mlk@iptm.ru

<sup>2</sup>*Shubnikov Institute of Crystallography RAS, 119333, Moscow, Russia*

LiNbO<sub>3</sub> (LN) is very perspective ferroelectric material for domain engineering. Our recent works were directed to elaboration of electron beam (EB) recording of periodical domains (PD) on non-polar (Y,X) surfaces of LN crystals. Correlation between EB exposure and planar PD patterns parameters, as well a depth of their location under the surface depending on EB energies were obtained [1]. Here we report the features of EB technique applied to PD creation in planar optical waveguides on the Y, X-cuts of the LN. The planar PD patterns ( $\Lambda = 4\text{-}7\mu\text{m}$ ) were fabricated by an EB in already prepared waveguide layers. We used the He-implanted planar optical waveguide on the X-cut (He<sup>+</sup> energy  $\sim 450$  keV) (He-LN waveguide) [2]. The depth of the implanted layer was  $D = 1.4 \mu\text{m}$  [2]. And we used the Ti-indiffused waveguide on the Y-cut (Ti-LN waveguide); the Ti diffusion depth reached more than  $10 \mu\text{m}$  [3]. PD patterns were recorded in the SEM JSM-840A with NanoMaker lithography system. Exposure technique was described in [1-3]. To visualize PD patterns a PFM in lateral mode and selective wet etching were applied.

For He-LN waveguide it was found, that growth of domains is inhibited by structurally disturbed layer produced by He implantation [2]. As a result violations of the PD regularities observed when the domains growth occurs beyond the He-implanted damaged barrier. When the domains are formed above the structurally disturbed area a regularity of PD is preserved. Acceleration voltages  $U=10$  and  $15$  kV have an optimum effect to domain structure. In the given case the domain thickness ( $T_d$ ) corresponds to  $T_d \leq D$ .

In the Ti-LN waveguide the best domain gratings were recorded at higher acceleration voltages ( $U = 25$  kV). In this case the domain thickness  $T_d$  could be reached more than  $\sim 4\text{-}5 \mu\text{m}$  [1]. Ti concentration in the Ti-LN waveguide diminishes gradually with a crystal depth [3]. Series etching of the waveguide showed that most regular PD patterns formed in areas of waveguide with a minimum concentration of metal. The results obtained permit us to match the EB irradiation parameters to the waveguide features to form the best PD patterns with optimum characteristics of the gratings.

The work was partially supported by the RFBR №16-02-00439-a.

1. L.S. Kokhanchik, R.V. Gainutdinov, T.R. Volk, *Phys.Sol.St.* **57**, 49 (2015).
2. T.R. Volk, L.S. Kokhanchik et al, *J Lightwave Technology* **33**, 4761 (2015).
3. L.S. Kokhanchik, M.V. Borodin, S.M. Shandarov et al, *Phys.Sol.St.* **52**,1722, (2010).

## Formation of periodic domain patterns by electron beam irradiation in lithium niobate

D.S. Chezganov<sup>1,2</sup>, E.O. Vlasov<sup>1</sup>, V.A. Kvashnin<sup>1</sup>, A.R. Akhmatkhanov<sup>1,2</sup>, M.A. Chuvakova<sup>1</sup>, D.K. Kuznetsov<sup>1</sup>, V.Ya. Shur<sup>1,2</sup>

<sup>1</sup>*Institute of Natural Sciences, Ural Federal University, 620000 Ekaterinburg, Russia*  
*dmitchezganov@gmail.com*

<sup>2</sup>*Labfer Ltd., 620014 Ekaterinburg, Russia*

The formation of ferroelectric domains by electron beam (e-beam) irradiation of polar surfaces in single crystals of 5 mol% MgO-doped lithium niobate (MgOLN) has been studied experimentally and by computer simulation [1,2]. The periodical domain patterns in have been produced and effective second harmonic generation (SHG) has been demonstrated.

The irradiation with different doses, periods and width of stripe scanning was performed by scanning electron microscope (Auriga Crossbeam, Carl Zeiss) driven by e-beam lithography system (Elphy Multibeam, Raith). Two exposure modes were used: arrays of dots and stripes. The irradiated surface of 1-mm-thick Z-cut MgOLN wafer was covered by 2.5- $\mu\text{m}$ -thick resist layer and opposite surface – by solid electrodes. The domain patterns were visualized by optical microscopy.

The dependences of the isolated domain sizes on dose, period of irradiated areas and width of stripe scans have been measured. It was shown that the quality of periodical domain patterns depends on the thickness of resist layer and electron energy. Four types of the domain structure appeared after stripe scanning were revealed. The irradiation parameters for the most uniform patterning were revealed. It was shown that resist layer and optimal irradiation parameters allowed to create high-quality periodically poled MgOLN.

The distribution of space charge and electric field were studied by computer simulation. The mechanism of domain nucleation and growth was proposed and explained in terms of the kinetic approach [3].

The developed technique was used for high quality periodical poling in MgOLN with 6.89  $\mu\text{m}$  period for SHG of green light. The homogeneity of the periodical poling was confirmed by uniform SHG efficiency.

The equipment of the Ural Center for Shared Use “Modern nanotechnology” UrFU was used. The research was made possible in part by RFBR (15-32-21102-mol\_a\_ved), by Government of the Russian Federation (Act 211, Agreement 02.A03.21.0006) and by President of Russian Federation grant for young scientists (Contract 14.Y30.16.8441-MK).

1. D.S. Chezganov et al., *Ferroelectrics* **476**, 117(2015).
2. V.Ya. Shur et al., *Appl. Phys. Lett.* **106**, 232902 (2015).
3. V.Ya. Shur, *J. Mater. Sci.* **41**, 199 (2006).

## Formation of nanodomain structures and snowflake domains during fast cooling of lithium tantalate crystals

M.S. Kosobokov, V.Ya. Shur, E.A. Mingaliev, D.K. Kuznetsov,  
P.S. Zelenovskiy

*Institute of Natural Sciences, Ural Federal University, 620000, Ekaterinburg, Russia*

Uniaxial ferroelectric lithium tantalate  $\text{LiTaO}_3$  (LT) is one of the most versatile materials for wide range of applications in electro-optical, nonlinear-optical, piezoelectric, and pyroelectric devices due to combination of unique characteristics. Many applications of LT involve creating stable precise domain structures with proper shapes and geometry (domain engineering) [1].

The studied samples are 0.5-mm-thick plates of Z-cut optically polished congruent LT (CLT) produced by Oxide Co., Japan.  $\text{CO}_2$  laser with wavelength 10.6  $\mu\text{m}$  and variable pulse duration was used for irradiation of Z+ polar surface. The static domain patterns were revealed by selective chemical etching. The relief corresponding to the domain structure was visualized by several microscopic methods: optical microscopy (Olympus BX51, Japan), Scanning Electron Microscopy (Auriga CrossBeam Workstation, Carl Zeiss, Germany), Confocal Raman Microscopy (Ntegra Spectra, NT-MDT, Russia).

Formation of the original dendrite snowflake-shape domains during fast cooling after heating above phase transition temperature by pulsed laser irradiation was revealed in CLT crystals. The effect was attributed to polarization reversal under the action of spatially nonuniform pyroelectric field. Two stages of domain shape evolution at the surface were separated: (1) growth of circular domains by sideways motion of the domain walls, (2) backswitching leading to formation of the snowflake domains. The simulated spatial distribution of the pyroelectric field in regular two-dimensional structure was used for explanation of the obtained results. The backswitching process near the surface has been attributed to change of the sign of the pyroelectric field. The snowflake shape of residual domains has been attributed to formation of isolated nanodomain fingers and hampering of their merging [4].

The equipment of the Ural Center for Shared Use «Modern Nanotechnology», Ural Federal University has been used. The research was made possible by Russian Scientific Foundation (Grant No. 14-12-00826).

1. V.Ya. Shur, E.V. Nikolaeva, et al., *Appl. Phys. Lett.* **79**, 3146 (2001).
2. V.Ya. Shur, M.S. Kosobokov, et al., *J. Appl. Phys.* **119**, 144101 (2016).

**Gd-doped ceria-based micro-electro-mechanical devices**

E. Mishuk, I. Lubomirsky

*Department of Materials and Interfaces, Weizmann Institute of Science, 76100, Rehovot, Israel*

Gd-doped ceria (GDC), one of the most studied oxygen ion conductors, was recently found to exhibit electrostrictive effect exceeding “classical (Newnham’s) electrostriction” by at least two orders of magnitude. GDC is a lead-free and completely inert with respect to Si compound, which makes it very attractive for a variety of integrated MEMS applications.

Using only Si-compatible processes, we fabricated membranes, bridges and cantilevers based on GDC films ( $\sim 1 \mu\text{m}$ ) with high aspect ratio (1:1000). Several types of electrode materials were tested and found to have a crucial role in device functionality.

Micromachining employed patterning of GDC films with chemical wet etch or by lift-off using sacrificial aluminum layer. The devices were coated with a film of Teflon to passivate surface corrosion processes. Well-passivated micro-cantilevers (500  $\mu\text{m}$  long) showed a deflection of a few microns, however, corrosion in air impedes their characterization.

More durable, large area ( $\sim 4 \text{ mm}^2$ ) membranes show an electrostrictive strain and can withstand  $\sim 0.01\%$  strain without any detectable degradation or fatigue even after  $\sim 6 \cdot 10^9$  operation cycles. The vertical displacement magnitude, induced by alternating voltage, can reach a few  $\mu\text{m}$ . For some electrode materials, the high contact resistance (at the GDC/electrode interface) impairs the response at low frequencies.

Further development of GDC-based devices has a promise to develop into a viable alternative to existing electromechanically active materials.

## Characterization of the lead free piezoelectric ceramics by piezoresponse force microscopy

D.O. Alikin<sup>1</sup>, A.P. Turygin<sup>1</sup>, J. Walker<sup>2</sup>, A.S. Abramov<sup>1</sup>, J. Hreščak<sup>3</sup>, A. Bencan<sup>3</sup>, B. Malic<sup>3</sup>, T. Rojac<sup>3</sup>, V.Ya. Shur<sup>1</sup>, A.L. Kholkin<sup>1,4</sup>

<sup>1</sup>*Institute of Natural Sciences, Ural Federal University, 620000, Ekaterinburg, Russia*

<sup>2</sup>*Materials Research Institute, Pennsylvania State University, University Park, PA, USA*

<sup>3</sup>*Electronic Ceramic Department, Jožef Stefan Institute, Ljubljana, Slovenia*

<sup>4</sup>*Physics Department & CICECO, University of Aveiro, 3810-193 Aveiro, Portugal*

The piezoelectric device market is dominated by lead containing Pb(Zr<sub>1-x</sub>Ti<sub>x</sub>)O<sub>3</sub> (PZT) based materials because of its versatility and robust functional properties. The toxicity of lead however has raised health concerns and in the last two decades legislative changes have stimulated intensive research into suitable lead-free PZT alternative materials. Among the numerous lead-free oxides and solid solution systems investigated for their piezoelectric potential K<sub>1-x</sub>Na<sub>x</sub>NbO<sub>3</sub> (KNN) and BiFeO<sub>3</sub> (BFO) based systems have received enormous attention following publications by Saito et al. and Wang et al., which reported piezoelectric constants for KNN comparable to PZT and high remnant polarizations of BFO approximately double those of PZT [1,2].

Despite the significant focus on KNN and BFO, and the subsequent high volume of scientific publications, commercial realization of their piezoelectric properties has not been forthcoming, as both materials experience difficulties with synthesis in the bulk ceramic form with digestible piezoelectric coefficients. We believe that detailed local study of the domain structure and domain wall motion in lead-free ceramics by piezoresponse force microscopy (PFM) can give fresh insight into understanding of macroscopic ceramics properties and give a way to significant improvement of their electromechanical performance. In this contribution, we provide a way to separate phase content and domain structure of bulk piezoelectric ceramics and propose new methods for study of the domain structure based on the advanced statistical approach. Domain wall motion was studied by direct visualization of the domain structure change after local polarization reversal.

The equipment of the Ural Center for Shared Use «Modern Nanotechnology», Ural Federal University has been used. The research was made possible in part by RFBR (Grants 16-32-60083-mol\_a\_dk) and by Ministry of Education and Science of the Russian Federation (UID RFMEFI58715X0022).

1. J. Wang, J.B. Neaton, H. Zheng et al, *Science* **299**, 1719 (2003).
2. Y. Saito, H. Takao, T. Tani et al, *Nature* **432**, 84 (2004).

**Finite element simulation of effective properties of microporous piezoceramic material with metallized pore surfaces**

A.V. Nasedkin<sup>1</sup>, A.A. Nasedkina<sup>1</sup>, A.N. Rybyanets<sup>2</sup>

<sup>1</sup>*I.I. Vorovich Institute of Mathematics, Mechanics and Computer Science, Southern Federal University, 344090, Rostov-on-Don, Russia  
nasedkin@math.sfedu.ru*

<sup>2</sup>*Physics Research Institute, Southern Federal University, 344090, Rostov-on-Don, Russia*

Piezoceramic composite materials and, in particular, porous piezoceramic materials with enhanced exploitation characteristics are being actively developed in the recent years. Lately, the third author of this abstract has suggested an original method of transportation of micro- and nanoparticles of various substances into micro- and nanoporous piezoceramic materials, respectively. Application of this method enables to obtain porous piezoceramic materials inside which on the boundaries of the ceramic matrix with pores metal or polymer particles are deposited.

This research presents the first numerical results on the calculation of effective properties of such microporous piezoceramic materials. The investigation was based on a complex approach which included the effective moduli method for the mechanics of composites, modeling of representative volumes, finite element solution of the set of static problems of the piezoelectricity theory with special boundary conditions and postprocessing of the computation results.

The representative volume was built in the following way. At the first stage the cubic lettuce of identical piezoelectric cubic finite elements was defined. Then the random number generator chose the finite elements which material properties were modified as material properties of pores. The most nontrivial stage consisted in finding the faces of contact of piezoelectric elements with porous elements. After this stage a part of the contact faces of piezoelectric and porous elements with the help of the random number generator was covered by shell elastic elements. This resulted in the generation of the representative volume which included cubic piezoelectric finite elements, pore elements and shell elastic elements. Static problems of the piezoelectricity theory for an inhomogeneous representative volume were solved numerically with the help of ANSYS finite element package, using programs written in ANSYS APDL.

The results of the numerical experiments on solving the test problems enabled to estimate the influence of the metallization of the pore surfaces on the values of effective moduli of piezoelectric materials, which were obtained by the method of micro- or nanoparticles transportation into ceramic matrices.

The research was done in the framework of the RFBR project 16-01-00785.

## Investigations of residual stresses in barium titanate pressed powder and their effects to the properties of the ferroelectric phase transition

I.V. Zaytseva<sup>1,2</sup>, A.S. Krylov<sup>3</sup>, A.M. Pugachev<sup>1</sup>, V.K. Malinovsky<sup>1</sup>,  
N.V. Surovtsev<sup>1</sup>, Yu.M. Borzdov<sup>2,4</sup>

<sup>1</sup>*Institute of Automation and Electrometry RAS, 630090, Novosibirsk, Russia*  
*apg@iae.nsk.su*

<sup>2</sup>*Novosibirsk State University, 630090, Novosibirsk, Russia*

<sup>3</sup>*L. V. Kirensky Institute of Physics, RAS, 660036, Krasnoyarsk, Russia*

<sup>4</sup>*V. S. Sobolev Institute of Geology and Mineralogy, RAS, 630090, Novosibirsk, Russia*

Recently it was shown that high pressure treatment of BaTiO<sub>3</sub> powder not only increases a density of a sample, but also modifies characteristics of the phase transition [1, 2]. In particular, it was suggested that relaxor-like properties of the pressure-treated barium titanate powders are effects of residual mechanical stresses, which caused by pressure treatment and can be erased by thermal annealing [1, 2]. However, an interrelation between the residual stress and the width of the ferroelectric phase transition was not established. To estimate the residual stresses in pressure-treated BaTiO<sub>3</sub> powder a diamond anvil cell EasyLab  $\mu$ ScopeDAC were used. Quasihydrostatic pressure was applied to the powder with the simultaneous measurement of the Raman spectrum. E-phonon line (about 307 cm<sup>-1</sup>) position was found as a function of the applied mechanical stresses. This dependence was used to evaluate a value of a residual stresses after the pressure treatment. Residual pressures were decreased by a temperature annealing. The dependence of residual stresses from the applied stresses was obtained.

To characterize the ferroelectric phase transition from the second harmonic generation technique was used [1, 2]. It was shown that in BaTiO<sub>3</sub> powder the residual stress generated by the pressure treatment change the temperature and width of the phase transition. A quasilinear correspondence between of the phase transition characteristics (the temperature and width) and the residual stress was found.

Acknowledgment. This work was supported by Russian Foundation for Basic Research (Grants N 15-02-04950 and N 14-02-00189).

1. J. Zhu, C. Jin, W. Cao, X. Wan *Appl. Phys. Lett.* **92**, 242901 (2008).
2. A.M. Pugachev, V.I. Kovalevsky, V.K. Malinovsky, Yu.M. Borzdov, N.V. Surovtsev *Appl. Phys. Lett.* **107**, 102902 (2015).
3. A.M. Pugachev, V.I. Kovalevskii, N.V. Surovtsev, S. Kojima, S.A. Prosandeev, I.P. Raevski, S.I. Raevskaya *Phys. Rev. Lett.* **108**, 247601 (2012).

**Domain wall motion in  $\text{PbZr}_{0.3}\text{Ti}_{0.7}\text{O}_3$  epitaxial thin film in temperature range from 4 to 295 K: experimental study and theoretical modeling**

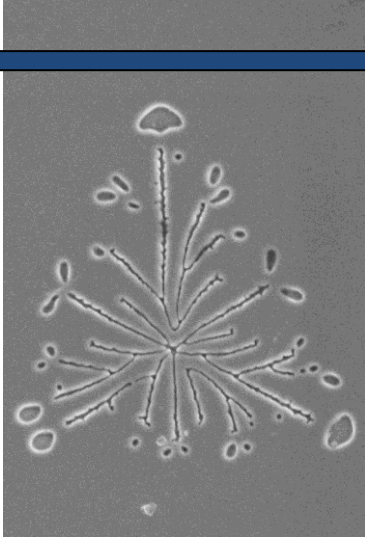
N.V. Andreeva, A.F. Vakulenko, A.V. Filimonov

*Peter the Great St. Petersburg Polytechnic University, 195251, St. Petersburg, Russia  
vakulenko705@gmail.com*

We study the growth of ferroelectric domains in thin epitaxial PZT film with thickness of 60 nm by piezoresponse force microscopy (PFM), in a temperature range from 4 to 295 K. Measurements were carried out using a cryogenic atomic force microscope AttoAFM I (Attocube Systems, Germany) equipped with an external lock-in amplifier SR844 (Stanford Research Systems, CA) and a functional generator FC120 (Yokogawa Electric Corporation, Japan). Nanoscale domains writing was done by applying negative DC voltage pulses with different duration to the bottom electrode while keeping the grounded PFM tip in contact with the film surface at a fixed point. The pulse duration has been varied in the range from millisecond and up to tens of seconds. In order to minimize the influence of native polarization distribution on the domain formation, film was initially poled in the upward direction by scanning the surface at a positive DC voltage applied between the PFM tip and the bottom electrode. The effective domain diameter  $D$  has been calculated from the reversed domain area.

We demonstrated that nanoscale ferroelectric domains can be created by short voltage pulses applied between the PFM tip and the extended bottom electrode even at temperatures as low as 4 K. It was found that the domain size increases gradually with increasing voltage at a given pulse duration. The results of low-temperature domain dynamics indicate that the translation motion of  $180^\circ$  walls in thin PZT film has the form of a creep process. Nevertheless, we observed a weak temperature dependence of the domain lateral expansion. To explain this experimental result we use COMSOL Multiphysics software to model the influence of the surface layer with different from the film dielectric properties on the domain growth. This layer could be represented by the polar phase of ice formed at low temperature or by the dead layer on the film surface.





---

## **POSTER PRESENTATIONS**

## Voltage imaging of ferroelectric domain structures created by electron beam technique in lithium niobate crystals

L.S. Kokhanchik<sup>1</sup>, R.V. Gainutdinov<sup>2</sup>

<sup>1</sup>*Institute of Microelectronics Technology and High Purity Materials RAS, 142432 Chernogolovka, Russia*  
 mlk@iptm.ru

<sup>2</sup>*Shubnikov Institute of Crystallography RAS, 119333 Moscow, Russia*

Lithium niobate crystals (LN) with periodic domain structures (PS) are of great interest to the realization of nonlinear frequency conversion of optical radiation. The most common method of PS creation in LN is a field-switching of spontaneous polarization ( $P_s$ ) under the electric field applied to structured electrodes. To solve some problems, especially in integrated optics, direct electron beam (e-beam) recording of PS in LN is developed. The use of simple and nondestructive methods of observation and diagnostic of PS is an urgent task of the domain engineering.

Here, we report about express control and investigation of PS in LN crystals using the low voltage scanning electron microscopy (SEM) [1, 2]. Usefulness of low voltage SEM to imaging of domain structures created by e-beam is discussed as far as we know for the first time.

In Figure 1 there are several voltage images of PS obtained by an e-beam technique in different LN crystals. The voltage images were mapped with other PS images: after chemical etching of the samples and using piezoresponse force microscopy (PFM) technique. The nature of the observed voltage contrast in the domain area is discussed; it is concluded on the usefulness of the method to the domain imaging after their e-beam recording. Method enables to quickly control the quality of the PS and explore the features of the domain structures in the used crystals.

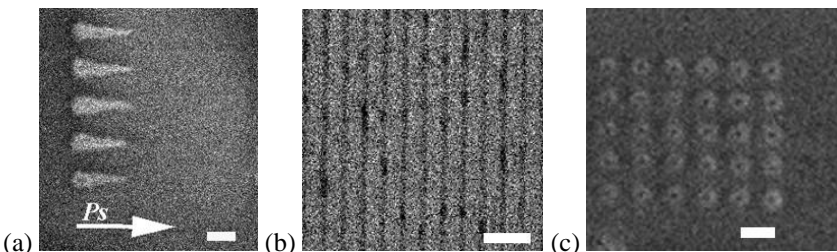


Figure 1. Voltage images of LN domain structures obtained by e-beam irradiation: a) single domains on Y-cut; b) single domains on Z-cut; c) PS on Z-cut. The white label bar corresponds to 20  $\mu\text{m}$ .

1. R. Le Bihan, *Ferroelectrics*, **97**, 19 (1989).
2. A.A. Sogr, *Ferroelectrics*, **97**, 47 (1989).

## Shape of isolated domains created by focused ion beam in lithium niobate and lithium tantalate single crystals

E.O. Vlasov<sup>1</sup>, D.S. Chezganov<sup>1,2</sup>, L.V. Gimadeeva<sup>1</sup>, D.O. Alikin<sup>1</sup>,  
A.R. Akhmatkhanov<sup>1,2</sup>, M.A. Chuvakova<sup>1</sup>, V.Ya. Shur<sup>1,2</sup>

<sup>1</sup>*Institute of Natural Sciences, Ural Federal University, 620000, Ekaterinburg, Russia  
evg.vlasov@labfer.usu.ru*

<sup>2</sup>*Labfer Ltd., 620014, Ekaterinburg, Russia*

The shapes of isolated domains created by focused ion beam irradiation have been studied in congruent (CLN), MgO-doped (MgOLN), stoichiometric lithium niobate (SLN) and congruent lithium tantalate (CLT) single crystals.

The irradiation of  $Z^+$ -polar surfaces covered by resist layer was performed by workstation Auriga Crossbeam (Carl Zeiss) driven by ion-beam lithography system Elphy Multibeam (Raith) using dot exposure mode with different charge dose. The domains were visualized after selective chemical etching by optical, piezoresponse force and confocal Raman microscopies (CRM). The irradiation of all crystals led to formation of through isolated domains. The difference of domain shape at the opposite polar surfaces and its evolution with dose increase were revealed.

In MgOLN the initially triangle domain shape at low dose on the  $Z^+$  polar surface of changed to hexagonal one and then to circular at high doses.

In CLN the domain shape changed with dose increase from rounded hexagon to three-ray star at  $Z^+$ -polar surface and from triangular to dendrite at non-irradiated  $Z^-$  surface while the hexagonal shape conserved in the bulk.

In SLN the circular isolated domains shape with hexagonal aureole appeared at  $Z^+$  surface. This aureole width enlarged with dose. The hexagonal domain shape in the bulk was shown by CRM. The circle shape at the surface can be attributed to backswitching in a 500-nm-thick surface layer.

In CLT the isolated domains at  $Z^+$  surface were circular-shaped with complicated multiple small circles inside. However, the domain shape at the  $Z^-$  surface conserved the triangle shape.

The observed domain shapes were attributed to change of screening effectiveness caused by reduction of the resist layer thickness by ion beam etching.

The equipment of the Ural Center for Shared Use “Modern nanotechnology” UrFU was used. The research was made possible in part by RFBR (15-32-21102-mol\_a\_ved), by Government of the Russian Federation (Act 211, Agreement 02.A03.21.0006) and by President of Russian Federation grant for young scientists (Contract 14.Y30.16.8441-MK).

## Morphology of charged domain walls in lithium niobate with inhomogeneous bulk conductivity

V.I. Pryakhina, D.O. Alikin, I.S. Palitsin, A.S. Abramov, S.A. Negashev, V.Ya. Shur

*Institute of Natural Sciences, Ural Federal University, 620000, Ekaterinburg, Russia  
viktoria.pryakhina@urfu.ru*

Charged domain walls (CDWs) with metallic-like conductivity look quite attractive for applications in modern nanoelectronics. These walls can be used as mobile interfaces for future electronic circuits due to possibility to locate and shift domain walls by external electric field. The possible usability of the materials with CDWs is strongly connected with methods which allow to control their periodicity [1].

In this contribution, we demonstrate the creation of self-organized stable CDWs by polarization reversal in lithium niobate  $\text{LiNbO}_3$  single crystals with spatially inhomogeneous bulk conductivity. The annealing in vacuum in the temperature range 650-850°C allowed us to increase the electrical conductivity at the surface and in the bulk up to  $10^{-11}$ – $10^{-9}$  S. Spatially inhomogeneous distribution of the electric field has been in situ measured by interferometric method [2].

We showed that head-to-head and tail-to-tail CDWs possess qualitatively different morphology and growth mechanisms [2]. The polarization reversal in uniform applied electric field in single domain sample started from Z- polar surface represented the propagation of the dense net of nanodomain rays which led to formation of the head-to-head CDWs. Tail-to-tail CDWs appeared in the crystal bulk. It was shown that the threshold field for formation of head-to-head domain walls ( $E_{\text{th}} = 12$  kV/mm) is essentially lower than for the tail-to-tail ones ( $E_{\text{th}} = 18$  kV/mm). The CDWs morphology depends on the applied electric field and wall growth velocity. The CDWs have been inspected in details by piezoelectric force microscopy at the surfaces and by confocal Raman microscopy in the bulk. The dependence of CDWs geometrical parameters on the treatment conditions has been extracted.

The evolution of CDWs has been discussed in terms of the kinetic approach [3]. The obtained knowledge can be used for development of the domain wall engineering in the crystals of  $\text{LiNbO}_3$  family.

The equipment of the Ural Center for Shared Use “Modern Nanotechnology” Ural Federal University has been used. The research was made possible in part by Government of the Russian Federation (Act 211, Agreement 02.A03.21.0006).

1. P.S. Bednyakov et al., *Scientific Reports* **5**, 15819 (2015)
2. V.I. Pryakhina et al., *Ferroelectrics* **476**, 109-116 (2015)
3. V.Ya. Shur, *J. Material Science* **41**, 199-210 (2006)

## Local polarization reversal in injected charge by the grounded tip on the non-polar cuts of lithium niobate crystal

A.P. Turygin, D.O. Alikin, Ju.M. Alikin, V.Ya. Shur

*Institute of Natural Sciences, Ural Federal University, 620000, Ekaterinburg, Russia  
anton.turygin@urfu.ru*

The intensive study of the domain structure evolution in single crystals of lithium niobate (LN) is stimulated by needs of domain engineering applied for laser frequency conversion based on LN with periodical micro- and nano-domain structures and development of the storage devices with ultra-high density [1,2]. The investigation of the domain evolution under application of the local electric field produced by conductive tip of the scanning probe microscope on polar surface is one of the most informative [2]. Moreover the domain growth on non-polar surfaces of LN investigated recently by this method allowed to reveal the detail information about forward growth of isolated domains [3,4].

In this work we provide experimental research of the domain growth during polarization reversal on non-polar (X and Y) cuts of congruent LN. The field and pulse duration dependences of the domain sizes have been measured.

The new effect of self-assembled formation of the domain chains during scanning by grounded SPM tip has been discovered. The effect had been attributed to the backswitching under the action of electric field produced by the injected charges [5] and charged domain walls. We demonstrated non-uniformity and unipolarity of the charge injection in LN and showed their influence on geometrical parameters of backswitched domain structure. It was shown by Kelvin probe microscopy that during application of the switching pulse the injected charge propagated over the distance about tens of microns from the tip. The measured relaxation time of the injected charge is about several hours.

The equipment of the Ural Center for Shared Use “Modern Nanotechnology” UrFU was used. The research was made possible in part by the Ministry of Education and Science of RF (UID RFMEFI59414X0011) and by Russian Science Foundation (Grant 14-12-00826).

1. V.Ya. Shur, *J. Mat. Sci.* **41**, 199 (2006).
2. V.Ya. Shur, A.R. Akhmatkhanov, I.S. Baturin, *Appl. Phys. Rev.* **2**, 040604 (2015).
3. D.O. Alikin, A.V. Ievlev, A. P. Turygin, A.I. Lobov, S.V. Kalinin, V.Ya. Shur, *Appl. Phys Lett.*, **106**, 182902 (2015).
4. A.V. Ievlev, D.O. Alikin, A.N. Morozovska, O.V. Varenyk, E.A. Eliseev, A.L. Kholkin, V.Ya. Shur, S.V. Kalinin, *ACS nano*, **9**, 769 (2014).
5. S.O. Fregatov, A.B. Sherman, *Phys. Solid State*, **41**, 457 (1999).

## Investigation of electric conductivity in single crystals of lithium niobate and lithium tantalate family at elevated temperatures

A.A. Esin, A.G. Neustroev, A.R. Akhmatkhanov, V.Ya. Shur

*Institute of Natural Sciences, Ural Federal University, 620000, Ekaterinburg, Russia  
alexander.esin@urfu.ru*

The bulk intrinsic electric conductivity is considered to be one of the main parameters governing the screening of residual depolarization field and thus the domain kinetics in the crystals of lithium niobate (LN) and lithium tantalate (LT) family [1]. Despite this fact, there is a lack of reliable experimental data at elevated temperatures up to 220°C.

We present the direct electrometric measurements of the electric conductivity in single crystals of LN and LT family in the temperature range 100 – 220°C [2]. The recirculating silicone oil thermostat was used to maintain sample temperature precisely. The staircase-like voltage pulse with amplitude 200 V was applied to the sample and the current response was measured by Keithley 6430 electrometer and analyzed. The original technique of compensation of pyroelectric current was used.

Experimentally measured temperature dependences of the bulk electrical conductivity along the polar direction followed the Arrhenius law with activation energy ranging from 1.0 to 1.2 eV (Fig. 1). It was shown that the bulk intrinsic conductivity became the main mechanism of screening at the temperatures above 160°C.

The weak anisotropy of the conductivity has been revealed in MgO doped LN single crystals.

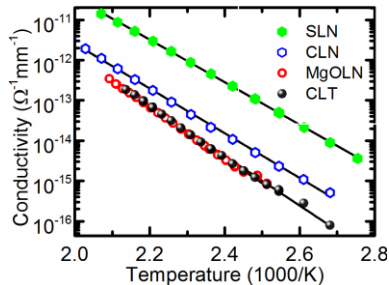


Figure 1. Temperature dependence of the bulk conductivity along the polar directions.

The equipment of the Ural Center for Shared Use “Modern Nanotechnology”, Ural Federal University was used.

1. V.Ya. Shur, E.L. Rummyantsev, *Ferroelectrics*, **191**, 319 (1997).
2. A.A. Esin, A.R. Akhmatkhanov, V.Ya. Shur, *Ferroelectrics*, **496**, 102 (2016).

## Field distribution in the vicinity of the perturbations at the moving plane domain wall

A.R. Udalov<sup>1</sup>, V.Ya. Shur<sup>1</sup>, A.L. Korzhenevskii<sup>2</sup>

<sup>1</sup>*Laboratory of Ferroelectricity, Institute of Natural Sciences, Ural Federal University, 620000, Ekaterinburg, Russia*  
artur.udalov@urfu.ru

<sup>2</sup>*Institute for Problems of Mechanical Engineering RAS, 199178, St. Petersburg, Russia*

The domain kinetics during polarization reversal, being an attribute of ferroelectrics, has been studied intensively. The lack of the domain wall shape stability during sideways domain wall motion is very important problem for creation of the precise tailored domain structures [1,2].

It is known that the local domain wall motion velocity in ferroelectric is defined by the spatial distribution of the electric field. We considered the three-layered ferroelectric capacitor representing ferroelectric plate oriented perpendicular to polar axis (F) between two dielectric (D) layers covered by electrodes. 2D boundary problem with arbitrary boundary conditions was solved to determine spatial distribution of electric field.

The surface charge density distribution was calculated for uniform motion of  $180^\circ$  plane domain wall with triangular perturbation. The retardation of the bulk screening of depolarization field produced by bound charges at the boundary of F and D layers was taken into account using 2D isotropic relaxation equation on charge density.

2D Fourier-image of the polar component of electric field in F layer was obtained analytically with subsequent transition to expression of spatial components of the electric field.

It was demonstrated that the lower value of the electric field at the perturbation leads to its growth. The obtained results allow to explain the lack of domain wall shape stability revealed experimentally in lithium niobate for highly non-equilibrium switching conditions.

The research was made possible in part by Government of the Russian Federation (Act 211, Agreement 02.A03.21.0006).

1. V.Ya. Shur, E.L. Rummyantsev, *Ferroelectrics* **151**, 171 (1994).
2. V.Ya. Shur, *J. Mater. Sci.* **41**, 199 (2006).

## Self-organized domain kinetics in lithium niobate single crystals at elevated temperatures

M.A. Chuvakova, A.A. Esin, A.R. Akhmatkhanov, V.Ya. Shur

*Institute of Natural Sciences, Ural Federal University, 620000, Ekaterinburg, Russia*  
*M.A.Chuvakova@urfu.ru*

The domain kinetics has been studied in single crystals of congruent lithium niobate (CLN) during polarization reversal at elevated temperature with artificial dielectric layer. The domain structure evolution was analyzed in details using *in situ* optical visualization. The field dependence of the domain shape was studied.

The polarization reversal was carried at 250°C out in Z-cut optical-grade polished samples of CLN (Crystal Tech., USA) with polar surfaces covered by metal electrodes and Z+ polar surface covered by artificial dielectric layer. Single rectangular field pulse with amplitude from 5 to 11 kV/mm was applied for polarization reversal.

The unusual scenario of the domain structure evolution representing self-organized domain growth was revealed by *in situ* visualization. Polarization reversal in external electric field with different amplitudes allowed to obtain the field dependence of the domains shape. The geometrical parameters of obtained static domain structures were measured using high resolution scanning electron microscopy after shallow selective chemical etching. The main stages of the domain structure evolution were separated. The visualization of domain structure in the bulk using Raman confocal microscopy allowed to measure the averaged depth of self-organized domain structures.

Comparison of the obtained results with domain kinetics and shape of isolated domains during switching of congruent lithium tantalate and stoichiometric lithium niobate crystals at elevated temperatures 250-275°C will be presented [1,2].

The equipment of the Ural Center for Shared Use “Modern Nanotechnology” UrFU was used. The research was made possible by Russian Science Foundation (grant 14-12-00826).

1. V.Ya. Shur, D.S. Chezganov, M.S. Nebogatikov, I.S. Baturin, M.M. Neradovskiy, *J. Appl.Phys.* **112**, 10 (2012).
2. V.Ya. Shur, A.R. Akhmatkhanov, D.S. Chezganov, A.I. Lobov, I.S. Baturin, M.M. Smirnov, *Appl. Phys. Lett.* **103**, 242903 (2013).



## Highly efficient nonlinear waveguides in LiNbO<sub>3</sub> fabricated by a combination of Soft Proton Exchange and electron beam periodic domains writing

M.M. Neradovskiy<sup>1,2</sup>, E.A. Neradovskaya<sup>1</sup>, D.S. Chezganov<sup>1,3</sup>, L.V. Gimadeeva<sup>1</sup>, E.O. Vlasov<sup>1</sup>, M.A. Chuvakova<sup>1</sup>, P. Baldi<sup>2</sup>, H. Tronche<sup>2</sup>, F. Doutre<sup>2</sup>, V.Ya. Shur<sup>1,3</sup>, M.P. De Micheli<sup>2</sup>

<sup>1</sup>*Institute of Natural Sciences, Ural Federal University, Ekaterinburg 620000, Russia  
maxim.neradovskiy@gmail.com*

<sup>2</sup>*Laboratoire de Physique de la Matière Condensée, University of Nice-Sophia Antipolis, Nice 06100, France*

<sup>3</sup>*Labfer Ltd., Ekaterinburg 620014, Russia*

The production of highly efficient nonlinear waveguides as a result of combination of Soft Proton Exchange and electron beam periodic domains writing has been studied in LiNbO<sub>3</sub> (LN).

The investigated samples were prepared on a Z-cut 0.5-mm-thick single-domain plates of congruent LN (CLN). The SPE process [1] was carried out in benzoic acid bath diluted by 3.1% lithium benzoate (BL) at 300°C for 72 hours, using a SiO<sub>2</sub> mask on Z<sup>-</sup>-polar surfaces to fabricate the channel waveguides with different width. The irradiation was performed by scanning electron microscope (Auriga Crossbeam, Carl Zeiss) attached with electron-beam lithography system (Elphy Multibeam, Raith).

The dependence of geometric parameters of established domain structures (transverse size, shape, depth) on the irradiation conditions (accelerating voltage, current, charge dose, period, the initial size of the design elements) were measured. The obtained results have been used to optimize the periodical poling procedure in channel waveguides, which allowed obtaining a nonlinear conversion efficiency of up to 48%/(Wcm<sup>2</sup>) in SHG experiments. Therefore, it is possible to get state-of-the-art SHG efficiency by periodic domain patterning after the waveguides fabrication. In this work we demonstrated this way of processing is particularly interesting as it allows adjusting the poling period to the waveguides characteristics when the device has to operate at a very precise wavelength.

The equipment of the Ural Center for Shared Use “Modern nanotechnology” UrFU was used. The research was made possible in part by RFBR (15-32-21102-mol\_a\_ved), by Government of the Russian Federation (Act 211, Agreement 02.A03.21.0006) with financial support of young scientists in terms of UrFU development program and for the joint supervision of doctorate thesis by government of France.

1. P. De Micheli, *Ferroelectrics*, **340**, 49 (2006).

## Effect of the processing conditions on vertical piezoresponse of PZT nanotubes prepared by electrophoretic method

D. Vasileva<sup>1</sup>, S. Vasilev<sup>1</sup>, M. Lanki<sup>2</sup>, A. Nourmohammadi<sup>2</sup>, V. Ya. Shur<sup>1</sup>,  
A.L. Kholkin<sup>1,3</sup>

<sup>1</sup>*Institute of Natural Sciences, Ural Federal University, 620026 Ekaterinburg, Russia  
kholkin@gmail.com*

<sup>2</sup>*Department of Nanotechnology Engineering, University of Isfahan, 81746-73441,  
Isfahan, Iran*

<sup>3</sup>*Physics Department & CICECO-Aveiro Institute of Materials, University of Aveiro,  
3810-193 Aveiro, Portugal*

Nanotubes of conducting materials such as carbon have recently received considerable attention. Microtubes of nonconducting BN and SiC have also been reported [1]. However, ferroelectric nanotubes made of oxide insulators, as reported in this work, have a variety of applications for pyroelectric detectors, piezoelectric inkjet printers, and terahertz emitters [2]. We report here fabrication of ferroelectric nanotubes made of lead zirconate titanate (PZT) by modified electrophoresis method. By using porous AAO templates it is also possible to produce regular arrays of discrete nanotubes.

Sol-gel electrophoresis technique was utilized to form the nanotubes on the pore walls. The alumina templates were prepared using various anodizing voltages and times to achieve different pore diameters and lengths. Phosphoric acid solution was employed as the anodizing electrolyte. Stabilized lead zirconate titanate sols were prepared using the corresponding precursors. Acetic acid was used as the modifier. The prepared sols were driven into the template channels under various electrophoretic voltages and times, and the effect of the electrophoresis parameters on the formation of nanotubes was investigated. The filled templates were dried at 100°C and sintered at 700°C. The investigations by scanning and transmission electron microscopy (SEM and TEM) demonstrated the tubular form of the lead zirconate titanate arrays. The SEM investigations also showed the nanotubes have been efficiently grown in the template pores. Further, vertical piezoelectric response was measured using Piezoresponse Force Microscopy. We confirmed the high piezoelectric properties with the longitudinal (axial) piezoelectric coefficient reaching 30 pm/V. The effect of the processing conditions on the measured response was also investigated and optimum conditions to maximize it were identified.

1. G. Mpourmpakis et al, *Nano Lett.* **6**, 1581 (2006).
2. J.F. Scott et al, *Nano Lett.* **8**, 4404 (2008).

## Determination of +Z and -Z surfaces of a lithium niobate crystal using the method of reflectance spectroscopy

V.D. Pararin, E. Panteley

*Samara State Aerospace University, 443086, Samara, Russia*  
 vpararin@mail.ru

The positive +Z and negative -Z crystal surfaces are usually determined using the piezoelectric, chemical and X-ray methods. The methods mentioned, however, are expensive, they involve contamination and mechanical loading of the substrate. Meanwhile, there are contactless optical methods that are of great interest and hold promise. Among the great variety of optical methods spectroscopy of images in the region of absorption is worth noting. Short-wavelength radiation of the ultra-violet band interacts actively with proper and impurity atoms of lithium niobate, defects of the surface layer.

A method of reflectance spectroscopy in the ultra-violet 190...250 nm range aimed at determining the sign of the polar surface is evaluated in the paper.

The reflection spectra of lithium niobate polar surfaces  $R_{+Z}$  and  $R_{-Z}$  were investigated by a Shimadzu UV-2450 spectrophotometer with peripheral equipment 206-14046. Congruent lithium niobate crystals of a Z-cut 0.55 mm thick were used as specimens. Prior to the investigation the crystals were cleared of organic and inorganic impurities.

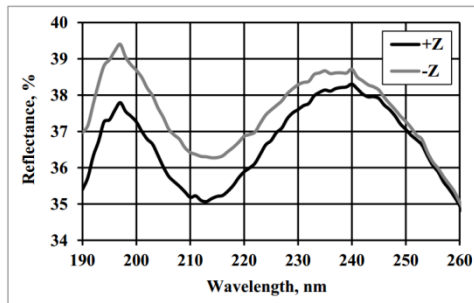


Figure 1. The reflection spectrum of the +Z and -Z surface

The investigation of crystal polar surfaces resulted in revealing the difference of reflection spectra, particularly noticeable in the range of 190...260 nm, persistent for all analyzed specimens. It follows from the data obtained that the reflection of the -Z surface exceeds that of the +Z surface by several per cent. This is sufficient to determine the required polar surface by simple photometric means. The method presented is distinguished by its simplicity and reliability in determining the sign of a polar surface. A stabilized radiating source with the wavelength below 260 nm is suitable for measurements. The method is efficient and does not impose any special requirements on the spectrum width and polarization of the radiating source.

## Isotropic and anisotropic diffraction of laser beam on periodically poled domain structures in lithium niobate

S.M. Shandarov<sup>1</sup>, A.E. Mandel<sup>1</sup>, A.V. Andrianova<sup>1</sup>, A.Yu. Kim<sup>1</sup>,  
G.V. Bolshanin<sup>1</sup>, S.V. Smirnov<sup>1</sup>, A.R. Akhmatkhanov<sup>2</sup>, V.Ya. Shur<sup>2</sup>

<sup>1</sup>*Tomsk State University of Control Systems and Radioelectronics, 634050, Tomsk, Russia*

<sup>2</sup>*Institute of Natural Sciences, Ural Federal University, 620000 Ekaterinburg, Russia*

Using relationships presented in [1], perturbations of the dielectric permittivity of two types are analyzed for PPLN created by alternating 180-degree domain walls parallel to the  $Z$  and  $Y$  crystallographic axes ( $Y$ -walls). For the first perturbation type, polarization along the  $x$  coordinate changes with the period  $\Lambda$  from  $-P_S$  to  $P_S$ , and for the second polarization type, it changes with the same period, but from  $P_S$  to  $-P_S$ . In this case it is assumed that the distances between the neighboring walls can differ from  $\Lambda/2$  by a certain value  $\pm\Delta x$ . It has been found that for the Fourier expansion of perturbations of the diagonal dielectric permittivity tensor components  $\Delta\varepsilon_{ii}(x)$  caused by both spontaneous quadratic electrooptical effect and elasto-optic contribution, the odd components with wave numbers  $K = 2\pi m/\Lambda$  ( $m = \pm 1, \pm 3, \pm 5, \dots$ ) for the domain structure with  $\Delta x = 0$  vanish. The pattern of the isotropic light diffraction on such ideal structure must contain the diffraction maxima only of even orders.

The Fourier expansion of nondiagonal component perturbations  $\Delta\varepsilon_{12}(x) = \Delta\varepsilon_{21}(x)$ , which can arise near the domain boundaries due to flexoelectric and elasto-optic effects [1], is characterized by all possible spatial harmonics. As a consequence, the pattern of anisotropic diffraction on the domain structure for the wave incident at a small angle to the  $Z$  axis in the  $XZ$  crystal plane must contain diffraction maxima of both even and odd orders.

The polarization structure of the 1st and 2nd order diffraction maxima is experimentally investigated for diffraction of laser radiation with a wavelength of 655 nm on a domain structure with spatial period of 9.43  $\mu\text{m}$  (Labfer Ltd) in a  $\text{LiNbO}_3: 5\% \text{MgO}$  single crystal sample by the repolarization method in an external spatially-periodic electric field. Qualitative agreement is obtained with the examined model for  $\Delta x \neq 0$  and  $\Delta\varepsilon_{12}(x) = \Delta\varepsilon_{21}(x) \neq 0$ .

1. S.M. Shandarov, A.E. Mandel, S.V. Smirnov, T.M. Akylbaev, A.R. Akhmatkhanov, V.Ya. Shur, *Ferroelectrics* **496**, 1 (2016).

**On expansion coefficients of the free energy in polarization revealed by harmonic analysis method in crystals of  $A_2BX_4$  group**

V.V. Gorbatenko<sup>1</sup>, B.N. Prasolov<sup>2</sup>, S.A. Gorbatenko<sup>1</sup>

<sup>1</sup>*Voronezh State Technical University, 394026 Voronezh, Russia*

<sup>2</sup>*Scientific and production firm "Sensor", 394061 Voronezh, Russia*

The decomposition coefficients values  $W_c$  by  $P_c$  series according to the theory of Landau-Devonshire on the basis of coordinates of dependence of the crystal  $Rb_2ZnCl_4$  free energy  $W_c$  from polarization  $P_c$  that were experimentally obtained using the harmonic analysis method are determined in the article. This research allowed to measure the members number in the decomposition  $W_c$  by  $P_c$  that are required to obtain the quantitative evaluations of the measurements results.

## Structural phase transformations of proton-exchanged layers of lithium niobate during annealing

S.S. Mushinsky<sup>1</sup>, V.I. Kichigin<sup>1</sup>, I.V. Petukhov<sup>1</sup>, M.A. Permyakova<sup>1</sup>,  
D.I. Shevtsov<sup>1</sup>

<sup>1</sup>Perm Scientific Instrument-Making Company  
sergey.mushinsky@gmail.com

<sup>2</sup>Perm State National Research University

Proton-exchanged waveguides in lithium niobate crystal are usually manufactured by means of treatment in the molten benzoic acid followed by annealing. As a result, stable  $\alpha$ -phase of solid solution  $H_xLi_{1-x}NbO_3$  is formed. Dynamics of structural phase transitions during annealing was investigated using optical microscopy.

Planar waveguides were formed in X-cut congruent lithium niobate (Crystal Technology). Proton exchange was conducted in the molten benzoic acid at 175°C during 2 hours. Sample annealing was conducted step by step (step was set to 1 hour) at 330°C, 350°C, 370°C. Total duration of annealing was 3 hours at 370°C, 5 hours at 350°C, 12 hours at 330°C.

Mode spectroscopy ( $\lambda = 0.633 \mu\text{m}$ ) was used to determine profile of extraordinary refractive index  $\Delta n_e(x)$ .  $\Delta n_e(x)$  was calculated using IWKB method. Dark field microscopy and polarized light microscopy (Olympus MX61) was used to visualize structure of proton-exchanged layers.

$\kappa$ -phase forms during annealing of planar waveguides. At first,  $\kappa$ -phase is precipitated in the form of single rounded particles. As annealing goes on, the number of  $\kappa$ -phase precipitations increases and they also get larger (Fig. 1a). Annealing during 6 hours and longer at 330 °C leads to the formation of  $\alpha$ -phase while  $\kappa$ -phase precipitations acquire specific shape and orientation aligned along certain crystallographic directions (Fig. 1b).

Further increase in annealing duration leads to decrease of  $\kappa$ -phase fraction in proton-exchanged layers and its gradual disappearance which is in a good agreement with mode spectroscopy data.

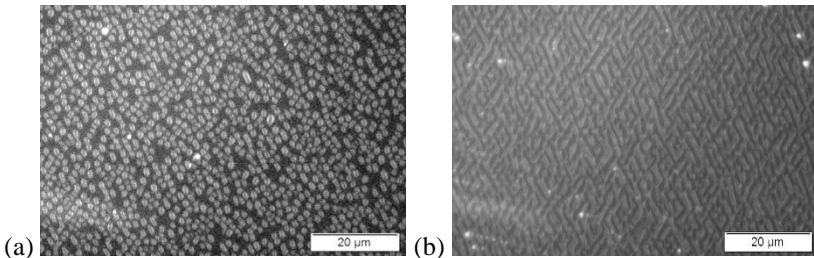


Figure 1. Structure of proton-exchanged layers in X-cut lithium niobate after (a) 3 hours and (b) 7 hours of annealing at 330°C.

## Micro-Raman study of phase composition and electro-optical properties of channel proton-exchanged LiNbO<sub>3</sub> waveguides

S.M. Kostritskii<sup>1</sup>, Yu.N. Korkishko<sup>1</sup>, V.A. Fedorov<sup>1</sup>, O.G. Sevostyanov<sup>2</sup>,  
I.M. Chirkova<sup>2</sup>

<sup>1</sup>*RPC Optolink Ltd, Zelenograd, 124489, Moscow, Russia*  
*skostritskii@optolink.ru, www.optolink.ru*

<sup>2</sup>*Kemerovo State University, 650043, Kemerovo, Russia*

All the above indicates the need to develop a nondestructive method for determining the phase composition and estimating the electro-optic coefficients in channel proton-exchanged waveguides. In order to solve this problem, we use micro-Raman spectroscopy, since Raman spectra of different phases are quite different from each other [1] and the use of a confocal microscope in a micro-Raman spectrometer provides high spatial resolution ( $\sim 1 \mu\text{m}$ ), enough for a detailed study of the cross section of channel waveguides and integrated optics systems based on them. For calibration of the micro-Raman data, we used samples of planar waveguides whose phase composition and electro-optic properties were determined by the IR and UV spectroscopy methods. This lets us establish clear correlations between the parameters of the micro-Raman spectra and the values of the electro-optic coefficients  $r_{13}$  and  $r_{33}$ , which we used to optimize the conditions for preparation of electro-optic phase modulators based on proton-exchanged channel waveguides in LiNbO<sub>3</sub> crystals. Micro-Raman spectroscopy allows for fast and easy analysis of the electro-optic properties of proton-exchanged waveguides, since there is no need for a number of complicated processing operations (polishing the ends, optical coupling and deposition of electrodes) with the integrated optics elements, which is required for optimization of the technology when using direct measurements of the electro-optic efficiency of waveguides.

All the previous studies showed a significant decrease in the electro-optic coefficients after proton exchange [1-3]. After high-temperature annealing, the effective values of the electro-optic coefficients are partially restored [1,2] and reach  $\sim 2/3$  of the values for the original LiNbO<sub>3</sub> crystal. Therefore the micro-Raman method is used to study annealed proton-exchanged channel waveguides which contain  $\alpha^*$ ,  $\alpha^{**}$ ,  $\kappa_1$ , and  $\kappa_2$  phases, depending on the processing conditions for their preparation. Thus, the results obtained allow us to optimize the process of preparation of electro-optic phase modulators based on proton-exchanged channel waveguides in LiNbO<sub>3</sub> crystals.

1. S.M. Kostritskii *et al*, *J. Appl. Spectr.* **82**, 234 (2015).
2. M. Rottschalk *et al*, *Opt. Commun.* **9**, 19 (1988).
3. H.G. Muller *et al*, *J. Appl. Phys.* **110**, 033539 (2011).

## Complex research of concentration structure rearrangement in $\text{LiNbO}_3\text{:Zn}$ (0.04÷5.84 mol. %) single crystals

N.V. Sidorov<sup>1</sup>, M.N. Palatnikov<sup>1</sup>, N.A. Teplyakova<sup>1</sup>, A.A. Yanichev<sup>1</sup>,  
R.A. Titov<sup>1</sup>, O.V. Makarova<sup>1</sup>, L.A. Aleschina<sup>2</sup>, A.V. Kadetova<sup>2</sup>

<sup>1</sup>*I.V. Tananaev Institute of Chemistry and Technology of Rare Elements and Mineral Raw Materials of the Russian Academy of Sciences Kola Science Center, Apatity, Russia*  
*sidorov@chemy.kolasc.net.ru*

<sup>2</sup>*Petrozavodsk State University, Petrozavodsk, Russia*

The change of incorporation mechanism for  $\text{Zn}^{2+}$  cations in  $\text{LiNbO}_3$  crystal structure was detected. The number of fractures on the concentration graphs of bands widths (five) is higher than known in literature number of thresholds (two).

Changes in secondary structure, optical and structure homogeneity were searched in  $\text{LiNbO}_3\text{:Zn}$  (0.04÷5.84 mol.%) crystals by Raman spectra, photoinduced light scattering, laser conoscopy, electron spectroscopy and X-ray analysis. Doping of  $\text{LiNbO}_3$  crystals by  $\text{Zn}^{2+}$  cations decreases photorefractive effect and coercive field although it leads to high structure inhomogeneity. Due to the Raman spectra at  $[\text{ZnO}] \approx 0.05\div 0.94$  mol.% cation sublattice is most ordered. In this concentrations Raman spectra bands widths are narrower than in congruent crystal and close to stoichiometric crystal, where cation sublattice is the most ordered and oxygen octahedrons  $\text{NbO}_6$  are perfect. Data on Raman spectra are in good agreement with full profile X-ray analysis. At  $[\text{ZnO}] \approx 1 \div 2$  mol. % parameter *c* of the unit cell has a minimum and parameter *a* increases. The minimum of the volume and periods of the unit cell is in crystals  $\text{LiNbO}_3$  (4.76 mol.% ZnO). During rise of  $[\text{ZnO}]$  these values increase. In all studied samples  $\text{Zn}^{2+}$  were occupying Li site. Shift of the optical transmission edge of crystal  $\text{LiNbO}_3$  (4.5 mol.% ZnO) to the shorter wavelengths also reveal ordering of the structure.

The change of incorporation mechanism of  $\text{Zn}^{2+}$  to  $\text{LiNbO}_3$  structure is detected in Raman spectra due to anisotropic expansion of the oxygen octahedra along the polar axis with the rise in  $\text{Zn}^{2+}$  concentration. The number of fractures on the dependence of bands widths (for forbidden  $630 \text{ cm}^{-1}$   $A_1(\text{TO})$  band were observed 5) is higher than known number of thresholds (2).

At  $[\text{ZnO}]$ : 0.03; 0.94; 1.12 and 1.59 mol.% photorefraction increased and at concentrations 0.05 and 4.5÷5.84 mol.% decreased in comparison with the congruent crystal. A decrease in photorefraction in  $\text{LiNbO}_3$  (4.5÷5.84 mol.% ZnO) might be caused by displacement of structural defects  $\text{Nb}_{\text{Li}}$  (the deepest electron traps) by  $\text{Zn}^{2+}$  cations. In crystal  $\text{LiNbO}_3$  (0.05 mol.% ZnO) structure units are the most ordered due to rise of shallow electron traps number (trapping levels). The probability of radiative recombination of photoexcited carriers without trapping by deep traps rises.



## Comparative Raman studies of $\text{Pb}(\text{Fe}_{1/2}\text{Nb}_{1/2})\text{O}_3$ single crystal, ceramics and epitaxial nanofilm

Yu.I. Yuzyuk<sup>1</sup>, I.P. Raevski<sup>1</sup>, S.I. Raevskaya<sup>1</sup>, W. Peng<sup>2,3</sup>, N. Lemée<sup>2</sup>, M.G. Karkut<sup>2</sup>, M.El. Marssi<sup>2</sup>, H. Chen<sup>4</sup>

<sup>1</sup>Research Institute of Physics and Faculty of Physics, Southern Federal University, 344090, Rostov-on-Don, Russia  
igorraevsky@gmail.com

<sup>2</sup>Laboratoire de Physique de la Matière Condensée, Université de Picardie Jules Verne, Amiens 80039, France

<sup>3</sup>State Key Laboratory of Functional Materials for Informatics, Shanghai Institute of Microsystem and Information Technology, Chinese Academy of Sciences, Shanghai 200050, China

<sup>4</sup>Institute of Applied Physics and Materials Engineering, Faculty of Science and Technology, University of Macau, Macau, China

Recently it was reported that in the epitaxial nanofilm of  $\text{Pb}(\text{Fe}_{1/2}\text{Nb}_{1/2})\text{O}_3$  (PFN) on the  $\text{SrTiO}_3$  substrate magnetic phase transition temperature is about 50 K higher than that in the bulk samples [1]. We carried out comparative Raman studies of the  $\text{Pb}(\text{Fe}_{1/2}\text{Nb}_{1/2})\text{O}_3$  single crystal, ceramics and 90-nm-thick  $\text{Pb}(\text{Fe}_{1/2}\text{Nb}_{1/2})\text{O}_3$  epitaxial film deposited by pulsed laser deposition technique on  $\text{SrRuO}_3$ -buffered (001)  $\text{SrTiO}_3$  substrate. It was found out that the bands at  $\approx 250 \text{ cm}^{-1}$  and  $\approx 700 \text{ cm}^{-1}$  in the Raman spectrum of the film, corresponding to Fe-O vibrational modes, are shifted by about  $20 \text{ cm}^{-1}$  to higher frequencies as compared to the bulk samples due to strengthening of the Fe-O bonds in nanoscale regions where Fe ions are expected to segregate into chemical clusters [2]. The results obtained are in line with the predictions of the recent first-principles calculations [3] that compressive misfit strain stimulates the disorder in the Fe and Nb distribution on the equivalent lattice sites, leading to an increase of magnetic phase transition temperature. Such disordering causes the changes in the Fe-sublattice of PFN seen in the Raman spectrum. The results obtained show that the so-called strain engineering can be successfully used to modify not only ferroelectric and related properties but also magnetic characteristics of multiferroic thin films and superstructures.

This work was partially supported by Ministry of Education and Science of the Russian Federation (research project 2132).

1. W. Peng, N. Lemee, M. Karkut, B. Dkhil, V. Shvartsman, P. Borisov, W. Kleemann, J. Holc, M. Kosec, R. Blinc, *Appl. Phys. Lett.* **94**, 012509 (2009).
2. I.P. Raevski, S.P. Kubrin, S.I. Raevskaya, D.A. Sarychev, S.A. Prosandeev, and M.A. Malitskaya, *Phys.Rev.B.* **85**, 224412 (2012).
3. S.A. Prosandeev, I.P. Raevski, S.I. Raevskaya, H. Chen, *Phys. Rev. B.* **92**, 220419(R) (2015).

## The effect of quenching on semiconductive properties and magnetic phase transition temperature of multiferroic $\text{Pb}(\text{Fe}_{1/2}\text{Nb}_{1/2})\text{O}_3$ ceramics

S.I. Raevskaya<sup>1</sup>, S.P. Kubrin<sup>1</sup>, I.P. Raevski<sup>1</sup>, C.-C. Chou<sup>2</sup>, H. Chen<sup>3</sup>, V.V. Titov<sup>1</sup>, M.A. Malitskaya<sup>1</sup>, D.A. Sarychev<sup>1</sup>, I.N. Zakharchenko<sup>1</sup>

<sup>1</sup>Research Institute of Physics and Faculty of Physics, Southern Federal University, 344090, Rostov-on-Don, Russia  
sveta.raevskaya@mail.ru

<sup>2</sup>National Taiwan University of Science and Technology, 106, Taipei, Taiwan, China.

<sup>3</sup>Institute of Applied Physics and Materials Engineering, Faculty of Science and Technology, University of Macau, 999078, Macau, China

Lead iron niobate  $\text{PbFe}_{0.5}\text{Nb}_{0.5}\text{O}_3$  (PFN)-based materials are among the promising multiferroics as they exhibit room-temperature magnetoelectric response [1]. In PFN the value of magnetic phase transition temperature  $T_M$  should depend dramatically on the degree of ordering of  $\text{Fe}^{3+}$  and  $\text{Nb}^{5+}$  cations, as such ordering lowers the number of the Fe-O-Fe links in the lattice. For the fully ordered PFN the estimates give  $T_M = 0$  K while for completely disordered case  $T_M \approx 300$  K. The typical  $T_M$  value observed most frequently for PFN is  $\approx 150$  K that is approximately halfway between calculated values for the fully ordered and completely disordered states. This fact as well as a large scatter of  $T_M$  values reported for PFN (from  $\approx 100$  K up to  $\approx 200$  K) are usually interpreted as an evidence of a partial ordering of  $\text{Fe}^{3+}$  and  $\text{Nb}^{5+}$  cations. The absence of superstructural reflections on XRD patterns of PFN is believed to be due to a local mesoscopic character of  $\text{Fe}^{3+}$  and  $\text{Nb}^{5+}$  ordering. Small dimensions of the ordered regions are due to the fact that the temperature of compositional order-disorder phase transition in PFN is rather low ( $\approx 900$  °C) and the ordering process is limited by a low diffusion rate. Thus  $T_M$  value of PFN ceramics is expected to depend on the cooling rate after sintering. We found out that  $T_M$  value of PFN ceramics sintered at  $1170$  °C and quenched to room temperature is about 20 K higher than that of ceramics from the same batch which was slowly cooled at a rate of 50 K/h. This result correlates with the assumption that the quenched sample is more disordered. The conductivity of the slowly cooled sample was several orders of magnitude lower than that of the quenched one. This difference is attributed to a higher concentration of oxygen vacancies in the quenched sample.

This work was partially supported by Ministry of Education and Science of the Russian Federation (research project 2132) and Research Committee of the University of Macau (Research & Development Grant for Chair Professor No RDG007/FST-CHD/2012).

1. V.V. Laguta, A.N. Morozovska, E.I. Eliseev, I.P. Raevski, S. I. Raevskaya, E.I. Sitalo, S.A. Prosandeev, L. Bellaiche. *J. Mater. Sci.* **51**, 5330 (2016).

**Size-dependent models of multiferroic materials with surface effects**A. V. Nasedkin

*I.I. Vorovich Institute of Mathematics, Mechanics and Computer Science, Southern Federal University, 344090, Rostov-on-Don, Russia  
nasedkin@math.sfedu.ru*

The simulation and experimental studies of magnetoelectrically active materials at various scale levels help to enhance the technologies of directed changing of the properties of these materials and provide a qualitative improvement of their characteristics.

Furthermore, it should be noted that the modeling of micro- and nanomaterials and devices has some specific features. It is known that a range of nanomaterials have abnormal mechanical properties that considerably differ from the properties of ordinary macrosized bodies. Thus, the experimentally observed fact is the increasing of the stiffness with reducing the sizes of nanoobjects. One of the factors that are responsible for this behavior of nanomaterials can be surface effects. As research of the recent years shows, for the bodies of submicro- and nanosizes the surface stresses play an important role and influence the deformation of the bodies in general. In connection to this, the actual problem can be an extension of this approach to the nanoscale elements of magnetoelectrically active composites and materials. Therefore, here it is logical to consider not only the mechanical surface effects, but also for the surface effects of electric and magnetic fields.

In present investigation the models of multiferroic materials account for their internal microstructure were developed in the framework of classic continuum approaches of solid mechanics and methods of composite mechanics. These models were used to construct new models of the micro- and nanosize bodies made of magnetoelectrically active materials that were additionally take into account the surface and micro local effects.

The finite element approximations were proposed for numerical solution of the formulated continuum problems, and the resolving finite element systems were obtained for static problems, eigenvalue problems, problems of steady oscillations and transient problems. For the majority of continuum models the finite element systems with symmetric quasidefinite matrices (matrices of saddle structure) were obtained. This allows us to use corresponding effective direct and iterative solvers for systems with symmetric quasidefinite matrices for both static and transient problems. It was also shown that here standard finite element software could be used with additional introduction of surface magnetoelectrically active films in the computation models of piezoelectric multiferroic materials with surface effects.

This work was supported by the Russian Science Foundation (grant number 15-19-10008).

**Electric polarization in bilayered ferromagnetic film**

Z.V. Gareeva<sup>1</sup>, F.A. Mazhitova<sup>2</sup>, R.A. Doroshenko<sup>1</sup>, T.T. Gareev<sup>3</sup>

<sup>1</sup>*Institute of Molecule and Crystal Physics, pr. Octyabtya 151, 450075, Ufa, Russia*

<sup>2</sup>*Bashkir State University, 450000 Ufa, Russia*

<sup>3</sup>*Moscow State University, 119991, Moscow, Russia*

Magnetoelectric phenomena become one of the most attractive fields of magnetism because of novel physics and promising potential for application. One of discussable items is magnetoelectric mechanisms with a particular focus on inhomogeneous magnetoelectricity leading to appearance of electric polarization of magnetic domain walls, improper polarization of multiferroics etc. [1, 2].

We explore electric polarization in bi – layered ferromagnetic film. Our findings show that magnetic inhomogeneity arising in a vicinity of interface in exchange coupled ferromagnetic film generates electric polarization that can be manipulated by external magnetic field. The magnetic inhomogeneity and the electric polarization can be localized close to interface, shifted from one layer to another or extended over entire structure dependent on the layer thicknesses, the relation between the constants of magnetic anisotropy. In ferromagnetic bi-layer with combined magnetic anisotropy one of the eight possible magnetic inhomogeneities differing by the direction of magnetization in the layers can be realized. Herewith four directions of electric polarization are possible. It indicates the principle possibility changing of the direction of electric polarization and correspondingly magnetization in the layers by an applied electric field in the films with negligible cubic magnetic anisotropy and coercitivity.

The work is supported by the Russian Foundation for Basic Research (grant №16-02-00336).

1. Y. Tokura, S. Seki, *Advanced materials* **22**, 1554 (2010).
2. A.K. Zvezdin, A.P. Pyatakov, *Phys. Usp.* **52**, 845 (2009).

**Magnetic properties of LiMPO<sub>4</sub> multiferroics**

N.V. Urusova<sup>1</sup>, S. Lee<sup>2</sup>, M.A. Semkin<sup>1</sup>, J.A. Barykina<sup>1,3</sup>, D.G. Kellerman<sup>3</sup>,  
A.N. Pirogov<sup>1,4</sup>

<sup>1</sup>*Institute of Natural Sciences of the Ural Federal University, 620083, Ekaterinburg, Russia*

*natali.urusova@mail.ru, urfu.ru*

<sup>2</sup>*Neutron Department, Korea Atomic Energy Research Institute, 305-600, Daejeon, Korea*

<sup>3</sup>*Institute of Solid State Chemistry of the Ural Branch of the RAS, 620137, Ekaterinburg, Russia*

<sup>4</sup>*Institute of Metal Physics of the Ural Branch of the RAS, 620990, Ekaterinburg, Russia*

The aims of this work are investigation of crystal and magnetic properties of LiMPO<sub>4</sub> (M = Ni, Co, Mn, Fe) multiferroics by neutron powder diffraction (NPD) and found correlation between magnetic structure and the type of 3d-transition ion. A large value of magnetoelectric effect are observed in materials of the lithium orthophosphates family [1]. These materials are characterized by the olivine-type crystallographic structure (space group *Pnma*) and an antiferromagnetic type of magnetic ordering at low temperatures.

Polycrystalline samples were synthesized by solid state reactions. Magnetic measurements were performed with SQUID magnetometer over temperature range from 2 K up to 300 K in zero field cold mode and at applied magnetic field 250 Oe. NPD patterns were recorded with the HRPD diffractometer, using the neutron wavelength of  $\lambda=1.834$  Å in HANARO reactor (Daejeon, Korea) and D2 diffractometer with  $\lambda = 1.805$  Å at the IVV-2M reactor (Zarechny, Russia) to study crystal and magnetic states. Calculation of NPD patterns were carried out using the “Fullprof” program.

Magnetic moment of 3d-transition ion is orientated along the *a*-crystallographic axis for LiMnPO<sub>4</sub>, along the *b*-axis for LiFePO<sub>4</sub> and along the *c*-axis for LiNi<sub>0.9</sub>Co<sub>0.1</sub>PO<sub>4</sub>. At low temperatures a magnetic moment value is about to equal 4.0  $\mu_B$  in LiMnPO<sub>4</sub>, LiFePO<sub>4</sub> samples and it is less twice for LiNi<sub>0.9</sub>Co<sub>0.1</sub>PO<sub>4</sub>. A magnetization decreases with an increasing of temperature and vanishes at Neel temperature  $T_N$ . It corresponds to second-order magnetic phase transition. The  $T_N$  values were determined from temperature dependences of the magnetic susceptibility. The  $T_N$  is 23 K for LiNi<sub>0.9</sub>Co<sub>0.1</sub>PO<sub>4</sub>, 37 K for LiMnPO<sub>4</sub> and 52 K for LiFePO<sub>4</sub>.

The research was supported by state program of FASE, subject “Potok”, No. 01201463334 and by the State contract (No. 1362) between Ural Federal University and Russian Federation Ministry of Education and Science.

1. X.-L. Pan, C.-Y. Xu, et al., *Electrochim. Acta* **87**, 303 (2013).

**Crystal structure of the  $(MFe_2O_4)_x+(BaTiO_3)_{1-x}$  multiferroic materials**

M.A. Semkin<sup>1</sup>, A.E. Susloparova<sup>1</sup>, T.S. Karpova<sup>2</sup>, A.P. Nosov<sup>2</sup>, A.N. Pirogov<sup>1,2</sup>

<sup>1</sup>*Ural Federal University, 620083, Ekaterinburg, Russia*  
*m.a.semkin@urfu.ru*

<sup>2</sup>*Institute of Metal Physics of the Ural Branch of the RAS, 620990, Ekaterinburg, Russia*

The aim our work is to study the crystal structure of the  $(MFe_2O_4)_x+(BaTiO_3)_{1-x}$  composite multiferroic materials depend on concentration, where  $x=(0.2-0.4)$  and  $M=(Ni \text{ or } Co)$ .

All samples were prepared by Pechini method. To synthesize the  $CoFe_2O_4$  (or  $NiFe_2O_4$ ) ferrite we used a thermal treatment of oxalates, coprecipitated from nitrate solutions. Initial materials were metallic iron, nickel and the  $Co(NO_3)_3 \cdot 6H_2O$  nitrate. Precursors were annealed at  $(900-1000)^\circ C$  for three hours. Mixing  $CoFe_2O_4$  and  $BaTiO_3$ , we made pellets of the  $(MFe_2O_4)_x+(BaTiO_3)_{1-x}$  samples, which were heat-treated at  $1150^\circ C$  for four hours. X-ray diffraction (XRD) patterns were recorded at room temperature using diffractometer BRUKER D8 Advance with  $Cu K_\alpha$  radiation ( $\lambda=1.5405 \text{ \AA}$ ). Calculations of XRD patterns have been carried out using the Fullprof program package [1].

Crystal structure of a  $CoFe_2O_4$  (or  $NiFe_2O_4$ ) subsystem possesses a cubic structure (space group  $Fd3m$ ). The Fe/Co ions particular occupy at the  $8a$  and  $16d$  positions site, oxide ions situation in  $32e$  position. Subsystem of a  $BaTiO_3$  possesses a tetragonal structure (space group  $P4mm$ ), with Ba-ions in  $1a$  positions site, the ions of titanium in  $1b$  site and O-ions occupy at  $1b$  and  $2c$ . The value of unit cell parameters of nickel ferrite increase with a concentration of a ferromagnetic component in multiferroic materials from  $a=b=c=(8.3337\pm 0.0003) \text{ \AA}$  for  $x=0.2$  up to  $a=b=c=(8.3359\pm 0.0008) \text{ \AA}$  for 0.4. At the same time the unit cell parameters of barium titanate (ferroelectric component) do not change with concentration  $x=(0.2-0.4)$  and equal to be  $a=b=(3.9944\pm 0.0002) \text{ \AA}$  and  $c=(4.0264\pm 0.0002) \text{ \AA}$ . In our work [2] we presented the dielectric constant  $\epsilon$  at low frequencies ( $10^2 \text{ Hz}$ ) and found  $\epsilon$  decreased from  $\sim 940$  for  $x = 0.2$  down to  $\sim 360$  for 0.4. An increasing of the frequency up to  $10^5 \text{ Hz}$  resulted in substantial lowering of the  $\epsilon$  constant by  $\sim 6.35$  times for  $x = 0.2$  and by to  $\sim 1.33$  times for  $x = 0.4$ . An qualitatively similar evolution of a dielectric permittivity with frequency and composition was observed for the  $(NiFe_2O_4)_x+(BaTiO_3)_{1-x}$  system. We assume what decreasing of the  $\epsilon$  in multiferroic materials associated with increased unit cell parameters of a ferromagnetic component.

This work was supported by the State contract (No. 1362) between Ural Federal University and Russian Federation Ministry of Education and Science.

1. J. Rodriguez-Corvajal, *J. Phys. B*, **55**, 192 (1993).
2. A.P. Nosov, M.A. Semkin and et al., *Sol. Stat. Phenom.* **233-234**, 371 (2015).

## Sonochemical method for magnetic powder production

A.Kh. Zhakina, Z.G. Akkulova, A.K. Amirkhanova, G.K. Kudaibergen,  
E.P. Vassilets, O.V. Arnt, A.R. Rapikov

*Institute of organic synthesis and coal chemistry of the Republic of Kazakhstan, 100000, Karaganda, Kazakhstan*  
gulshahar90@mail.ru

One of the most promising methods for synthesis of magnetic fluids in highly- and nano-dispersed condition is sonochemical method based on production of substance with needed properties using ultrasound exposure without use of special organic compounds, that is surface active substances [1, 2].

We have produced magnetic fluid (MF) with the help of coprecipitation from the iron sulfate (II) solution under the influence of ultrasound. We used ИЛ100-6/2 with operating frequency 22 kHz and maximal power 1200 W as the source of ultrasound. We used ammonium hydroxide as precipitator. In the process of research we have studied influence of solution exposure time and precipitator concentration on the process of stable magnetic fluid production. Comparative X-ray diffraction analysis of MF produced using sonochemical method (time = 75 min,  $C(\text{NH}_4\text{OH})=7,5\text{M}$ ), as well as coprecipitation method, showed identical peaks indexed in the area of interplanar space and corresponding to the following values:  $d=1,48\text{\AA}$ ,  $d=1,61\text{\AA}$ ,  $d=1,71\text{\AA}$ ,  $d=2,10\text{\AA}$ ,  $d=2,53\text{\AA}$ ,  $d=2,97\text{\AA}$  и  $d=4,50\text{\AA}$ .

In the process of the research we have studied influence of exposure time and precipitator concentration on the process of stable magnetic fluid production, the results were confirmed with the help of energy-dispersive microanalysis (Fig. 1).

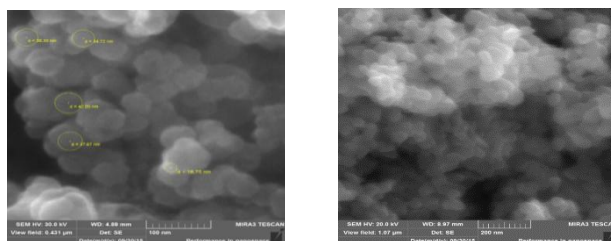


Figure 1. Results of X-ray energy-dispersive microanalysis of magnetic fluid element composition

1. E.H. Kim, H.S. Lee, B.K. Kwak, B.K. Kim, *J. Magn. Magn. Mater.* **289**, 328 (2005).
2. S. Laurent, D. Forge, M. Port, A. Roch, C. Robic, L. Vander Elst, R.N. Muller, *Chem. Rev.* **108**, 2064 (2008).

## Study of ferrite on the basis of nickel with the help of electronic microscopy

O.V. Arnt, A.Kh. Zhakina, A.K. Amirkhanova, E.P. Vassilets,  
G.K. Kudaibergen

*Institute for organic synthesis and coal chemistry of the Republic of Kazakhstan,  
Karaganda*

*oxana230590@mail.ru*

In order to produce nickel ferrites the magnetic fluid dispersed phase was functionalized by the nickel ions which led to production of complex ferrites. Despite intensive study of magnetic fluids the highly effective methods for their production is still current [1].

Image of topographical surface of produced ferrite can be seen on the Figure 1. The  $\text{NiFe}_2\text{O}_4$  ions, which can be seen on the image above, were produced with the help of  $\text{Fe}^{2+}$  and  $\text{Fe}^{3+}$  salts coprecipitation method and all divalent iron ions were substituted by  $\text{Ni}^{2+}$  ions. Phase composition  $\text{FeCl}_3:\text{NiCl}_2$  was used in proportion 2:1.

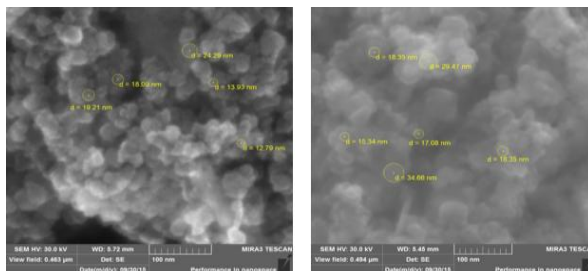


Figure 1. Image of ferrite made with the help of electronic microscopy ( $\text{NiFe}_2\text{O}_4$ ) on REM (coprecipitation, stabilizer  $\text{C}_{17}\text{H}_{33}\text{COOH}$ ,  $T = 80^\circ\text{C}$ ).

As we can see on the micro-image made with the help of raster electronic microscope introduction of nickel in the phase composition leads to changes in the relief of the surface and in the element composition of ferrite nanoparticles, which have spherical form.

Element composition images fully confirm ferrite composition ( $\text{NiFe}_2\text{O}_4$ ) and show Fe 79,8%, Ni 8,1% and O 12,1%. Presence of spherical nanoparticles in the magnetic fluid was confirmed with the help of raster electronic microscopy.

1. G. Helgesen, E. Svasand, A.T. Skjeltorp, *J. Phys.: Condens. Matter.* **20**, 204 (2008).



**Peculiarities of inhomogeneous magnetoelectric effect in rare earth magnets**

R.M. Vakhitov, A.T. Kharisov, Yu.E. Nikolaev

*Institute of Physics and Technology, Bashkir State University, 450076, Ufa, Russia  
VakhitovRM@Yahoo.com*

Currently, magnetoelectric materials attract growing attention due to the prospects of implementation in spintronics and data storage devices [1]. These materials include ferrite garnet crystals in which linear, quadratic and non – homogeneous (flexomagnetolectric) magnetoelectric effects [1, 2] were found out. In the latter case, the effect of magnetic domain wall displacement under the influence of non – uniform electric field occurring at room temperatures was discovered. The number of concomitant regularities has been revealed in [3] that have not received a complete explanation in the subsequent theoretical studies. Particularly, essential dependence of magnetoelectric effect on the crystallographic films orientation, dependence of the observable width of magnetic domain wall on the magnitude of electric field etc. [2] request the additional analysis.

In the present work the influence of electric field on the structure and properties of domain wall in ferrite – garnet films having the different crystallographic orientations has been explored. Euler – Lagrange equations describing the distribution of magnetization<sup>3</sup> in the considered magnets take into account the presence of cubic, induced uniaxial magnetic anisotropy and non – uniform magnetolectric interaction. Analysis of the equations shows that electric field leads to the transformation of 180<sup>0</sup> domain wall; it transforms from the Bloch wall to domain wall having quasi – Bloch structure whose angle  $\varphi$  characterizes the deviation of magnetization vector  $\mathbf{M}$  from domain wall plane. In this case “magnetic charges” arising in the rotation plane due to flexomagnetolectric mechanism induce electric polarization  $\mathbf{P}$  of domain wall. As a result domain wall is attracted or repelled from the source of electric field. We determined the dependences of polarization  $\mathbf{P}$  and domain wall width on material parameters, electric field  $\mathbf{E}$  and the wall chirality that are consistent with experimental data [3].

The work was supported by a grant from the Russian Fund for Fundamental Research (Project № №16-02-00336).

1. A.P. Pyatakov, A.K. Zvezdin, *Phys. Uspechi* **185**, 1077 (2015).
2. A.S. Logginov *et al.*, *JETP Lett.* **86** 115 (2007).
3. R.M. Vakhitov, A.T. Kharisov, Yu.E. Nikolaev, *Dokl.A.N.* **455**, 150 (2014).

## Magnetic phase and inhomogeneous micromagnetic structure in (210) - oriented film of iron garnets

R.M. Vakhitov, R.R. Iskhakova, A.R. Yumaguzin

*Institute of Physics and Technology, Bashkir State University, 450076, Ufa, Russia  
VakhitovRM@Yahoo.com*

The synthesized about 30 years ago, the ferrite-garnet films with an orientation (210) have proved on closer examination to be promising multifunctional materials that can be used in a magnetic recording [1], and in high-sensitivity sensors to visualize the small non-uniform fields [2] and etc. In particular, after the discovery of these films, the giant magnetoelectric effect (ME) [3] at room temperatures of them talked about as a magneto-electric materials. Also in subsequent studies new strong ME effect was discovered in them, which consisted in the displacement of domain walls (DW) under the influence of an external electric field. An interesting feature of the observed effect was its dependence on the orientation of the film: in the (210) -oriented films ME effect is manifested most strongly. Two possible mechanisms to explain the observed phenomenon has been suggested in the literature: the first - ME, the mechanism of which is due to the presence of inhomogeneous magnetoelectric interaction in these materials [3], the second - the conditions of the experiment and the characteristics of the orientation of the phase diagram of the studied films. Thus, from the above it follows that in order to explain the results of [4], it is necessary to analyze the homogeneous and inhomogeneous magnetic states possible in the film type (011) iron garnets, because similar studies have still not been carried out.

In this article we consider the orientation phase diagram of the type of film (210) garnet ferrite on which studied the possible they DW of different topologies. In particular, it was found that in the DW investigated materials generally have non-bloch structure, i.e. with the release of the magnetization vector of the plane of the DW. In this case, the mechanism is implemented flexomagnetoelectric DW induce charges in [3].

The work was supported by a grant from the Russian Fund for Fundamental Research (Project № 16-02-00336 A).

1. V.V. Randoshkin et. all. *Pisma v J. Zh. Tekh. Fiz.* **15**, 42 (1989).
2. S. Tkachuk et. all. *J. of Appl. Phys.* **105**, 07A524 (2009).
3. A.P. Pyatakov et. all. *Phys. Usp.* **58**, 981 (2015).
4. A.S. Logginov et. all. *Appl. Phys. Lett.* **93**, 182510 (2008).
5. A.F. Kabychenkov, F.V. Lisovskii, E.G. Mansvetova *JETP Lett.* **97**, 265 (2013).

**Percolation  $\text{La}_{0.7}\text{Sr}_{0.3}\text{MnO}_3/\text{C}$  composites**

Y.V. Kabirov<sup>1</sup>, T.I. Chupakhina<sup>2</sup>, V.G. Gavrilyachenko<sup>1</sup>, M.I. Evdokimov<sup>1</sup>,  
K.G. Abdulvakhidov<sup>1</sup>

<sup>1</sup>*Southern federal university, 344090 Rostov-on-Don, Russia*  
salv62@mai.ru

<sup>2</sup>*The Institute of Solid State Chemistry of the Ural Branch of the Russian Academy of Sciences, 620990 Ekaterinburg, Russia*

The percolation phenomenon is of great interest within the composite material science. Properties the percolation composites ( $\text{La}_{0.7}\text{Sr}_{0.3}\text{MnO}_3$ )/C are shown in our report. Novel magnetoresistive materials are attractive for various magnetic storage devices. Magnetoresistance (MR) in a magnetoresistive compound at room temperature can be enhanced by diluting with an insulator. In composites manufactured at diluting, a material of barrier layers influences on values and even on the sign of MR [1]. Only restricted interesting data on the positive MR (PMR) that is suitable for applications [2-5]. The aims of the present report are synthesis and study of the MR in composite ( $\text{La}_{0.7}\text{Sr}_{0.3}\text{MnO}_3$ )<sub>x</sub>C<sub>1-x</sub> materials at  $x = 0-85\%$ , where components are  $\text{La}_{0.7}\text{Sr}_{0.3}\text{MnO}_3$  (LSMO) and graphite (C). Composites are investigated by means of XRD and electronic microscopy. The sharp maximum of resistance lies near the percolation threshold. At 50%-60% of LSMO in LSMO/C composites, the maximum PMR values, corresponding to the region of the percolation threshold, are observed. The change of the sign of the temperature coefficient of resistivity (from the positive sign to the negative sign) near the percolation threshold is also consistent with the aforementioned performance. The possibility of achieving the high values of positive MR (up to 15%) at room temperature is shown for LSMO/C composite samples at  $H = 15$  kOe. In our opinion, the important reason of the manifestation of the PMR scattering of spin-polarized electrons can promote an abnormal diamagnetic response like that in C.

This study was supported by the Russian Foundation for Basic Research (project no. 14\_03\_00103).

1. J. M. De Teresa et al. *Phys. Rev. Lett.* **82**, 4288 (1999).
2. X. Zhang, Q.Z. Xue, D.D. Zhu. *Physics Letters A* **320**, 471 (2004).
3. P. Tian, X. Zhang, Q.Z. Xue. *Carbon* **45**, 1764 (2007).
4. Q.Z. Xue, X. Zhang, D.D. Zhu. *Physica B* **334**, 216 (2003).
5. Q.Z. Xue, X. Zhang. *Physics Letters A* **313**, 461 (2003).

## Piezoelectric and electro-optic properties of relaxor ferroelectric $\text{Pb}(\text{In}_{1/2}\text{Nb}_{1/2})\text{O}_3\text{-Pb}(\text{Mg}_{1/3}\text{Nb}_{2/3})\text{O}_3\text{-PbTiO}_3$

X. Liu, Y. Zhao, Q. Hu, Y.G. Zhuang, Z. Xu, X. Wei

*Electronic Materials Research Laboratory, Key Laboratory of the Ministry of Education & International Center for Dielectric Research, Xi'an Jiaotong University, Xi'an 710049, China*  
*eudora\_liu826@sina.com*

The relaxor-PT based ternary  $\text{Pb}(\text{In}_{1/2}\text{Nb}_{1/2})\text{O}_3\text{-Pb}(\text{Mg}_{1/3}\text{Nb}_{2/3})\text{O}_3\text{-PbTiO}_3$  (PIN-PMN-PT) crystals, which can be readily grown by modified Bridgman method with large size [1], have been received considerable attention due to its excellent piezoelectric and electro-optic properties.

Compared to the binary  $\text{Pb}(\text{Mg}_{1/3}\text{Nb}_{2/3})\text{O}_3\text{-PbTiO}_3$  (PMN-PT) crystals, the rhombohedral PIN-PMN-PT crystals possess comparative piezoelectric coefficients and electromechanical couplings, higher coercive field, and broadened temperature usage range [1]. Those results demonstrated that the ternary PIN-PMN-PT crystals are promising candidates for electromechanical devices where high temperature usage and ac field stability are required [2-4]. Furthermore, quasi-single domain tetragonal PIN-PMN-PT crystal can be obtained by high temperature poling technique. The optical transmittance of quasi-single domain tetragonal PIN-PMN-PT crystal is larger than that of multi-domain crystal and it have relatively high electro-optical coefficient, which have potential application value in future [5].

1. F. Li, S.J. Zhang, *J Appl Phys.* **109**, 014108 (2010).
2. F. Li, S.J. Zhang, *J Appl Phys.* **107**, 054107 (2010).
3. F. Li, S.J. Zhang, *J Am Ceram. Soc.* **93**, 2731 (2010).
4. S.J. Zhang, F. Li, *J Appl Phys Lett.* **97**, 132903 (2010).
5. C.T. Chen, J.Y. Zhang, *J Chin. Ceram. Soc.* **43**, (2015).

**Phenomenological model of relaxors for PMN-PT**R.F. Mamin<sup>1,2</sup>, D.A. Tayurskii<sup>2</sup><sup>1</sup>Zavoisky Physical-Technical Institute of RAS, 420029, Kazan Russia  
mamin@kfti.knc.ru<sup>2</sup>Kazan Federal University, Kremlevskaji street, 420000, Kazan, Russia

Relaxor ferroelectrics with a diffuse phase transition, which is usually called relaxors, are subject to continuously, intensive research [1-6]. Interest in these compounds is determined by a combination of ferroelectric, piezoelectric and optical properties and the ability to use these materials in optoelectronics and data storage systems. An important problem in this field is the determination of the nature of the relaxor behavior near the permittivity peak. Theory of phase transitions in systems with defects is considered and phenomenological theory of the diffuse phase transition has been proposed for  $(\text{PbMg}_{1/3}\text{Nb}_{2/3}\text{O}_3)_{1-x}(\text{PbTiO}_3)_x$  (PMN-PT). The temperature behavior and dispersion of the dielectric properties in the region of the diffuse phase transition has been associated with the dynamics of the charge delocalization on defects. The consideration has been performed on the basis of simple thermodynamic ideas in the framework of the phenomenological approach to the theory of phase transitions in the system with defects. A characteristic vibrational frequency of these formations and a dispersion of dielectric permittivity are determined by characteristic times both of the lattice and electron system. The probability distribution of relaxation time is obtained analytically. Appearance of relaxor behavior in PMN-PT with change of titanium concentration will have been also discussed. The experimental observed [5] delay time of phase transition at field after cooling at zero field had been also described in framework of that approach [6]. Good agreement between theory and the experimental data [5] is obtained.

The work is performed according to the Russian Government Program of Competitive Growth of Kazan Federal University. The reported study was partially supported by RFBR, research project No. 14-02-01154 a.

1. G.A. Smolenskii, V.A. Isupov, A.I. Agranovskaya et al., *Sov. Phys. Solid State* **2**, 2584 (1961).
2. L.K. Cross, *Ferroelectrics* **76**, 241 (1987).
3. W. Kleemann, *Int. J. Mod. Phys. B* **7**, 2469 (1993).
4. A.E. Glazounov., A.K. Tagantsev, *Phys. Rev. Lett.* **85**, 2192 (2000).
5. E.V. Colla, E.Yu. Koroleva, N.M. Okuneva, S.B. Vakhrushev, *Phys. Rev. Lett.* **74**, 1681 (1995).
6. R.F. Mamin, R. Blinc, *Ferroelectric Letters* **29**, n.1, 15-20 (2002).

## Photoconductivity and photostimulated current in PMN-PT

S.A. Migachev<sup>1</sup>, R.F. Mamin<sup>1,2</sup>, R.V. Yusupov<sup>2</sup>, A.A. Tirkiya<sup>1</sup>, M.F. Sadykov<sup>1</sup>

<sup>1</sup>Zavoisky Physical-Technical Institute of RAS, 420029, Kazan, Russia  
smigach@kfti.knc.ru

<sup>2</sup>Kazan Federal University, 420000, Kazan, Russia

Relaxor ferroelectrics are subject to intensive research [1-3]. Interest in these compounds is determined by a combination of ferroelectric, piezoelectric and optical properties. These materials are used in optoelectronics and data storage systems. For study of a properties of defect states of the relaxors the photoconductivity and the photostimulated current was measured in  $\text{PbMg}_{1/3}\text{Nb}_{2/3}\text{O}_3$  (PMN) and  $(\text{PbMg}_{1/3}\text{Nb}_{2/3}\text{O}_3)_{1-x}(\text{PbTiO}_3)_x$  (PMN-PT) single crystals. We also observed photocurrent at absent external bias through many hours after illumination under bias. On the basis of experimental data on the spectral dependence of the photoconductivity the characteristic form of the density of states defect levels and the characteristic energy intervals was determined for PMN and PMN-PT as well. The activation energy and the energy gap between the localization region of charge carriers on defects and the conduction band agree well with one another for PMN-PT. The values of the used parameters also agree with the experimental data on the conductivity. This allows us to conclude that the characteristic temperature range of the thermal localization of charge carriers on the defect levels lies between 350 and 700 K. Thus, the phenomenological model [4] for relaxor ferroelectrics can be applied for PMN-PT and the discovered defect states can take part in the formation of the diffuse phase transition and determine its dispersion properties. Effect of the light on the change of dielectric properties in PMN-PT samples is also investigated. In conclusion, the spectral dependence of the photoconductivity and photostimulated currents at zero external voltage has been studied. Based on the experimental data, the structure of the density of states of the defect levels and the possibility their participation in the formation of a diffuse phase transition is proposed. Thus the results of the investigations of the photoconductivity and photostimulated phenomena in PMN-PT are discussed.

The work is performed according to the Russian Government Program of Competitive Growth of Kazan Federal University. The reported study was partially supported by RFBR, research project No. 14-02-01154 a.

1. G.A. Smolenskii, V.A. Isupov, A.I. Agranovskaya et al., *Sov. Phys. Solid State* **2**, 2584 (1961).
2. L.K. Cross, *Ferroelectrics* **76**, 241 (1987).
3. W. Kleemann, *Int. J. Mod. Phys. B* **7**, 2469 (1993).
4. R.F. Mamin, T.S. Shaposhnikova, *JETP Letters* **101**, n.1, 29 (2015)

## Dielectric spectrum of a ferroelectric-soft PZT-based material in a relaxor phase

G.M. Akbaeva<sup>1</sup>, E.I. Sitalo<sup>1</sup>, V.G. Gavrilyachenko<sup>2</sup>, E.M. Panchenko<sup>1</sup>

<sup>1</sup>*Institute of Physics, Southern Federal University, 344090, Rostov-on-Don, Russia*  
gakbaeva@mail.ru

<sup>2</sup>*Physics Faculty, Southern Federal University, 344090, Rostov-on-Don, Russia*

The ferroelectric-soft PZT-based material represents a solid solution of a five-component system of  $\text{PbTiO}_3$ – $\text{PbZrO}_3$ – $\text{PbNb}_{2/3}\text{Zn}_{1/3}\text{O}_3$ – $\text{PbW}_{1/2}\text{Zn}_{1/2}\text{O}_3$ – $\text{PbW}_{1/2}\text{Mg}_{1/2}\text{O}_3$  with the addition of the  $\text{PbGeO}_3$  modifier. This modifier exhibits ferroelectric-relaxor properties [1] as follows: a diffuse maximum of a temperature dependence of dielectric permittivity  $\varepsilon(T)$ , a temperature-frequency dispersion of  $\varepsilon$ , and this means a dielectric relaxation that can be described in terms of the Vogel–Fulcher law.

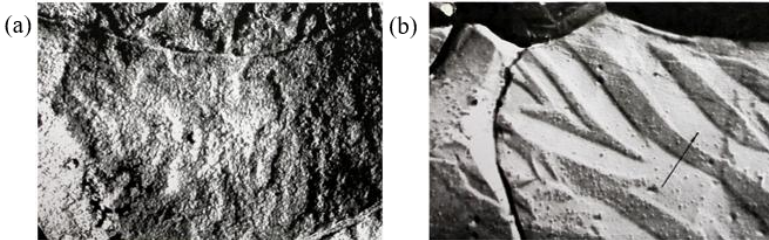


Figure 1. Micrographs of the etched non-poled ceramic of the aforementioned composition at the magnification  $\times 34350$  (a) and of the poled ceramic at the magnification  $\times 21600$  (b).

As follows from the micrographs of the ceramic microstructure (Fig. 1), a “tweed structure” observed in a non-poled ceramic sample and ferroelectric domains in a poled ceramic sample also suggest that the studied composition is related to ferroelectric-relaxors.

In the present work, dielectric spectra were studied within ranges over and under the maximum of dielectric permittivity (i.e., in the relaxor phase), and in these spectra, there are regions of the Debye-type dispersion. Features of the obtained spectra are discussed.

1. A.I. Burkhanov, A.V. Shilnikov, Yu.N. Mamakov, G.M. Akbaeva, *Physics of Solid State* **44**, 1665 (2002, in Russian).

## Nanoscale piezoelectric properties of PLZT ceramics: effect of surface disorder

E.A. Neradovskaya<sup>1</sup>, M.M. Neradovskiy<sup>1</sup>, A.P. Turygin<sup>1</sup>, V.V. Fedoroviy<sup>1</sup>, V.Ya. Shur<sup>1</sup>, A.L. Kholkin<sup>1,2</sup>, D.A. Kiselev<sup>3</sup>

<sup>1</sup>*Institute of Natural Sciences, Ural Federal University, Ekaterinburg, 620000, Russia*  
*Elizaveta.kolchina@urfu.ru*

<sup>2</sup>*Physics Department & CICECO, University of Aveiro, 3810-193 Aveiro, Portugal*

<sup>3</sup>*National Research Technological University "MISiS", Moscow, 119049 Russia*

$\text{Pb}_{1-x}\text{La}_x(\text{Zn}_{0.65}\text{Ti}_{0.35})_{1-x/4}\text{O}_3$  (PLZT x/65/35) ceramics are widely used in optical devices, actuators, sensors and modulators [1] due to their outstanding electromechanical, piezoelectric and electrooptical properties [2]. These materials are disordered ferroelectrics and are characterized by the presence of normal micron-sized domains along with labyrinthlike structures due to disorder. It is therefore necessary to understand and to control the domain states in relaxors that are directly related to their performance as sensors and actuators

PLZT x/65/35 ceramic samples with  $x = 6 - 9.75\%$  produced by Latvian Academy of Sciences and Jozef Stefan Institute, Slovenia were under investigation. PLZT ceramics from Latvian Institute of Physics were produced by peroxohydroxopolymer method. On the contrary, samples from Jozef Stefan Institute were prepared by a conventional mixed-oxide method from commercial oxides.

In order to compare PLZT x/65/35 ceramics of different compositions produced by different methods both dielectric and nanoscale properties have been studied. Nanoscale domain structure have been acquired by piezoresponse force microscopy (PFM).

The dielectric permittivity of PLZT x/65/35 decreases rapidly at entire temperature range with increasing La concentration for both set of samples following typical relaxor behavior.

The grain size and correlation length in different grains have been measured. The spatial dependence of the correlation length inside grain have been revealed for PLZT 9.75/65/35. Also correlation length was found to depend on the size of the grain. Another important feature of the observed grain effect is that the average value of the piezoelectric response (proportional to the average value of the polarization) also decreases upon approaching grain boundary closely following the correlation length dependence.

The temperature dependence of piezoresponse have been measured in PLZT 9/65/35 ceramics showing variation upo approaching freezing temperature.

1. G.H. Haertling, *Ferroelectrics* **75**, 25 (1987).
2. A.L. Kholkin, I.K. Bdkin, V.V. Shvartman, A. Orlova, D. Kiselev, A.A. Bogomolov, S.-H. Kim, *MRS Proc.* 838 (2004).



## Band-like electrical transport in $\text{Pr}_{1-x}\text{Ca}_x\text{MnO}_3$ manganites

L.S. Kadyrov<sup>1,2</sup>, T. Zhang<sup>3</sup>, E.S. Zhukova<sup>1,2,4</sup>, V.B. Anzin<sup>1,2</sup>, V.G. Trotsenko<sup>5,6</sup>,  
V.I. Torgashev<sup>5</sup>, M. Dressel<sup>4</sup>, B.P. Gorshunov<sup>1,2,4</sup>

<sup>1</sup>Moscow Institute of Physics and Technology, Dolgoprudny, 141700, Russia  
vasiliytrotsenko@live.ru

<sup>2</sup>A.M. Prokhorov General Physics Institute, RAS, Moscow, 119991, Russia

<sup>3</sup>Key Laboratory of Materials Physics, ISSP, CAS, Hefei, 230031, China

<sup>4</sup>Physikalisches Institut, Universität Stuttgart, 70569, Stuttgart, Germany

<sup>5</sup>Faculty of Physics, Southern Federal University, 344090, Rostov-on-Don, Russia

<sup>6</sup>Laboratory of Condensed Matter Physics, University of Picardy, 80039, Amiens, France

By using coherent source and pulsed terahertz spectroscopy techniques and infrared Fourier-transform spectroscopy, broad-band ( $5$  to  $3000\text{ cm}^{-1}$ ) spectra of conductivity and dielectric permittivity of polycrystalline manganites  $\text{Pr}_{1-x}\text{Ca}_x\text{MnO}_3$  with  $x = 0.3, 0.4$  and  $0.5$  are measured at temperatures  $10$ - $300\text{ K}$ . Three spectral components are revealed at terahertz frequencies: a) the Drude-like response of free charge carriers; b) the resonance centered at  $40$ - $60\text{ cm}^{-1}$ ; c) the relaxational dispersion around  $10$ - $20\text{ cm}^{-1}$ . The Drude component is assigned to the band-like response of small polaronic charge carriers. It is shown that the amplitude of this free-carrier conductivity is thermally activated with the activation energy changing from  $95$ - $140\text{ meV}$  above  $120$ - $170\text{ K}$  to  $2.6$ - $4.3\text{ meV}$  at lower temperatures (Fig. 1). The temperature driven crossover at  $120 - 170\text{ K}$  is associated with setting in of the magnetic order. The nature of the terahertz resonance at  $40$ - $60\text{ cm}^{-1}$  is assigned to the transition between Stark split  $\text{Pr}^{3+}$  electron states that gain optical activity due to coupling to acoustical phonons. The relaxation at  $10$ - $20\text{ cm}^{-1}$  is caused by delocalized polarons whose response is governed by their dynamics in presence of random localizing potential.

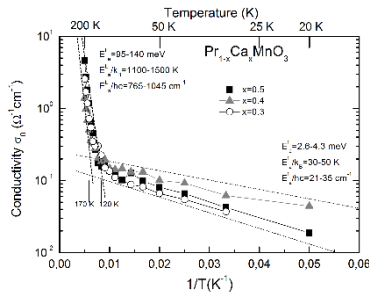


Figure 1. DC conductivity of  $\text{Pr}_{1-x}\text{Ca}_x\text{MnO}_3$  polycrystalline samples obtained by least-square fitting of the terahertz-infrared spectra. Dashed lines show ranges of activation energies describing variation of conductivity at high ( $E_a^h$ ) and low ( $E_a^l$ ) temperatures.

## Structural characterization of $\text{La}_{0.25}\text{Ca}_{0.75}\text{MnO}_3$ thin films grown by pulsed laser deposition

V.G. Trotsenko<sup>1,2</sup>, V.I. Torgashev<sup>1</sup>, Yu.I. Yuzyuk<sup>1</sup>, M. El Marssi<sup>2</sup>, A. Lahmar<sup>2</sup>

<sup>1</sup>Faculty of Physics, Southern Federal University, 344090, Rostov-on-Don, Russia  
vasiliytrotsenko@live.ru

<sup>2</sup>Laboratory of Condensed Matter Physics, University of Picardy, 80039, Amiens, France

We report the growth of well-crystallized and highly oriented  $\text{La}_{0.25}\text{Ca}_{0.75}\text{MnO}_3$  thin films on (100)  $\text{SrTiO}_3$  substrates by pulsed laser deposition at the substrate temperatures  $680^\circ\text{C}$  and  $700^\circ\text{C}$ , with the oxygen pressure 0.2 mbar and 0.3 mbar. Crystal structure and phase characterization were determined by X-ray diffraction (XRD) ( $\theta - 2\theta$ ,  $\varphi$ ,  $\omega$  scans, rocking curves, reciprocal space maps) using  $\text{Cu K}\alpha$  radiation at room temperature. According to X-ray diffraction the films consist of single phase c-axis oriented material. The pseudocubic lattice parameters and the volume of the unit cells calculated from the XRD patterns are shown as a function of combination of temperature and oxygen pressure in Fig 1. We find a strong dependence of the lattice constant on the substrate temperature and the oxygen pressure. It can be easily seen that the pseudocubic lattice parameters  $a_p$  and  $b_p$  approach each other at  $680^\circ\text{C}$  and 0.3 mbar. This means that crystal structure turns from orthorhombic to more tetragonal. This can be attributed to a complex dependency of amount  $\text{Mn}^{4+}$  on the substrate temperature and the oxygen pressure.

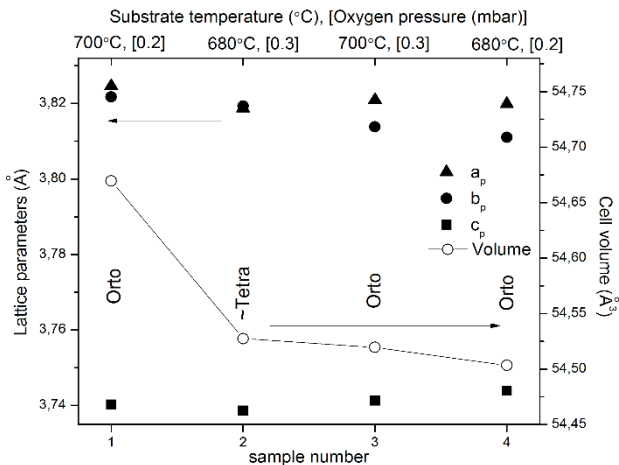


Figure 1. The combination of the substrate temperature and the oxygen pressure dependence of the pseudocubic lattice parameters  $a_p, b_p, c_p$  and volume of  $\text{La}_{0.25}\text{Ca}_{0.75}\text{MnO}_3$  thin films at room temperature. The lattice parameters  $a_p, b_p$  and  $c_p$  were determined from  $\theta - 2\theta$  scans of LCMO (112), (011) and (002) peaks, respectively.

**Strain effects in multiferroic superlattices**

A.S. Anokhin<sup>1</sup>, A.G. Razumnaya<sup>2</sup>, Yu.I. Yuzyuk<sup>2</sup>, Yu.I. Golovko<sup>1</sup>,  
V.M. Mukhortov<sup>1</sup>

<sup>1</sup>*Southern Scientific Center of RAS, Rostov-on-Don, 344006, Russia*  
*razumnaya2@yandex.ru*

<sup>2</sup>*Southern Federal University, Faculty of Physics, Rostov-on-Don, 344090, Russia*

Multiferroic materials like bismuth ferrite, are the subject of intensive investigations because they are very promising candidates for device applications in spintronics and multiple-state memories that can be addressed both electrically and magnetically. Epitaxial multiferroics exhibit strong sensitivity of magnetic and/or ferroelectric properties towards lattice strain. Thus, multilayer films and superlattices offer a very efficient way of strain engineering to design materials with enhanced magnetoelectric responses.

We investigated the  $\text{Bi}_{0.98}\text{Nd}_{0.02}\text{FeO}_3/\text{Ba}_{0.8}\text{Sr}_{0.2}\text{TiO}_3$  superlattice (BNFO/BST SL) using X-ray diffraction and Raman spectroscopy techniques with the aim to clarify the peculiarities of crystal structure and lattice distortions within multilayer heterostructure. The superlattice consisting of 20 BNFO/BST pairs, was grown by rf-sputtering on the (001) MgO single crystal. Detailed analysis of the XRD patterns shows that the thickness of the BNFO and BST layers equal to 4 and 6 nm, respectively. The modulation period of the SL was about 10 nm. The out-of-plane parameters of the BNFO and BST layers were found to be 0.3975 nm and 0.4032 nm, respectively. Note, that the lattice parameters of both layers are markedly larger than those that are observed in the bulk samples of the same compositions.

Polarized Raman spectra of BNFO/BST SL differ significantly from the spectra of the one-component BNFO and BST films and other SL, consisting of alternating BNFO and BST layers. In particular, the parallel-polarized spectrum of the BNFO/BST SL contains a dominating band at  $705\text{ cm}^{-1}$ . We assume that this feature originates from the highly strained BNFO layers, where the two-dimensional epitaxial strains in the SL's layers induce the distortions in  $\text{FeO}_6$  octahedra and the high-frequency symmetrical stretching mode appears in the Raman spectra. We propose that distortion in  $\text{FeO}_6$  octahedra is enforced by the epitaxial strain and induces enhanced magnetic properties in the BNFO/BST SL.

This study was supported by the Russian Foundation for Basic Research (project No. 16-32-00033 mol\_a). One of the authors (A.G.R.) thanks grant of President RF No. SP-1359.2016.3.

**Lattice distortions and lattice dynamics of the multiferroic heterostructures**

D.V. Stryukov<sup>1,2</sup>, A.G. Razumnaya<sup>1</sup>, Yu.I. Yuzyuk<sup>1</sup>, O.A. Bunina<sup>3</sup>,  
V.M. Mukhortov<sup>2</sup>

<sup>1</sup>*Southern Federal University, Faculty of Physics, 344090, Rostov-on-Don, Russia*  
razumnaya2@yandex.ru

<sup>2</sup>*Southern Scientific Center of RAS, 344006, Rostov-on-Don, Russia*

<sup>3</sup>*Southern Federal University, Research institute of physics, 344090, Rostov-on-Don, Russia*

A comparative study of crystal structure and Raman spectra of the epitaxial BiFeO<sub>3</sub> films on a cubic (001) and (111) MgO substrates was performed. The epitaxial BiFeO<sub>3</sub> (BFO) films were grown by rf-sputtering on a cubic MgO substrates with different orientations using Ba<sub>0.8</sub>Sr<sub>0.2</sub>TiO<sub>3</sub> (BST) buffer layers with the thickness of 100 nm. The thickness of BFO films was 100 nm. These heterostructures were investigated by means of X-ray diffraction and micro-Raman scattering with the aim to determine the features of the crystal structure and the lattice dynamics.

According to X-ray diffraction examination, the crystal structure of the BFO and BST layers in BFO/BST/(001)MgO heterostructure is monoclinic or tetragonal with the out-of-plane lattice parameters  $c=0.3955$  nm and  $c = 0.4005$  nm in BFO and BST layers, respectively. Note that both layers have close values of the in-plane lattice parameters,  $a = 0.399$  nm. At room temperature, the structure of the BFO and BST layers in the BFO/BST/(111)MgO heterostructure is described by the rhombohedral symmetry. In the hexagonal setting the out-of-plane parameter  $c=0.6914$  nm of BST layer is larger than that one  $c=0.6861$  nm of the BFO layer, while their in-plane parameter is  $a = 0.555$  nm.

The polarized Raman spectra of the heterostructures have been measured in the normal backscattering geometry. The parallel polarized spectra of both samples are dominated by the lines corresponding to the upper BFO layer, and does not contain the very intense  $A_1(\text{TO})$  component of the soft mode of the BST layer. The cross-polarized spectrum of the BFO/BST/(001)MgO film contains the characteristic lines of the BFO and  $A_1$  symmetry modes of the BST layers. The presence of  $A_1$  fully symmetrical modes in the cross-polarized spectrum excludes the tetragonal symmetry of these layers. Thus, the BFO and BST layers in the BFO/BST/(001)MgO heterostructure are characterized by monoclinic symmetry.

This study was supported by the Russian Foundation for Basic Research (project No. 16-32-00033 mol\_a). One of the authors (A.G.R.) thanks grant of President RF No. SP-1359.2016.3.

## Dielectric spectroscopy of the binary system solid solutions $(1-x)\text{BiFeO}_3$ - $x\text{BaTiO}_3$

N.A. Boldyrev, E.I. Sitalo, L.A. Reznichenko

*Research Institute of Physics, Southern Federal University, Rostov-on-Don, Russia  
nboldyrev@sfnu.ru*

Bismuth ferrite ( $\text{BiFeO}_3$ , BFO) is the multiferroic material with perovskite structure. Solid solutions based on it have recently been the subject of intense search. The aim of this work is establishing regularities of the structural and dielectric characteristics formations in the binary system solid solutions  $(1-x)\text{BiFeO}_3$ - $x\text{BaTiO}_3$  ( $0.10 \leq x \leq 0.50$ ,  $\Delta x = 0.10$ ). The second component of this solid solution is classic ferroelectric barium titanate ( $T_C = 393$  K), which is widely used in the piezoceramic manufacturing.

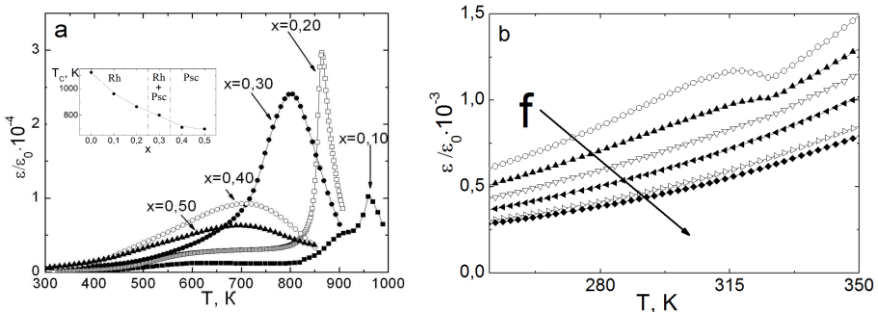


Figure 1. Dependencies  $\varepsilon/\varepsilon_0(T)$  for all researched samples ( $f = 100$  kHz) and for  $x = 0.50$  sample in the temperature range  $(250 \div 350)$  K.

Relative permittivity measurements shows that introduction of  $\text{BaTiO}_3$  have led to a monotonic reduction of the ferroelectric-paraelectric phase transition temperature and dielectric constant maximum blurring (Fig. 1a). It can be related with the compositional disorder in the A- and B-positions of perovskite cell. Some relative permittivity behavior anomalies were observed in the temperature range  $(100 \div 350)$  K (Fig. 1b). Work discusses relations between observed phenomena and material crystal chemical structure features, nano-domain structures formation and evolution, Maxwell-Wagner relaxation.

This work was supported by the Ministry of Education and Science of the Russian Federation: projects №№ 1927, 213.01-2014/012-IG and 3.1246.2014/K (the basic and project parts of the state task) and performed on equipment of Collective usage center "Electromagnetic, electromechanical and thermal properties of solids" of the Research Institute of Physics, Southern Federal University.

## Dielectric spectroscopy of the binary system solid solutions (1-x)BiFeO<sub>3</sub>-xCdTiO<sub>3</sub> in the low-frequency region

A.V. Turik, N.A. Boldyrev, E.I. Sitalo

Research Institute of Physics, Southern Federal University, Rostov-on-Don, Russia  
nboldyrev@sfnu.ru

Solid solutions based on bismuth ferrite (BiFeO<sub>3</sub>) have recently been the subject of intense search. The aim of this work is establishing dielectric characteristics formations regularities of the binary system solid solutions (1-x)BiFeO<sub>3</sub>-xCdTiO<sub>3</sub> (0.10 ≤ x ≤ 0.50, Δx = 0.10). High temperature dielectric measurements have shown there is a regions with negative values of real part ε' of complex permittivity  $\epsilon = \epsilon' - i\epsilon''$  in the low-frequency area in the some samples. For explanation of observed phenomena we use technique described in [1] and based on using the parallel circuit including the capacity C, having only the real part, and the complex conductivity  $G = 1/R = (G_1 - iG_2)$ . This parallel connection allowed us to describe adequately experimental data and passing the real part of the complex capacity C\* or permittivity  $\epsilon^* = \epsilon^{*'} - i\epsilon^{*''}$  through zero.

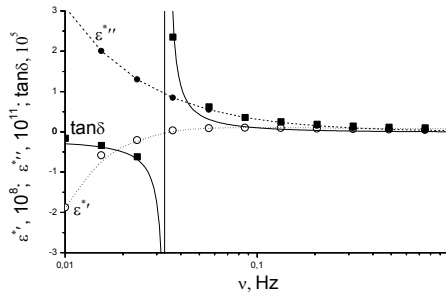


Figure 1. Experimental dielectric spectra of 0.6BiFeO<sub>3</sub>-0.4CdTiO<sub>3</sub> ceramics at 923 K (points) and calculated frequency dependences of  $\epsilon^{*'}$ ,  $\epsilon^{*''}$  and  $\tan \delta$ .

Critical frequency, at which condition  $\epsilon^{*'}=0$  is fulfilled, is determined. The presence of negative  $\epsilon^{*'}$  values at low frequencies  $\nu < \nu_c \sim 3.4 \cdot 10^{-2}$  Hz is equivalent to an occurrence of the parallel resonance. This type of resonance phenomena arises owing to a mutual compensation of the capacity and hopping conductivity contributions to the real part of the dielectric permittivity.

This work was supported by the Ministry of Education and Science of the Russian Federation: projects №№ 1927, 213.01-2014/012-IG and 3.1246.2014/K (the basic and project parts of the state task) and performed on equipment of Collective usage center "Electromagnetic, electromechanical and thermal properties of solids" of the Research Institute of Physics, Southern Federal University.

1. A.V. Turik, A.S. Bogatin, *Functional Materials Letters* **8**, 1550035 (2015).

## Comparison of the structures of Y–Mn–O system (YMnO<sub>3</sub>, YMn<sub>2</sub>O<sub>5</sub>, and Y<sub>2</sub>Mn<sub>2</sub>O<sub>7</sub>)

V.V. Lyutikova<sup>1</sup>, A.V. Nazarenko<sup>2</sup>, S.V. Chagovets<sup>1</sup>, A.G. Rudskaya<sup>1</sup>,  
M.F. Kupriyanov<sup>1</sup>

<sup>1</sup>The Department of Physics, Southern Federal University, 344090 Rostov-on-Don,  
Russia  
arudskaya@yandex.ru

<sup>2</sup>Southern Scientific Center, Russian Academy of Sciences, 344006 Rostov-on-Don,  
Russia

Manganite yttrium (YMnO<sub>3</sub>) belongs to the group of double oxides having the chemical formula ABO<sub>3</sub>, where A and B are trivalent ions (A – all lanthanide Ln – La, Ce, Pr, Nd, Sm, Eu, Gd, Tb, Dy, Ho, Er, Tm, Yb, Lu, and ions are Bi, In, Ga, Sc, and Y; B – ions Al, V, Cr, Mn, Fe, Co, Ni, Ga, In, Sc). There are also known B – Cu and Ti structures.

The hexagonal phase YMnO<sub>3</sub> at temperatures below  $T_N = 74$  K is antiferromagnetic and ferroelectric below  $T_C = 913$  K. The symmetry of the hexagonal phase is described by the space group  $P6_3cm$ . Above  $T_C$  YMnO<sub>3</sub> hexagonal structure is maintained, but the symmetry is increased to the space group  $P6_3/mmc$ . The parameters of the unit cell vary from  $a_H = 6.148$  Å,  $c_H = 11.400$  Å ( $P6_3cm$ ) to the parameters  $a_H' = 3.619$  Å,  $c_H' = 11.340$  Å ( $P6_3/mmc$ ), that is, during the phase transition with decreasing temperature from the paraelectric phase  $P6_3/mmc$  to the ferroelectric  $P6_3cm$  multiplication of the elementary cell along the axes ( $x, y$ ) ( $a_H = \sqrt{3} a_H'$ ) is changed.

It is stated that the Mn ions are surrounded by five oxygens forming a trigonal bipyramid. Y ions occupy positions surrounded by eight oxygen in chains along the  $z$  axis.

In the orthorhombic phase YMnO<sub>3</sub> ( $o$ ) unlike the hexagonal phase YMnO<sub>3</sub> ( $h$ ), the Neel temperature  $T_N$  is below 30 – 40 K. Earlier made various research YMnO<sub>3</sub> of orthorhombic phase ( $o$ ) stated that at temperatures above 50 K, the structure is characterized by a space group  $Pbnm$  ( $Pnma$ ), and below  $T_N = 30$  K is characterized by a space group  $P2_1nm$ .

YMnO<sub>3</sub> and solid solutions can be formed both with hexagonal and perovskite structures depending on the preparation conditions (temperature, pressure). Furthermore, in Y–Mn–O phase system there are also formed and YMn<sub>2</sub>O<sub>5</sub> and Y<sub>2</sub>Mn<sub>2</sub>O<sub>7</sub>. Monitoring of these phases formation conditions is very difficult. In any case, our experiments on solid phase synthesis of such compounds led to the formation of a hexagonal phase YMnO<sub>3</sub> only.

The structures of the multiferroic RMn<sub>2</sub>O<sub>5</sub>, where R – Tb, Ho, Dy and YMn<sub>2</sub>O<sub>5</sub> are characterized by disproportionate magnetic structures with orthorhombic  $Pbam$  phase.

Compounds  $Y_2Mn_2O_7$ ,  $Ho_2Mn_2O_7$ ,  $Yb_2Mn_2O_7$  are characterized by pyrochlore type structures which exhibit antiferromagnetic domains switching effects of electric fields. Such structures are decomposed in nanocrystalline objects.

The report will present the results of crystal-chemical analysis of Y–Mn–O system ( $YMnO_3$ ,  $YMn_2O_5$  and  $Y_2Mn_2O_7$ ) structures correlation.

This work was financially supported by the Ministry of Education and Science of the RF: themes №№ 1927, 213.01-2014/012-VG and 3.1246.2014/K (the basic and project parts of the state task).



## Effect of $\text{PbNi}_{1/3}\text{Nb}_{2/3}\text{O}_3$ on the structure, dielectric and piezoelectric properties of multicomponent solid solutions based on PMN-PT

M.V. Talanov, L.A. Shilkina, L.A. Reznichenko

*Research Institute of Physics, Southern Federal University, 344090, Rostov-on-Don, Russia*  
 tmikle-man@mail.ru

Solid solutions based on relaxor ferroelectrics  $\text{PbMg}_{1/3}\text{Nb}_{2/3}\text{O}_3$  (PMN),  $\text{PbZn}_{1/3}\text{Nb}_{2/3}\text{O}_3$  (PZN),  $\text{PbNi}_{1/3}\text{Nb}_{2/3}\text{O}_3$  (PNN), and classical ferroelectric  $\text{PbTiO}_3$  (PT) are of considerable interest owing to high values of piezoelectric, dielectric, optical, and pyroelectric parameters which makes it possible to use these objects in various devices: actuators, sensors, and transducers. However, the binary system based on the above compounds characterized by a one-dimensional morphotropic region and therefore extreme properties are manifested in a very narrow concentration range, which limits the choice of materials on the basis of these systems. The aim of this study was to establish the influence of PNN on the composition-structure-property correlations in the ceramics of the multicomponent system PMN(m)-PNN(n)-PZN(y)-PT(x).

Fig. 1 shows graphs showing the evolution of piezoelectric and dielectric properties of the ceramics by varying the concentration PNN (n) and PT (x). Detailed results will be presented in the report.

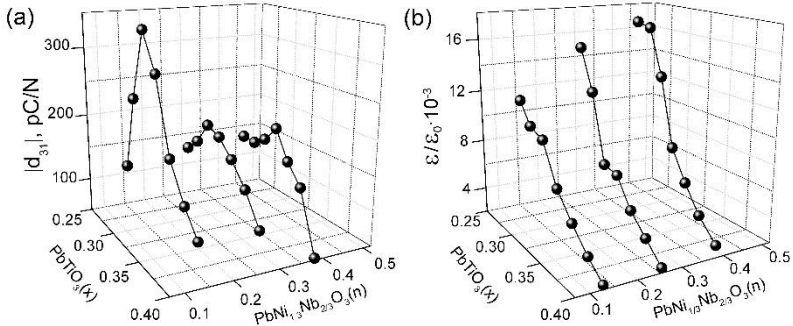


Figure 1. Dependencies of the piezoelectric coefficient  $d_{31}$  (a) and dielectric constant (b) of the studied ceramics at room temperature on concentration PNN (n) and PT (x).

This work was supported by the grants of the Ministry of Education and Science of the Russian Federation (basic and project tasks of the state: themes number 1927 213.01-2014 / 012-VG, Task № 3.1246.2014 / K), RFBR (No. 16-32-00144 moll\_a.) and SP-96.2016.1 using the collective use center equipment "Electromagnetic, electromechanical and thermal properties of solids" Institute of physics, Southern federal University.

## The dielectric dispersion of the $\text{PbTiO}_3\text{-PbZrO}_3\text{-PbNb}_{2/3}\text{Mg}_{1/3}\text{O}_3\text{-PbGeO}_3$ solid solutions: the evolution of the response in the transition from the classical to the relaxor ferroelectric state

A.A. Pavelko, L.A. Reznichenko

Research Institute of Physics, Southern Federal University, 344090, Rostov-on-Don, Russia  
 aapavelko@sfnu.ru

Study of the dispersion properties of multi-component system ceramic solid solutions on the basis of a well-known binary systems  $(1-x)\text{PbZrO}_3\text{-}x\text{PbTiO}_3$  (PZT),  $(1-x)\text{PbNb}_{2/3}\text{Mg}_{1/3}\text{O}_3\text{-}x\text{PbTiO}_3$  (PMN-PT) allowed to calculate the degree of diffuseness and a measure of tailing, characterizing the smearing of the phase transition (PT) and the degree of deviation of the dielectric constant temperature dependencies in vicinity of PT from the Curie-Weiss law. This allows one to set proportional ratio of basic binary systems PMN-PT and PZT in the system in accordance with the character of ferroelectric (FE) properties manifestations of its solid solutions (FE-relaxors,  $\text{FER} \leftrightarrow \text{FE with diffuse PT}$ ,  $\text{DPT} \leftrightarrow \text{classical FE}$ , CFE).

An investigation of the solid solutions electrical parameters behavior under the strong biasing DC electric fields has confirmed the classification adopted above. The obtained results make it possible to determine the concentration regions where the solid solutions shows different FE properties, and to predict the presence of the specified properties of the materials in unexplored areas of the phase diagram (Fig. 1).

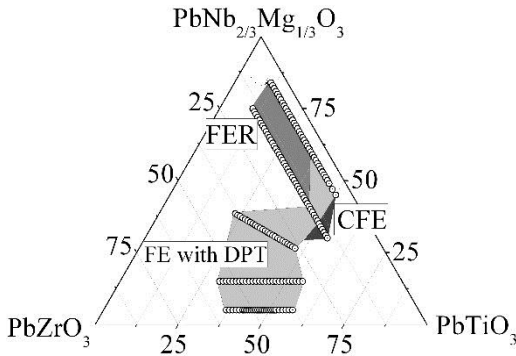


Figure 1. The phase diagram of the system  $\text{PbZrO}_3\text{-PbNb}_{2/3}\text{Mg}_{1/3}\text{O}_3\text{-PbGeO}_3$ , highlighted areas refers to different FE properties of solid solutions.

This work was financially supported by the Ministry of Education and Science of the Russian Federation: grant of the President of RF № MK-3232.2015.2; themes № 1927, № 213.01-2014/012-VG and № 3.1246.2014/K (the basic and project parts of the state task).

**Optical and dielectrical properties of the  $(\text{Ba}_{0.5}\text{Sr}_{0.5})\text{Nb}_2\text{O}_6/\text{Pt}(111)/\text{Si}(001)$** A.P. Kovtun<sup>1,2</sup>, S.P. Zinchenko<sup>2</sup>, A.V. Pavlenko<sup>1,2</sup>, G.N. Tolmachev<sup>1,2</sup><sup>1</sup>*Research Institute of Physics, Southern Federal University, 344090, Rostov- on-Don, Russia  
tolik\_260686@mail.ru*<sup>2</sup>*Southern Scientific Center, Russian Academy of Sciences, 344006 Rostov- on-Don, Russia*

Heterostructures based on ferroelectric films of barium strontium niobate are promising environments for micro- and nanoelectronics. The aim of this work was to study the optical anisotropy films  $(\text{Ba}_{0.5}\text{Sr}_{0.5})\text{Nb}_2\text{O}_6$  (BSN) on the substrate Pt(111)/Si(001).

RF sputtering gas discharge BSN films produced in an atmosphere of pure oxygen at  $P = 0.5$  Tr. The optical properties of the films were analyzed using the measured angular dependence of the intensity of the specular reflected probe radiation H- polarization on the structure of the film-substrate.

It was found that the films have a preferred crystallographic orientation in the [001] direction and have natural unipolarity, which proved by the analysis of dielectric and piezoelectric characteristics.

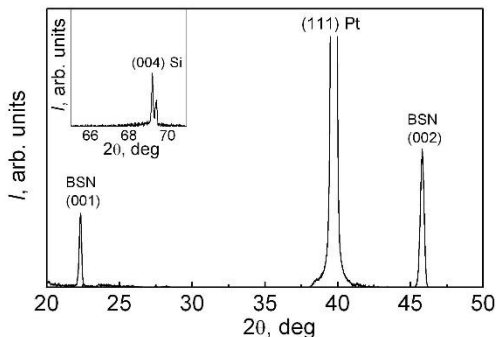


Figure 1. The XRD pattern of the heterostructure BSN/(111)Pt/(001)Si.

It is found that the film material BSN optical characteristics (i.e., the values of  $u$ ) is equivalent to a uniaxial negative ( $n_0 > n_e$ ) BSN single crystal whose optical axis is perpendicular to the substrate.

This study was supported by the Ministry of Education and Science of the Russian Federation (theme №. 3.1246.2014/K), the RFBR (№ 15-08-05711 A) and the SP-1689.2015.3.

## The method of experimental determination of microwave-absorbing characteristics of composite materials

A.G. Abubakarov<sup>1</sup>, J.A. Reyzenkind<sup>1</sup>, M.A. Lerer<sup>2</sup>, L.A. Reznichenko<sup>1</sup>,  
M.B. Manuilov<sup>2</sup>, Y.M. Noykin<sup>2</sup>, A.B. Kleshnikov<sup>2</sup>, S.V. Crutiev<sup>2</sup>

<sup>1</sup>*Research Institute of physics southern Federal University, 344090, Rostov-on-Don, Russia*  
*abubakarov12@mail.ru, http://ip.sfedu.ru/*

<sup>2</sup>*Physical faculty of southern Federal University, 344090, Rostov-on-don, Russia*

Radio-absorbing materials are materials, composition and structure which ensures effective absorption of electromagnetic energy in a certain wavelength range.

The purpose of this work is to determine the parameters that characterize a comprehensive study of microwave absorption of new composites based on ferroelectrics and multiferroics.

The samples are placed in the waveguide and closes with two foam for fixing of the measuring sample in the measuring path of the line. Measurements in a wide frequency range of module and phase, using a vector network analyzer (P4M-18, Micran),  $S_{11}$  and  $S_{21}$ .

The complex permittivity  $\epsilon$  is sought from the condition of minimizing the sum of squared deviations of measured and calculated  $S_{11}$  and  $S_{21}$ . The calculations are carried out using commercial software CSTMicrowaveStudio. This task is multi-parameter, since  $\epsilon$  depends on the frequency.

In the absence of dissipative losses, the energy conservation law gives the following relationship between the modules of the coefficients of the scattering matrix:  $S_{11}^2 + S_{21}^2 = 1$ ;  $S_{12}^2 + S_{22}^2 = 1$ . Further calculations in the following formulas: Let the matrix elements of the measuring line without a sample  $S_{ij}^0$ , and the elements of the scattering matrix of the measurement line with the sample  $S_{ij}$ ; The absorption line measurement without a sample  $L_0 = 1 - |S_{11}^0|^2 - |S_{21}^0|^2$ ; The absorption of the measuring line with the sample  $L_1 = 1 - |S_{11}|^2 - |S_{21}|^2$ ; The microwave absorption of the sample is calculated as follows  $L = L_1 - L_0 = (1 - |S_{11}|^2 - |S_{21}|^2) - (1 - |S_{11}^0|^2 - |S_{21}^0|^2) = |S_{11}|^2 - |S_{21}|^2 - |S_{11}^0|^2 - |S_{21}^0|^2$ ; Find a complete absorption of the measured sample:  $1 - L$ .

This work was financially supported by the Ministry of Education and Science of the Russian Federation: themes №№ 1927, 213.01-2014/012-VG and 3.1246.2014/K (the basic and project parts of the state task), Grant of President of Russian Federation № SP-3330.2016.3.

**Formation of the crystalline structure and properties of complex heterogeneous system «BiFeO<sub>3</sub>» by solid phase synthesis**

L.A. Shilkina, L.A. Reznichenko, I.A. Verbenko

*Research Institute of Physics, Southern Federal University, 344090 Rostov-on-Don, Russia*

*ilich001@yandex.ru*

Speed, performance and memory capacity of computers is constantly growing in full accordance with the famous Moore's law (performance of computers doubles every two years). However, further improvement of information technology involves the creation of new materials that combine several ways to record, store and play back data. High-temperature multiferroics are the most promising in this area. In this case bismuth ferrite has record potential operating temperatures. However, there are a number of technological factors that hinder its practical application. They are thermodynamic instability, insufficiently high magnetoelectric coefficients, high coercive fields and conductivity.

In this work the processes of phase formation BiFeO<sub>3</sub> were investigated. It was established that the mechanism of phase formation in the Bi<sub>2</sub>O<sub>3</sub>-Fe<sub>2</sub>O<sub>3</sub> system by solid-phase synthesis is realized with the participation of impurity phases (Bi<sub>25</sub>FeO<sub>40</sub>, Bi<sub>2</sub>Fe<sub>4</sub>O<sub>9</sub>). This leads to local stoichiometry disturbances, partial loss of oxygen, the appearance of oxygen vacancies, which are clustering and removed by crystallographic shear. At temperatures above 800°C vacancies are ordered and more complex macroscopic the defects appear. Then, degradation and slow processes of decomposition ceramics are occurred. This leads to increased instability of dialectical properties.

This work was financially supported by the Ministry of Education and Science of the Russian Federation: themes №№ 1927, 213.01-2014/012-VG and 3.1246.2014/K (the basic and project parts of the state task). Scholarship of President of Russian Federation № SP-3197.2016.3. The work performed on equipment of Collective use center "Electromagnetic, electromechanical and thermal properties of solids" of the Research Institute of Physics, Southern Federal University.

## Relaxation of polarization in $(\text{K}_{0.5}\text{Na}_{0.5})(\text{Nb}_{0.93}\text{Sb}_{0.07})\text{O}_3$ ferroelectric ceramics modified by $\text{BaTiO}_3$

A.I. Burkhanov<sup>1</sup>, K. Bormanis<sup>2</sup>, G.M. Akbaeva<sup>3</sup>, A.V. Zhirkov<sup>1</sup>, M. Antonova<sup>2</sup>, M. Livinsh<sup>2</sup>

<sup>1</sup>Volgograd State University of Architecture and Civil Engineering, Volgograd, 400074, Russia  
burkhanov@inbox.ru

<sup>2</sup>Institute of Solid State Physics, University of Latvia, Riga, LV-1063, Latvia

<sup>3</sup>Institute of Physics, Southern Federal University, Rostov-on-Don, 344090, Russia

Due to the high toxicity lead and lead compounds do not meet modern ecological requirements for which reason in recent years attention is paid to lead-free ferroelectric materials. Solid solutions on the basis of alkali metal niobates, for example, potassium sodium niobate (KNN), are considered the most promising at the moment [1].

We have studied the low- and infra-low processes of polarization relaxation in  $(1-x)(\text{K}_{0.5}\text{Na}_{0.5})(\text{Nb}_{0.93}\text{Sb}_{0.07})\text{O}_3-x\text{BaTiO}_3+0.5\text{mol.}\% \text{MnO}_2$  ( $x = 0.02, 0.04$ ) (KNNSB- $x$ ) ceramics prepared by conventional solid-state sintering [2]. The temperature dependence of the effective dielectric permittivity  $\epsilon'_{\text{eff}} = P/(\epsilon_0 \cdot E)$  and dielectric loss  $\epsilon''_{\text{eff}} = S/(\epsilon_0 \cdot \pi \cdot E^2)$ , where  $P$  – polarization,  $E$  – the amplitude of the sinusoidal field employed to measure polarization loops,  $\epsilon_0$  – electric constant, and  $S$  – the loop area of the sample with  $x = 0.02$  in the region of the broad tetragonal-to-orthorhombic phase transition at  $T \sim 70\text{-}90^\circ\text{C}$  are shown in Fig. 1.

It is found, that, despite of the essential diffusion of the para-electric to ferroelectric phase transition caused by barium additives to the KNN ceramics, the features of the polarization relaxation in the investigated samples noticeably differ from the behavior of the low frequency relaxations in relaxors on the basis of PMN.

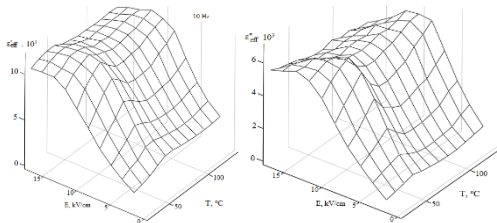


Figure 1. Effective dielectric permittivity  $\epsilon'_{\text{eff}}$  and dielectric loss  $\epsilon''_{\text{eff}}$  as functions of the sinusoidal field intensity and temperature of KNNSB-0.02.

1. H.E. Mgbemere, R.P. Herber, G.A. Schneider, *Journal of the European Ceramic Society* **29**, 3273 (2009).
2. I. Smeltere, M. Antonova, A. Kalvane, K. Bormanis, M. Livinsh, *Physics of the Solid State* **54**, 994 (2012).

## Formation of nanodomain structures in ferroelectric films by interfering hypersound beams

V.V. Krutov, A.S. Sigov, A.A. Shchuka

Moscow Technological University MIREA, 119454, Moscow, Russia  
v\_krutov@mirea.ru, <http://www.mirea.ru>

Description of double pulse heterothermal technology for quick formation of regular domain structures (RDS) by means of hypersound is presented in [1]. The technological setup is intended for RDS formation both in volumetric *c*-cut ferroelectric crystals and in *c*-axis-oriented ferroelectric films.

The essential advantage of this technique is the short work cycle duration, commensurable with the domain switching time. There is the basis to expect the record-breaking short work cycle duration  $t \leq 0.25$  ms of RDS formation in PZT films.

New data [2] on the influence of sample thickness on thermal characteristics testify to reduction of thermal diffusivity coefficient at reduction of thickness. This fact creates rather favorable conditions of application of double pulse heterothermal technology for formation of micro- and nanodomain structures in films and thin samples since it allows one to create "long-living" temperature lattices.

Conditions of RDS formation by means of the technology in view of new data on heat transfer in films are defined and estimated values of the basic technological parameters of RDS formation in PZT samples are received.

By our estimations (and on the basis of data [2]) for PZT demanded microwave generator power decreases approximately 2 times at reduction of sample thickness from 1 mm to 0.24 mm and less.

It is shown that for RDS formation with the period of 800 nm (similar structures in PZT are created in [3]) it is required microwave generator power no more than 20 mW. The obtained power value is much less than the power of serially released measuring microwave generators.

1. V.V. Krutov, A.S. Sigov, A.A. Shchuka, *Ferroelectrics* **476**, 69 (2015).
2. O.V. Malyshkina, A.A. Movchikova, O.N. Kalugina, A.V. Daineko, *Ferroelectrics*, **424**, 28 (2011).
3. A.K.S. Kumar, P. Paruch, J. Triscone, *Appl. Phys. Lett.* **85**, 1757 (2004).

**Dielectric response of thin film structures based on PZT**

M.V. Kamenshchikov<sup>1</sup>, A.V. Solnyshkin<sup>1</sup>, I.P. Pronin<sup>2</sup>

<sup>1</sup>*Department of condensed matter physics, Tver State University, 170002, Tver, Russia  
Mikhailkamenshchikov@yandex.ru*

<sup>2</sup>*Laboratory ferroelectricity and magnetism physics, Ioffe Institute, 194021,  
St. Petersburg, Russia*

Recently thin films are widely used in microelectronics. PZT-based structures occupy one of leading position among the materials for microelectromechanical systems (MEMS), microwave devices, piezoelectric and pyroelectric sensor devices, etc. However, some properties of thin PZT films are not well understood. The aim of this work was to investigate dielectric properties of PZT-based thin films according to synthesis temperatures.

Thin film capacitor structures of Pt/PZT(54/46)/Pt were studied in this work. The films were deposited on silicon substrates by two-stage (ex-situ) RF-magnetron sputtering method. The PZT layer was produced with excess of lead oxide and then annealed at temperatures  $T_{\text{ann}} = 540 - 570$  °C. The thickness of the PZT layer is about 500 nm.

C-V characteristics were obtained to determine the internal electric fields of the Pt/PZT(54/46)/Pt structures. The value of the internal field was determined from an offset of capacitance-voltage characteristics peak along the y-axis. The peak offsets for films synthesized at temperatures of 540 – 550°C increase reaching a maximum value at  $T_{\text{ann}} = 550$ °C and then decreases in the region of 555 – 570°C. The extremum (minimum) of dependences of dielectric constant on the synthesis temperature were observed at  $T_{\text{ann}} = 550-555$ °C too. The reason of extremes dependences with increasing of the synthesis temperature is the microstructure change of the samples. These films consist of spherulitic polycrystalline blocks, the size of which at temperatures of 540 – 570°C first decreases and then increases reaching a minimum value at  $T_{\text{ann}} = 550$ °C. Another significant factor affected the properties of the films is the content of the excessive lead in PZT. The dependence of excessive lead content in the studied films with increasing synthesis temperature demonstrate a maximum at  $T_{\text{ann}} = 550$ °C.

The influence of the frequency and the amplitude of the test signal on the properties of the capacitance-voltage characteristics were obtained for analyze the contribution of the domain mechanism to the dielectric response of these structures. It was determined that the dielectric constant of the ferroelectric film is not associated with a domain mechanism must be determined from the high-frequency measurement in the smallest test signal at the large bias.

This work was supported by RFBR, project № 16-32-00420 mol\_a.



**The theoretical investigation of the structural transitions in thin ferroelectric films**

T.O. Petrova<sup>1</sup>, R.A. Gerasimov<sup>1</sup>, O.G. Maksimova<sup>2</sup>, A.V. Maksimov<sup>2</sup>

<sup>1</sup>*Mathematics, Mechanics and Computer Sciences, Southern Federal University, 344006, Rostov-on-Don, Russian Federation*  
*to\_87@bk.ru*

<sup>2</sup>*Physics Department, Cherepovets State University, 162600, Cherepovets, Russian Federation*

The purpose of this study is to investigate the influence of free surface on structural phase transitions from an ordered to a disordered state in thin ferroelectric films.

We used the modified version of the classic three-dimensional the anisotropic Heisenberg model, energy constants of which are determined by the chemical structure of films. The temperature dependences of the long-range orientational order parameter (the average cosine of the angle between dipoles and the direction of their preferred orientation) are calculated for different film thickness. We take into account a depolarization field, which arises on the free surface of the ferroelectric. It is assumed that the this field proportional to the order parameter and its value is determined from the condition of self-consistency. Calculations are carried out on the base of the Monte Carlo method. The dependences of the order parameter on the distance from the free surface are calculated.

It is shown that the effective thickness of the surface layer depends on the temperature of the film. Nearby the phase transition point, its thickness increases indefinitely.

This study was funded by Russian Science Foundation (the research project No.15-19-10008).

## Piezoresponse force microscopy studies of domains in $\text{PbFe}_{1/2}\text{Nb}_{1/2}\text{O}_3$ ceramics

M.A. Bunin, I.P. Raevski

*Research Institute of Physics and Faculty of Physics, Southern Federal University, 344090, Rostov-on-Don, Russia*

*bunin.m.a@gmail.com*

$\text{PbFe}_{1/2}\text{Nb}_{1/2}\text{O}_3$  is a promising basic material for many applications. However up to now there is no data on its domain structure. The scope of the present work was the study of  $\text{PbFe}_{1/2}\text{Nb}_{1/2}\text{O}_3$  ceramics by piezoresponse force microscopy (PFM) method. At room temperature this ceramics has a rhombohedral symmetry. The measurements were performed using AFM Veeco Multimode VS and MESP tip with spring constant value  $k \sim 3.5$  N/m. Conventional contact-mode PFM technique was used. The surface topography (1), the PR amplitude (2) and Inphase (3) (amplitude of the PR signal is multiplied by the sine of the phase signal) images were obtained simultaneously (Figure 1). The surface topography image (1) shows that intergrain boundaries

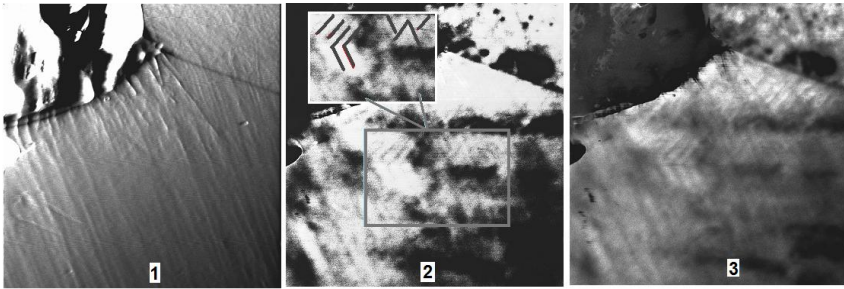


Figure 1.  $5 \times 5 \mu\text{m}^2$  PFM images of the polished  $\text{PbFe}_{1/2}\text{Nb}_{1/2}\text{O}_3$  ceramics' surface.

in the ceramics studied are very thin. Both PR and PR Inphase images (2) and (3) demonstrate the presence of parquet-like stripes pattern within the grain. For the PR- amplitude image (2) the most distinct area is highlighted in the inset in panel (2) where these stripes are outlined by bold lines. The angles between the stripes appeared to be either  $110 \pm 4^\circ$  (in the left part of the inset) or  $67 \pm 4^\circ$  (in the right part of it). These stripes seem to be ferroelectric domains. Very similar patterns of  $110^\circ$ -domains were observed by electron microscopy in the  $0.9\text{PbFe}_{1/2}\text{Nb}_{1/2}\text{O}_3 - 0.1\text{PbZrO}_3$  rhombohedral ceramics.

This work was partially supported by Ministry of Education of the Russian Federation (research project 2132).

## A comparative x-ray diffraction study of ferroelectric thin films and superlattices

Y.A. Tikhonov<sup>1</sup>, A.G. Razumnaya<sup>1</sup>, Y.I. Yuzyuk<sup>1</sup>, I.N. Zakharchenko<sup>1</sup>,  
Sh. Pavunny<sup>2</sup>, N. Ortega<sup>2</sup>, A. Kumar<sup>2</sup>, R.S. Katiyar<sup>2</sup>

<sup>1</sup>*Faculty of Physics, Southern Federal University, 344090, Rostov-on-Don, Russia*  
tikhonov.yuri@yandex.ru

<sup>2</sup>*Department of Physics and Institute for Functional Nanomaterials, University of Puerto Rico, San Juan, PR 00931-3343 USA*

Currently ferroelectrics can be used as components of microelectronic devices to enhance their properties, reduce size or decrease power consumption. Properties of ferroelectrics highly depend on their structure, which can be tuned in a variety of ways in ferroelectric superlattices, bringing new possibilities for creation of functional devices with outstanding performance.

Structural features of a number of ferroelectric thin films  $\text{Ba}_{1-x}\text{Sr}_x\text{TiO}_3$  and two types of superlattices  $\text{BaTiO}_3/\text{Ba}_{1-x}\text{Sr}_x\text{TiO}_3$  and  $\text{BaTiO}_3/\text{Ba}_{0.5}\text{Sr}_{0.5}\text{TiO}_3$  were investigated using x-ray diffraction. All specimens were synthesized on the MgO (001) substrates by pulsed laser deposition technique. Concentration of strontium in thin films varied from 0.0 to 0.7 as in BST layers of  $\text{BaTiO}_3/\text{Ba}_{1-x}\text{Sr}_x\text{TiO}_3$  superlattices.  $\text{BaTiO}_3/\text{Ba}_{0.5}\text{Sr}_{0.5}\text{TiO}_3$  superlattice samples distinguished by number of laser pulses used to vaporize individual components ( $\text{BaTiO}_3$ ,  $\text{Ba}_{0.5}\text{Sr}_{0.5}\text{TiO}_3$ ) which resulted to different values of modulation period. Values of microstrains and sizes of coherent scattering regions were estimated using numerical data treatment. In addition, modulation period of superlattices was calculated. The unit cells parameter  $c$  in the direction normal to substrate was evaluated from experimental diffraction patterns for all samples.

Parameter  $c$  decreases linearly as concentration of strontium increases in  $\text{Ba}_{1-x}\text{Sr}_x\text{TiO}_3$  thin films. All thin film samples show high structural quality. Diffraction patterns of all superlattice samples revealed presence of main peak and satellites. Structural quality of  $\text{BaTiO}_3/\text{Ba}_{1-x}\text{Sr}_x\text{TiO}_3$  superlattices enhances with increasing concentration of strontium. Structural quality of  $\text{BaTiO}_3/\text{Ba}_{0.5}\text{Sr}_{0.5}\text{TiO}_3$  samples enhances with increasing periodicity. We discuss the structural features of the samples and compare distinctive traits of thin films and superlattices.

This study was supported by the Russian Science Foundation (grant N 14-12-00258).

## Electric response of lithium niobate thin film structures

K.D. Baklanova<sup>1</sup>, S.I. Gudkov<sup>1</sup>, M.V. Kamenshchikov<sup>1</sup>, A.V. Solnyshkin<sup>1</sup>,  
D.A. Kiselev<sup>2</sup>

<sup>1</sup>*Department of condensed matter physics, Tver State University, 170002, Tver, Russia  
cauchyandtaylor@gmail.com*

<sup>2</sup>*Department of materials science, semiconductors and dielectrics, National University  
of Science and Technology MISiS, 119049, Moscow, Russia*

Lithium niobate  $\text{LiNbO}_3$  (LN) is a promising ferroelectric material for optoelectronic and microelectronic devices. However, some properties of LN thin films are not well explored. The aim of this work was to investigate photoelectric and dielectric properties of LN thin films according to synthesis method.

Thin film Cu/LN/Si and Al/LN/ITO structures were studied in this work. The films were deposited on substrates by RF-magnetron sputtering and laser ablation methods. The thickness of the LN layer ranged from 100 to 500 nm.

Electric response was obtained by illuminating the sample rectangular modulated pulses with frequency range from 1 Hz to 20 kHz. The radiation source was a laser module CLM - 1845 IR - 980. Radiation wave-length was 980 nm, power - 220 mW. Fig. 1 shows kinetics of electric response of LN thin

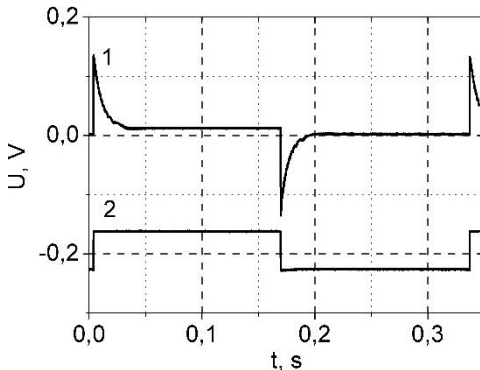


Figure 1. Kinetics of electric response of Cu/LNO/Si thin films (1). (2) – Reference signal: frequency – 3 Hz, wave-length – 980 nm, power – 220 mW.

films deposited by RF-magnetron sputtering methods. It is easy to see that response consist of two parts: unstationary and stationary signals ("shelf"). Kind of response such as "shelf" indicates the presence of stationary photoconductivity in these structures. The photocurrent short-circuited about 0.05 V.

*I-V* characteristics of this film a similar to a diode characteristics. Current limited by space charge is the main conduction mechanism.

Dielectric response of LN thin films was investigated. Also the influence of films microstructure on their electrophysical characteristics is discussed.

This work was supported by RFBR, project № 16-32-00420 mol\_a.

## Electromechanical properties of Gd-doped ceria ceramics and thin films measured by laser interferometry

A. Ushakov<sup>1</sup>, E. Mishuk<sup>2</sup>, N. Yavo<sup>2</sup>, V. Ya. Shur<sup>1</sup>, A.L. Kholkin<sup>1,3</sup>,  
I. Lubomirsky<sup>2</sup>

<sup>1</sup>*Institute of Natural Sciences, Ural Federal University, Ekaterinburg 620026, Russia  
bddah23@gmail.com*

<sup>2</sup>*Department of Materials and Interfaces, Weizmann Institute of Science, Rehovot 76100, Israel*

<sup>3</sup>*Physics Department & CICECO-Aveiro Institute of Materials, University of Aveiro, 3810-193 Aveiro, Portugal.*

Materials developing mechanical stress/strain in response to applied electric field have found numerous applications in the modern science and technology. In electrostrictive materials such as  $\text{PbMg}_{1/3}\text{Nb}_{2/3}\text{O}_3$  the electrostriction coefficient typically increases with decreasing of dielectric constant and mechanical stiffness and can reach  $10^{-16} \text{ m}^2/\text{V}^2$  at best. Recently Korobko et al<sup>1</sup> have found that the oxide materials with high enough concentration of oxygen vacancies (e. g. Gd-doped ceria) can develop giant electrostriction well beyond the expectations.

In this work, we report the study of Gd-doped ceria electromechanical performance by Michelson interferometer<sup>2</sup> (sensitivity up to 5 femtometers). Measurements in thin films and bulk ceramics (Fig. 1) revealed a strong dependence of the electrostriction signal on the driving frequency. This fact was attributed to the high resistance of electrodes. Measurement on thin films (single beam interferometer) showed a strong substrate bending similar to that of PZT thin films. Time dependences of the electrostriction in Gd-doped ceria will be reported as well. The mechanisms of the giant electrostriction will be discussed.

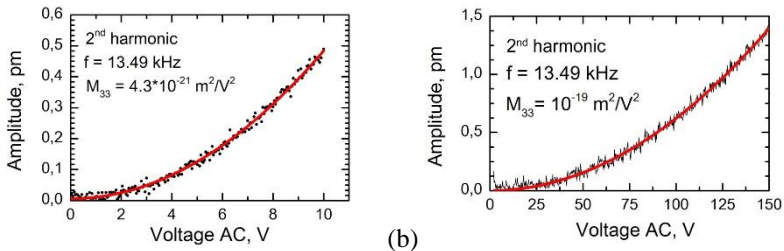


Figure 1. Voltage dependencies of the displacements of CGO-based (a) thin films and (b) bulk ceramics.

1. R. Korobko, A. Patlolla, A. Kosoy, E. Wachtel, H.L. Tuller, A.I. Frenkel, I. Lubomirsky, *Adv. Mat.* **24**, 5857 (2012).
2. A. Kholkin, C. Wüthrich, D. Taylor, N. Setter, *Rev. Sci. Instr.* **67**, 1935 (1996).

## Application of tip enhanced Raman scattering on various nanostructural objects

V.Ya. Shur<sup>1</sup>, M.S. Nebogatikov<sup>1</sup>, A.A. Arkhipov<sup>1</sup>, A.N. Arkhipova<sup>2</sup>,  
S.G. Kazarian<sup>2</sup>

<sup>1</sup>*Ural Federal University, 620000, Yekaterinburg, Russia*  
*alexey.arkhipov92@gmail.com*

<sup>2</sup>*Imperial College London, London, Great Britain*

Enhancement of Raman scattering on the surface of metal nanoparticles (Ag, Au, Cu) with sizes ranged from 10 to 100 nm is connected with the excitation of plasmon resonance that increase the local electric field inside of nanoparticles, and intensity of RS signal, which is proportional to the field [1].

Tip enhanced Raman scattering (TERS) has been realized by using: (1) gold coated silicon AFM tips and (2) silver tips electrochemically etched from wire with diameter 0.3 mm in a drop of 10% aqueous HNO<sub>3</sub> solution. The tip's radius was achieved down to 30 nm, which was enough to observe enhancement of the Raman signal. The hot spot with enhanced signal was detected for various materials. The TERS microscopy was applied for rhodamine 6G inhomogeneity (Fig. 1) and the bundle of carbon nanotubes. The obtained resolution of the images about 50 nm is significantly better than the resolution of images obtained by confocal microscopy.

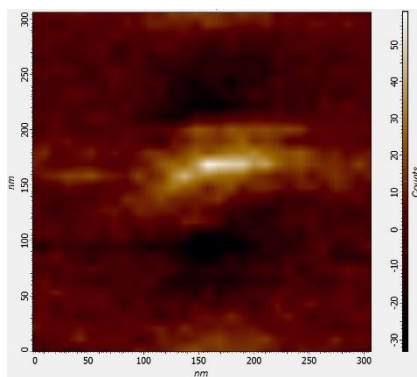


Figure 1. Image of the rhodamine 6G inhomogeneity obtained by TERS microscopy.

3. M. Fleischmann, P.J. Hendra, A.J. McQuillan, *Chem. Phys. Lett.* **26**, 163 (1974).

## Study of mechanical properties of ferroelectric metamaterials using computer modelling

R.A. Gerasimov<sup>1</sup>, V.A. Eremeyev<sup>1</sup>, T.O. Petrova<sup>1</sup>, V.I. Egorov<sup>2</sup>, O.G. Maksimova<sup>2</sup>, A.V. Maksimov<sup>2</sup>

<sup>1</sup>*Southern Federal University, 344006, Rostov on Don, Russia  
roman-gerasimoff@yandex.ru*

<sup>2</sup>*Cherepovets State University, 162602, Cherepovets, Russia*

For hybrid discrete-continuous model describing system consisting of flexible substrate and ferroelectric polymeric coating we provide computer modelling of its mechanical properties on different levels of stretching and bending deformations and at various temperatures. The substrate is modelled within the linear elasticity with the Hooke law while for the coating we use the discrete model. For description of interactions in polymeric coatings we implement the Stockmayer potential. The latter is a Lennard-Jones potential with additional term which describes the dipole interactions that is the Keesom energy. Using the Monte-Carlo method with the Metropolis algorithm the equilibrium configuration of the system is determined. We obtain dependencies of the energy, force, bending moment and Young's modulus for various levels of deformations and for different values of temperature. We demonstrated that in the polymeric coating there is a deformation induced structural transition from ordered ferroelectric state to unpolarized one. So, the surface polymeric coating gradually ceases to affect the dynamics of the investigated system dependencies of parameters for tension and for bending. The comparison of theoretical results with known experimental data on deformations of similar systems.

1. R.C. Advincula, W.J. Brittain, K.C. Caster, J. R  he, *Polymer Brushes: Synthesis, Characterization, Applications*, 483 (2004)
2. A.V. Maksimov, O.G. Maksimova, *Polymer Science*, **45**, 859 (2003)
3. O.I. Vinogradova, A.V. Belyaev, *J. Phys.: Condens. Matter* **23**, 184104 (2011).
4. J. Bico, U. Thiele, D. Quere, *Colloid Surf. A: Physicochem* **206**, 41 (2002).

**Tricolor ferroelectric superlattice**A.G. Razumnaya<sup>1</sup>, Yu.I. Yuzyuk<sup>1</sup>, N. Ortega<sup>2</sup>, R.S. Katiyar<sup>2</sup><sup>1</sup>*Southern Federal University, Faculty of Physics, Rostov-on-Don, 344090, Russia  
razumnaya2@yandex.ru*<sup>2</sup>*University of Puerto Rico, San Juan, Puerto Rico, 00931 United States*

The superlattices consisting of several alternating ferroelectric layers with repeated periods can possess better functional parameters over one-component thin films of the same compositions or have new properties which are not observed in individual layers. In the present work, the tricolor BaTiO<sub>3</sub>/(Ba<sub>0.5</sub>Sr<sub>0.5</sub>)TiO<sub>3</sub>/SrTiO<sub>3</sub> (BT/BST/ST) superlattice was grown by pulsed laser deposition on a cubic (001) MgO substrate. The total thickness of superlattice was about 1 μm. The sample was studied using X-ray diffraction with the aim to determine the structural characteristics provided by the lattice mismatch between the alternating layers. To reveal the lattice dynamics we performed micro-Raman study in a broad temperature range of 80–700 K.

The modulation period, the lattice parameters of the layers and orientation relationships between the layers and the substrate were determined by X-ray diffraction. It was found that the modulation period of the BT/BST/ST superlattice is 150 Å and the unit cell parameters *c* of the BT, BST, and ST layers are 0.4080 nm, 0.3935 nm, and 0.3926 nm, respectively.

An analysis of the temperature-dependent Raman spectra of the BT/BST/ST superlattice showed that the frequency of the *E*(TO) soft mode is 90 cm<sup>-1</sup> at 80 K and monotonically increases with temperature up to 103 cm<sup>-1</sup> at 600 K with simultaneous increase in its half-width from 90 to 140 cm<sup>-1</sup>. The temperature dependence of the integrated intensity of *E*(TO) soft mode suggests that the BT/BST/ST superlattice undergoes a transition from the ferroelectric to paraelectric phase at ~ 610 K and Curie temperature is upshifted with respect to bulk BT (*T*<sub>c</sub> ~ 398 K).

Thus, the application of layers of different compositions when preparing multilayer superlattices makes it possible to produce heterostructures with desirable characteristics and to perform a fine adjustment of their parameters due to the deformations of alternating epitaxial layers.

This study was supported by the Russian Science Foundation (grant N 14-12-00258).



## **Destruction of cpm and simulation of currents time dependence in cpm at simultaneous action of an electric field and mechanical load**

P.A. Bakulin, I.V. Kochergin, L.V. Zhoga

*Federal State Educational Institution of Higher Professional Education Volgograd State University of Architecture and Civil Engineering, Volgograd, 400074, Russia  
todestriebe@ya.ru*

Operating conditions piezoceramic elements in external mechanical (MP) and electrical fields (EP) do the actual study of the properties of such materials and their resistance to cyclic and extreme loads, which can lead to loss of the electrical properties and even to destruction. In this work, the task - to get the dependence of ferroelectric destructive stress on the external electric field, using a relaxation model of brittle solids [1].

Samples examined in a static electric field along the polarization against polarization and annealed at 500 ° C. The paper presents experimental results of durability and leakage current versus time for the ferroelectric PZT, part of which lies in the vicinity of the area morphotropic from rhombohedral border. Data are presented as computer modeling relaxation processes by which it can be said that the change in circuit current due to a change in the model occurrence ferroelectric polarization current in [1-3] by Shil'nikov and Nesterov coefficients, but their ratio, which shows how the conductivity of the sample is changed slightly.

Reducing ferroelectric strength in the electric field is the result of not only the emergence of local elastic stresses due to the inverse piezoelectric effect, but also the relaxation in the process of destruction.

Mechanical load significantly affects the appearance of the kinetic characteristics of the leakage current in the case of small electric field strengths, and significantly weaker at high electric fields. Qualitatively, the effect is also different, namely, in the case of small (less than half the electrical strength) electric field leakage current increases, and in the case of large (before electric/mechanic breakdown) it decreases.

1. V.V. Shpeizman, L.V. Zhoga, *Physics of Solid State* **47**, 843 (2005).
2. V.N. Nesterov, A.V. Shil'nikov, *Ferroelectrics* **265**, 153 (2002).
3. A.V. Shil'nikov, V.N. Nesterov, A.I. Burkhanov, *Ferroelectrics* **175**, 145 (1996).

## Specialties of low-frequency relaxation of ferroelectric ceramics (PZT)

Yu. I. Yurasov<sup>1,2</sup>, A.V. Turik<sup>1</sup>, L. A. Reznichenko<sup>1</sup><sup>1</sup>Research Institute of Physics, Southern Federal University, 344090, Rostov-on-Don, Russia

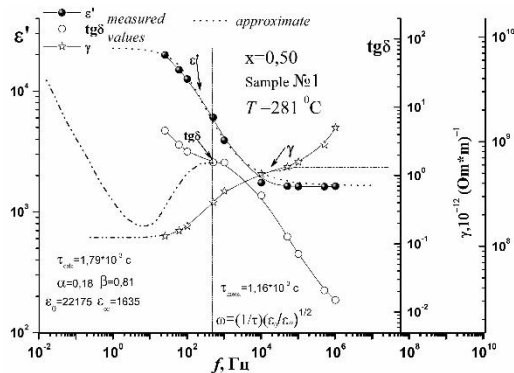
yucomp@ya.ru, ip.sfedu.ru

<sup>2</sup>Southern Scientific Centre Russian Academy of Sciences, 344006, Rostov-on-Don, Russia

The report presents the analysis of temperature dependency of electric conductivity  $\gamma$ , real and imaginary parts of dielectric constant  $\epsilon'$ ,  $\epsilon''$ . It has indicated the specific features of relaxation processes within the system  $(1-x)\text{PbZrO}_3-x\text{PbTiO}_3$  (PZT) in the range of alternating electric field with frequency ranging from  $4 \cdot 10^{-1}$  to  $10^5$  Hz. The field of deep relaxation of  $\gamma$ ,  $\epsilon'$ ,  $\epsilon''$  has been defined.

Figure 1 (for sample  $x=0.50$  ( $T=281^\circ\text{C}$ )) shows both the dependence of measured quantity  $\epsilon'$ , dielectric loss factor  $\text{tg}\delta$  and  $\gamma$  from  $f$  and the graph  $\epsilon'(f)$ , approximated using a formula Gavriiliak-Negami (dash-line), and “reconstructed” graphs  $\text{tg}\delta(f)$  and  $\gamma(f)$ .

Relaxation timing using a formula in Fig. 1 has resulted in  $\tau_{\text{meas}}=1,16 \cdot 10^{-3}$  that corresponds with  $\tau_{\text{calc}}=1,79 \cdot 10^{-3}$  c, defined in accordance with approximate formula Gavriiliak-Negami.

Figure 1. Dependence  $\epsilon'(f)$ ,  $\text{tg}\delta(f)$  and  $\gamma(f)$ .

The report considers physical mechanisms of the observed phenomena.

This work was financially supported by the Ministry of Education and Science of the Russian Federation: themes №№ 1927, 213.01-2014/012-VG and 3.1246.2014/K (the basic and project parts of the state task).

## Correlations structure, prehistory of thermodynamic, crystal structure, landscape of grain, and the macroscopic properties in ferroelectric ceramics with alkali and alkaline earth metal niobates

J.Y. Zubarev, L.A. Shilkina, L.A. Reznichenko

Research Institute of Physics, Southern Federal University, 344090 Rostov-on-Don, Russia  
yzubarev@sfnu.ru

Features of modern technology are the intensification of the processes associated with the growth of temperatures and frequencies. Put forward more stringent requirements for the selection of functional materials thermally loaded structures. It seems reasonable to use for this purpose the ferroelectric ceramic composition:  $(1-x)\text{NaNbO}_3 - x\text{Sr}_2\text{Nb}_2\text{O}_7$  - (SSI) and  $(1-x)\text{NaNbO}_3 - x\text{Ca}_2\text{Nb}_2\text{O}_7$  - (SSII), where  $\text{NaNbO}_3$  – antiferroelectric (AFE) it's a composite with a Curie temperature is ( $T_C$ ) 630K,  $\text{Sr}_2(\text{Ca}_2)\text{Nb}_2\text{O}_7$  - it is layered (L) perovskite (P) ferroelectrics (FE) with  $T_C = 1600\text{K}$  и  $T_C = 2100\text{K}$ , respectively.

The figure shows the phase diagrams of SSI, SSII; the independence of the major electrical characteristics from  $x$ . The report discusses the details of the established correlations structure, prehistory of thermodynamic, crystal structure, landscape of grain, and the macroscopic properties and draw a conclusion about the practical applicability of solid solution near  $\text{NaNbO}_3$  - in microwave technology; near  $\text{Sr}_2(\text{Ca}_2)\text{Nb}_2\text{O}_7$  in a high-temperature technology.

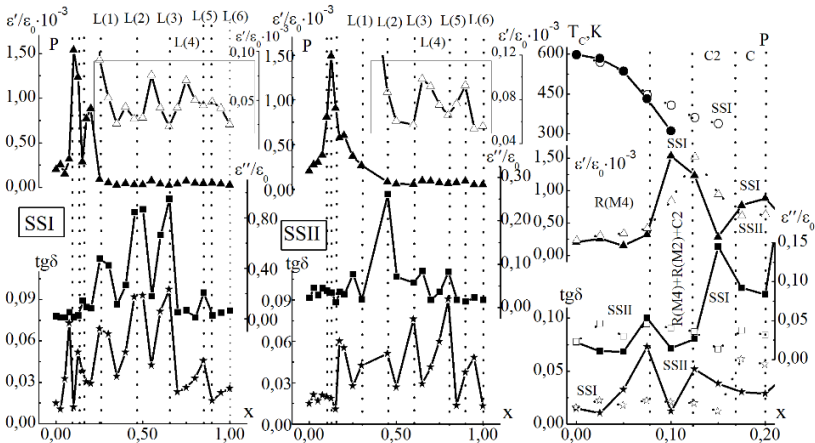


Figure 1. Dependences of  $\varepsilon'/\varepsilon_0$ ,  $\varepsilon''/\varepsilon_0$ ,  $\text{tg}\delta$  и  $T_C$  from  $x$ .

This work was financially supported by the Ministry of Education and Science of the Russian Federation: themes №№ 213.01-11/2014-21, 213.01-2014/012-БГ, and 3.1246.2014/К), СП-1689.2015.3, and performed on equipment of Collective use center of Southern Federal University.

**Piezo ferroelectric ceramics based on highsensitivity functional composition**

I.N. Andryushina, K.P. Andryushin, L.A. Reznichenko, L.A. Shilkina

*Research Institute of Physics, Southern Federal University, 344090 Rostov-on-Don, Russia*

*futur6@mail.ru*

Electrically active piezoelectric materials that form the basis of modern piezotechnique for a long time not considered in classical physics of solids as an objects worthy of serious scientific research. A significant obstacle to its "path to physics" was the fact that in these "dirty", it was thought, the objects cannot be studied physical phenomena and laws, exempt from many uncontrollable factors. In connection with the above, the purpose of the work is to establish the regularities of the formation of the dielectric (loss), piezoelectric (piezo sensitivity) and ferroelastic (mechanical quality factor, Poisson's ratio, the speed of sound) based on the PZT- system without method of hot pressing (HP), but with preservation of properties, inherent of hot pressing samples. The objects of the study were made by solid solutions of three and four component systems (pure and modified): (1)  $\text{PbTiO}_3\text{-PbZrO}_3\text{-PbNb}_{2/3}\text{Zn}_{1/3}\text{O}_3\text{-PbNb}_{2/3}\text{Mg}_{1/3}\text{O}_3 + \text{MnO}_2$ , (2)  $\text{PbTiO}_3\text{-PbZrO}_3\text{-PbW}_{1/2}\text{Cd}_{1/2}\text{O}_3$ , (3)  $\text{PbTiO}_3\text{-PbZrO}_3\text{-PbW}_{1/2}\text{Cd}_{1/2}\text{O}_3 + \text{Ta}_2\text{O}_5$ , in which highly sensitive functional medium can be realized. All samples obtained by convention all ceramic technology (CCT), which includes a two-stage solid-phase synthesis.

The obtained results indicates that the resulting material (1) made by CCT, has good compatibility piezocharacteristic ( $\epsilon_{33}^T/\epsilon_0 = 416$  is the relative dielectric constant of the polarized samples,  $K_p = 0.35$  coefficient of electromechanical coupling of the planar oscillation modes,  $|d_{31}| = 38\text{pC/N}$  - piezoelectric modulus,  $|g_{31}| = 10.3 \text{ mV}\cdot\text{m}/\text{N}$ - piezoelectric coefficient (piezosensitivity),  $\text{tg}\delta = 1.45$  - the angle of dielectric losses,  $Q_M = 1224$ - mechanical quality factor) with samples of the material PCR-3, previously developed at research institute of physics SFU and obtained by HP method. However down of quality factor indicates that the production of this material by CCT, leading to an increase in its segnetosoft that confirmed an increase of dielectric loss tangent ( $\text{tg}\delta$ ) almost 3 times. This phenomenon is probably due to the higher conductivity of the object. In two other materials received by the CCT, the loss of property was about 30 %, in spite of very high relative density ( $\rho_{\text{rel}(1)} = 93,40 \%$ ;  $\rho_{\text{rel}(2)} = 95,10 \%$ ;  $\rho_{\text{rel}(3)} = 92,81 \%$ ), which can be explained by imperfection technology adapted to these two specific composition.

This work was financially supported by the Ministry of Education and Science of the RF: themes №№ 1927, 213.01-2014/012-VG and 3.1246.2014/K (the basic and project parts of the state task). Scholarship of President of RF № SP-3197.2016.3. The work performed on equipment of CUC "Electromagnetic, electromechanical and thermal properties of solids" of the Research Institute of Physics, Southern FU.

**Maxwell-Wagner effects in barium-strontium titanates and bismuth ferrite ferroelectric ceramics**

S.V. Khasbulatov, A.A. Pavelko, S.P. Kubrin, K.A. Sadykov, L.A. Reznichenko

*Research Institute of Physics, Southern Federal University, 344090, Rostov-on-Don, Russia*

*said\_yahaevich@mail.ru*

Solid solutions based on barium-strontium titanate (BST) and multiferroic bismuth ferrite ( $\text{BiFeO}_3$ ) occupy a special place among the known ferroelectric ceramic materials as the ancestors of materials families used, respectively, in the microwave technology and spintronics. Therefore, detailed investigations of the dielectric properties of the objects in a wide range of temperatures (10–800) K are of great interest.

Analysis of the results revealed at temperatures above the room one abnormal behavior of relative permittivity – the formation of one or more highly dispersive and relaxation maxima not related to the Curie temperature. The calculated parameters of the dielectric relaxation were characteristic of Maxwell-Wagner (MW) relaxation process, which is known to be associated with structural changes, and caused by changes at the grain structure level of the ceramics. Relaxation of this type occurs due to the presence of microscopic inhomogeneities in the dielectrics composition. It is often also referred to as polarization inhomogeneous dielectrics, or surface, or interlayer polarization, the cause of which is the accumulation of space charges or charges on the dielectric partition surfaces. It is shown that in the analyzed objects MW-relaxation may be associated with redox processes  $\text{Ti}^{4+} \leftrightarrow \text{Ti}^{3+}$ ,  $\text{Fe}^{3+} \leftrightarrow \text{Fe}^{2+}$ , and interphase rearrangements that are not accompanied by a change in the symmetry of the cell.

This work has been done on equipment of Collective use center "Electromagnetic, electromechanical and thermal properties of solids" of Institute of Physics, Southern Federal University.

This work was financially supported by the Ministry of Education and Science of the Russian Federation: themes №№ 1927, 213.01-2014/012-VG and 3.1246.2014/K (the basic and project parts of the state task).

## Composition, structure, electrophysical and thermofrequency properties sodium solutions of sodium-potassium-cadmium

K.P. Andryushin, I.N. Andryushina, L.A. Reznichenko, L.A. Shilkina

*Research Institute of Physics, Southern Federal University, 344090 Rostov-on-Don, Russia*

*kpandryushin@gmail.com*

Ferroelectric materials are widely used in electronic engineering (piezoelectric transmitters, pyroelectric infrared sensors and microwave telecommunication devices). Most of the piezoelectric ceramic materials are based on the lead- zirconate- titanate (PZT) system. However, there exists a group of Pb- free materials based on Na- Li and Na- K niobates possessing the unique properties. The closest to such materials in properties and answering the above- mentioned purposes are solid solutions (SSs) of the (Na, K)NbO<sub>3</sub> system that was chosen as a basic one.

The objects of study were the system  $(1-x-y)\text{NaNbO}_3 - x\text{KNbO}_3 - y\text{CdNb}_2\text{O}_6$  in which the first two components– NaNbO<sub>3</sub> ( $a = 5.512\text{Å}$ ,  $b = 5.557\text{Å}$ ,  $c = 15.54\text{Å}$ ) and KNbO<sub>3</sub> ( $a = 5.695(4)\text{Å}$ ,  $b = 5.7213(3)\text{Å}$ ,  $c = 3.9739(2)\text{Å}$ ) – crystallize in the perovskite structural type, while the third component (y) belongs to the columbite one with the following parameters:  $a = 5.848(4)\text{Å}$ ,  $b = 14.7817(10)\text{Å}$ ,  $c = 5.1419(4)\text{Å}$ . In what follows, its chemical formula will be reduced to the perovskite structural type ABO<sub>3</sub> (Cd<sub>0.5</sub>NbO<sub>3</sub>).

Four groups of SSs were found to have the promising parameters making them potentially attractive for being used in a midfrequency range ( $2000 < \varepsilon_{33}^T/\varepsilon_0 < 2250$ ), in UHF- devices ( $\varepsilon_{33}^T/\varepsilon_0 < 700$ ,  $K_P \sim 0.40$ ,  $V_1^E > 5.0$  km/s), in high- sensitivity accelerometers and ultrasonic flaw detectors ( $\varepsilon_{33}^T/\varepsilon_0 = 500 \div 700$ ,  $g_{33} \sim 30$  mV·m/N), and in the devices operating in force regimes ( $Q_M \approx 1000$ ,  $K_P \approx 0.20$ ).

In the region adjacent to NaNbO<sub>3</sub> there exists the interval of critical values of the total electronegativity of the A elements (473 ÷ 477 kJ/g.at.) being a division between the traditional inverse dependences of the dielectric permittivity on the homogeneous deformation parameter and the abnormal direct ones.

The report discusses the physical mechanisms of the observed phenomena.

This work was financially supported by the Ministry of Education and Science of the RF: themes №№ 1927, 213.01-2014/012-VG and 3.1246.2014/K (the basic and project parts of the state task). Scholarship of President of RF № SP-3197.2016.3. The work performed on equipment of CUC "Electromagnetic, electromechanical and thermal properties of solids" of the Research Institute of Physics, Southern FU.

**Surface modification of ZnO by plasma and laser treatment**

V.P. Afanasjev<sup>1</sup>, N.V. Mukhin<sup>1</sup>, G.A. Konoplev<sup>1</sup>, D.N. Redka<sup>1</sup>, E.I. Terukov<sup>2</sup>

<sup>1</sup>*Saint Petersburg Electrotechnical University "LETI", 197376 Saint-Petersburg, Russia  
dnredka@gmail.com*

<sup>2</sup>*A.F. Ioffe Physical-Technical Institute of the Russian Academy of Sciences, 194021  
Saint-Petersburg, Russia*

The aim of this work was to investigate the surface modification of zinc oxide, its optical and electrophysical properties by plasma and laser treatment.

The ZnO films were prepared by chemical vapor deposition using the organometallic compounds at a low pressure.  $(C_2H_5)_2Zn$  and deionized water were used as precursors. Their concentration ratio was  $[H_2O]:[DEZ] = 5:6$ . The ZnO films were doped by boron using a gas mixture of 2%  $B_2H_6$  in hydrogen.

Plasma treatment of Boron-doped ZnO aimed at surface modification of the films has been performed in RF magnetron sputtering systems at ambient temperature and typical pressure of about 60 Torr. For the treatment the samples were placed on a target holder directly above the magnet as the sputtered target. This position of the samples provides strong magnetic field in the vicinity of the treated sample which increases the efficiency of ionization of Ar atoms by electron impacts and, therefore, increases the density of plasma and flux of Ar ions toward treated surface. As a result one can expect decrease of the treatment time without increasing the RF power density [1]. The treatment times ranged from 5 to 17 minutes for the power density with typical value of  $1.3W/cm^2$ .

Laser treatment of ZnO films made at the wavelength 355 nm with various levels of radiation power density ( $6...24 GW/cm^2$ ). At high radiation power density an increase in surface resistance caused by violation of the uniformity of the film due to its partial destruction [2]. The samples were characterized by scanning electron microscopy, atomic force microscopy and Raman spectroscopy methods. Optical properties of films before and after the treatment were measured using SenSol Haze Tester system and Varian Cary 5000 spectrophotometer providing information on total and diffused transmission and thickness of the films. Electrical conductivity, carrier concentration, and mobility were measured by Ecopia HMS 5000 Hall Effect measurement system.

Optical and electrical properties (Haze spectra, carrier concentration, mobility, and resistivity) of ZnO thin films deposited on glass substrates were studied by plasma and laser treatment. It was shown that 5 min plasma treatment can be sufficient to perform a transformation of the surface morphology of ZnO layers from V-type to U-type without deterioration of optical and electrical properties. Longer treatment results in over flattening of the surface followed by reduction of light scattering along with degradation of electronic properties. By pulse laser treatment we can increase light scattering while maintaining the values of the electrical resistance.

The work was supported by the grant of the Russian Science Foundation (project № 14-12-00327).

1. D. Andronikov, A. Abramov, E. Terukov, A. Vinogradov, A. Ankudinov, V. Afanasjev, *Semiconductors* **49**, 823 (2015).
2. V.S. Levitskii, D.N. Redka, E.I. Terukov, *Ferroelectrics* **496**, 163 (2016)



## Graphene and polyvinylidene fluoride polymer ferroelectric composites for multifunctional applications

V.S. Bystrov<sup>1</sup>, I.K. Bdikin<sup>2</sup>, S. Kopyl<sup>3</sup>, G. Goncalves<sup>3</sup>, A.V. Sapronova<sup>4</sup>,  
T. Kuznetsova<sup>5</sup>, V.V. Bystrova<sup>6</sup>

<sup>1</sup>*Institute of Mathematical Problems of Biology RAS, 142290 Pushchino, Russia*  
vsbys@mail.ru

<sup>2</sup>*National Research University of Electronic Technology MIET, 124498 Moscow, Russia*

<sup>3</sup>*Dept. Mechanical Eng. & TEMA, University of Aveiro, 3810-193, Aveiro, Portugal*

<sup>4</sup>*UniResearch AS, University of Bergen, Norway*

<sup>5</sup>*University of Bergen, N-5008, Bergen, Norway*

<sup>6</sup>*Shmidt Institute of Physics of the Earth RAS, 123242 Moscow, Russia*

Multifunctional composites nanostructures with ferroelectric properties are very urgent for modern industry application [1]. The interest is focused on the graphene/graphene oxide (G/GO) and polyvinylidene fluoride (PVDF)/poly(vinylidene fluoride-trifluoroethylene) (P(VDF-TrFE)) piezo-/ferroelectric polymers, where G based nanostructures allowed us to create new porous nanomaterials, which provide new opportunities to develop emerging technologies for a molecular storage systems. Last study of the formation of CO<sub>2</sub>, CH<sub>4</sub>, N<sub>2</sub> hydrates in non-inter-lamellar structures in GO demonstrates that confinement and strong interaction of water with the hydrophilic surface of GO reduce water activity, that can lead to inhibition of gas hydrates nucleation [2] as highly functionalized GO surface interacts strongly with water molecules. Within the non-interlamellar structures, water readily crystallizes and transforms into solid phase such as hexagonal ice (the most energetically stable form). So, the development of related composite, based on G/GO/PVDF structures could be more useful for trapping gas hydrates. Another application of G/GO/PVDF structures based nanocomposites is the creation of energy harvesting units, such as hybrid nano-generators, consisting e.g. of patterned P(VDF-TrFE) with G electrodes and assembled on a micro-patterned polydimethylsiloxane (PDMS)-carbon nanotubes composite substrate [3]. In this work the new nanocomposite P(VDF-TrFE)-GO thin films are designed and investigated by piezo-response force microscopy. The distribution of the local piezoresponse poling area and Graphene sheet effect on these films was measured: rise of GO component to 2% reduces the piezo-response with approximately twice lower value of piezo-coefficient  $d_{33\text{eff}}$ . Molecular modeling of the polar/piezo-properties of new nanostructures was done in comparison with experimental data at the nanoscale.

The study was supported by RFBR 15-01-04924 and RSF Gr. 16-19-10112.

1. V.S. Bystrov et al., *J. Appl. Phys.* **116**, 066803 (2014).
2. D. Kim et al., *Phys. Chem. Chem. Phys.* **16**, 22717 (2014).
3. Ju-H. Lee et al., *Advanced Materials* **26**, 765 (2013).

## Polarization switching in ultrathin polyvinylidene fluoride homopolymer ferroelectric films

E.V. Paramonova<sup>1</sup>, S. Filippov<sup>1</sup>, V.E. Gevorkyan<sup>2</sup>, L.A. Avakyan<sup>2</sup>, X.J. Meng<sup>3</sup>, B.B. Tian<sup>3</sup>, J.L. Wang<sup>2</sup>, V.S. Bystrov<sup>1</sup>

<sup>1</sup>*Institute of Mathematical Problems of Biology RAS, 142290 Pushchino, Russia*  
vsbys@mail.ru

<sup>2</sup>*Southern Federal University, Physical Faculty, Rostov-on-Don, Russia*

<sup>3</sup>*Shanghai Institute of Technical Physics Chinese Academy of Science, 200083, Shanghai, China*

Our recent molecular modeling and molecular dynamic (MD) simulation of the polarization switching in the homopolymer (polyvinylidene fluoride (PVDF)/poly(vinylidene fluoride-trifluoroethylene) (P(VDF-TrFE)) Langmuir-Blodgett (LB) films were investigated and analyzed in comparison with the experimental data at the nanoscale [1]. Quantum-mechanical modeling and MD simulations showed that the polarization switching proceeds by the intrinsic homogeneous switching mechanism in accordance with the theory of Landau-Ginzburg-Devonshire (LGD) [1]. The values of the coercive field is within the  $E_C \sim 0.5 - 2.5$  GV/m, which is consistent with experimental data [2, 3]. Nevertheless, as it was established further, at the high values of the applied electric field and for most thick samples the polarization switching mostly correspond to the domain mechanism similarly to the known microscopic Kolmogorov–Avrami–Ishibashi (KAI) theory, describing bulk ferroelectric crystals and thick films [1, 2]. The performed analysis of data show that the critical sizes is  $\sim 10$  nm, while MD simulation show that beginning from 6-10 parallel polymer chains the non-homogeneous layered switching is started and have the formation of new layered domain structures. The value of the critical length starts from  $\sim (3 - 6)$  nm that is in line with experimental measurements [1, 3]. To clarify the new possible mechanism of the domain formation in the transition region we performed the density functional theory (DFT) calculations in local density approximations (LDA) in AIMPRO codes [4] using orthorhombic unit cell for PVDF model. Computed data shown that density of states (DOS) has energy gap  $E_g \sim 6.3$  eV in good comparison with other data [5]. The obtained data are the basis of the new approach for the description of the polarization switching in the transition homogeneous/unhomogeneous region for ultrathin polymer ferroelectrics, having new domains formation. Study was supported by RFBR grants 15-01-04924, 16-51-53017.

1. V.S. Bystrov et al, *Math.Biol.&Bioinf.* **10**, 372 (2015); *Physica B* **432**, 21 (2014).
2. V.M. Fridkin, S. Ducharme, *Ferroelectricity at the Nanoscale. Basics and Applications* 122 (2014).
3. J.L. Wang, et al., *Appl. Phys. Lett.* **104**, 182907 (2014).
4. <http://aimpro.ncl.ac.uk/> (accessed April 2016).
5. Chun-gang Duan et al., *Europhys. Lett.* **61**, 81 (2003).

**Electron work function of the modified HAP: 1. Synchrotron actions**

A.V. Bystrova<sup>1,2</sup>, Yu. D. Dekhtyar<sup>2</sup>, A.I. Popov<sup>3</sup>, V.S. Bystrov<sup>1</sup>

<sup>1</sup>*Institute of Mathematical Problems of Biology RAS, 142290 Pushchino, Russia  
aniria2003@mail.ru*

<sup>2</sup>*Biomedical Eng. & Nanotechnology Institute, Riga Technical University, Riga, Latvia*

<sup>3</sup>*Institute M. von Laue - P. Langevin, Grenoble, France*

Hydroxyapatite (HAP) is a well known multifunctional material for biomedical applications. When using HAP in implantology one deals with electron work function (eWF), determining an interaction between osteo-cells and a HAP surface covering implant. In this work a combined photo-electron emission technique (up to 6.5 eV) and photoluminescence synchrotron DESY measurements were used to study spectral HAP characteristics in a wide energy diapason so that to determine eWF changes during various HAP treatments [1]. Using the first principles calculations of HAP structure and electronic density of states (DOS) [2] as well as relevant synchrotron experimental data [1], we established: 1) excitation by synchrotron irradiation in a wide range leads to transfer of excited electrons from valence band A, B, C, and D peaks, 2) after relaxation of excited electrons and their trapping at the OH-vacancies of energy levels  $E_i$  in the middle of the forbidden gap  $E_g$ , the recombination of the electrons with holes at these energy levels occurred, 3) final irradiation of the luminescence photons with the average energy  $E_i \approx 2.95$  eV observed, the intensity of which is comparable with the intensity of computed DOS peaks (A, B, C, and D) in the valence band, from which electrons jumped. The data obtained are the first direct experimental registration of the existence of A, B, C, and D peaks in the HAP valence band (which was before only theoretically estimated). It explains the experimental data obtained on synchrotron irradiation of HAP samples after different treatments in accordance with observed changes in the intensities and eWF changes.

Determination of the eWF value  $\phi$  during treatment procedures of HAP modification shows that it has several different values of  $\phi_i$  at the same time for the same sample and changes with time. Comparison with computed values of eWF  $\phi_i$  obtained for various HAP defect models and analysis of these data allow us to make a conclusion about the main types of defects and its evolution in time. For the computed values of eWF  $\phi_i$ , which were approximately equal to the forbidden band  $E_g \sim \phi_i$  (in the approximation of small electronic affinity), we can reveal 4 main cases [1]: 1)  $\phi_0 = \sim 4.6 \pm 0.1$  eV for a pure hexagonal HAP unit cell, 2)  $\phi_1 = \sim 5.12 \pm 0.1$  eV for the HAP unit cell with H interstitial, 3)  $\phi_1 = \sim 5.15 \pm 0.1$  eV for the HAP unit cell with O vacancy, 4)  $\phi_1 = \sim 5.49 \pm 0.1$  eV for the HAP unit cell with OH vacancy. The work was partly supported by RFBR grant 15-01-04924.

1. A.V.Bystrova, et al., *Ferroelectrics* **475** 135 (2015).
2. V.S. Bystrov et al., *J. Phys. D: Appl. Phys.* **48**, 195302 (2015).

**Electron work function of the modified HAP: 2. Actions of HAP treatments**

A.V. Bystrova<sup>1,2</sup>, Yu. D. Dekhtyar<sup>2</sup>, A.I. Popov<sup>3</sup>, V.S. Bystrov<sup>1</sup>

<sup>1</sup>*Institute of Mathematical Problems of Biology RAS, 142290 Pushchino, Russia  
aniria2003@mail.ru*

<sup>2</sup>*Biomedical Eng. & Nanotechnology Institute, Riga Technical University, Riga, Latvia*

<sup>3</sup>*Institute M. von Laue - P. Langevin, Grenoble, France*

The analysis of the electron work function (eWF) evolution of the modified hydroxyapatite (HAP) during various treatments procedures under combined experimental measurements and computational modeling data were performed [1, 2]. As a results, after comparison of the data computed with experimental values of eWF  $A_i$  we established the following: 1) after first HAP heat treatment the sample have 2 values of the eWF:  $A_1 \sim 5.02 \pm 0.04$  eV,  $A_2 \sim 5.24 \pm 0.04$  eV, which are rather close to the cases of HAP with O vacancy and H interstitial; 2) after combined heat treatment with microwave irradiation samples have 3 values of the eWF:  $A_1 \sim 4.81 \pm 0.31$  eV,  $A_2 \sim 5.167 \pm 0.167$  eV,  $A_3 \sim 5.227 \pm 0.14$  eV, where the first is close to the initial pure HAP, the second - to the case of HAP with O vacancy and H interstitial, and the third - to the case of HAP with OH vacancy; 3) after combined heat treatment with procedure of hydrogenation here were registered 3 values of the eWF:  $A_1 \sim 4.84 \pm 0.04$  eV,  $A_2 \sim 5.175 \pm 0.04$  eV,  $A_3 \sim 5.49 \pm 0.1$  eV, where the first is close to initial pure HAP, the second - to the case of HAP with O vacancy and H interstitial, and the third - to the case of HAP with OH vacancy; 4) after combined heat treatment with procedure of hydrogenation and microwave irradiation finally were observed 2 values of the eWF:  $A_1 \sim 5.026 \pm 0.04$  eV,  $A_2 \sim 5.3 \pm 0.1$  eV, where the first is close to the cases of HAP with O vacancy and H interstitial, while the second - to the case of HAP with OH vacancy. In all the cases eWF data evolved after 25 months to the value of only one eWF with average value  $A_0 \sim 4.65 \pm 0.34$  eV, which mostly corresponds to the pure initial HAP and demonstrates a short rise to the average value  $A \sim 5.25 \pm 0.3$  eV after synchrotron action, which possibly occurs mainly due to quick formation of the OH vacancy. Additionally we observed that the defects emerged survive for 1-2 months, and then evolved to the initial pure HAP state starting from 11 months, except the last combined case 4, when the stable state with OH vacancy (with one WF:  $A_{11} \sim 5.415 \pm 0.14$  eV) was observed after 11 months period and then it was evolved to pure HAP state too. These observations and conclusions are very important for the HAP applications and technology of the new modified HAP fabrication for bones implantation and other biomedical purposes. The work was partly supported by RFBR grant 15-01-04924.

1. A.V. Bystrova, et al., *Ferroelectrics* **475**, 135 (2015).
2. V.S. Bystrov et al., *J. Phys. D: Appl. Phys.*, **48**, 195302 (2015).

## Infrared imaging for label-free non-invasive and minimally invasive disease diagnostics

S.A. M. Tofail,<sup>1</sup> C. Silien<sup>1</sup>, J. Bauer<sup>2</sup>, T. Soulimane<sup>3</sup>

<sup>1</sup>*Department of Physics and Energy and Materials & Surface Science Institute, University of Limerick, V94 T9PX, Limerick, Ireland  
tofail.syed@ul.ie*

<sup>2</sup>*Department of Biomedical Engineering, Wroclaw University of Science and Technology, 50-370, Wroclaw, Poland*

<sup>3</sup>*Department of Chemical and Environmental Sciences and Materials & Surface Science Institute, University of Limerick, V94 T9PX, Limerick, Ireland*

Disease pathology and its successive stages of development are molecular in origin and indicated by the respective chemistry of their molecular constituents. The ability to detect these molecular developments at the disease occurrence sites enables definitive and predictive *in vivo* diagnosis.

Infrared (IR) for medical imaging is currently restricted to thermal imaging but its ability, similar to Raman spectro-imaging, to detect the chemical constituents make it interesting for functional imaging *in vivo*. IR imaging can be used in non-invasive disease diagnosis and therapy monitoring. If successful, such imaging can provide both on-site and telemetric disease diagnosis. The unique ability of IR radiation in molecular fingerprinting with high sensitivity and quantification thus provide a huge opportunity for personalized and preventive diagnosis of diseases at a much earlier stage than it is currently possible through clinical *in vivo* imaging of morphological changes combined with off-site histopathology/cytology of biopsy samples. A robust IR imaging apparatus allowing fast, large field-of view IR imaging with sufficiently high lateral resolution is required for successful introduction of IR imaging for label free diagnosis.

Here we outline the pre-requisites for IR-based functional imaging for clinical diagnostics, and discuss some of the challenges overcome in high speed, large field of view IR imaging of biological samples.

1. E. Boerner, J. Bauer, M. Kuczkowska, H. Podbielska, B. Ratajczak, *J. Therm Anal Calorim.* **120**, 921 (2015).
2. N. Liu, M. Kumbham, P. Bianchini, A. Diaspro, S. A. M. Tofail, A. Peremans, C. Silien, *ACS Photonics* (2016 in press).
3. C. Silien, A. Peremans, N. Liu, S.A.M Tofail, D. Symens, *Differential Infra Red Nanoscopy System and Method*, WO2014106657 (2014).
4. S.A.M., Tofail, A., Mani, S., Daly, C. Silien, R. Mouras, *A spectroscopic imaging device*, EP15170819.5 (2015).

## PVDF-TrFE/BNNT: Piezoelectric system for mediating tendon repair through activation of voltage and stretch sensitive transmembrane receptors

M.A. Fernandez-Yague<sup>1</sup>, D. Zeugolis<sup>1</sup>, S.A.M. Tofail<sup>2</sup>, A. Pandit<sup>1</sup>, M.J.P. Biggs<sup>1</sup>

<sup>1</sup>Centre for Research in Medical Devices (CURAM), National University of Ireland, Galway, Ireland  
tofail.syed@ul.ie

<sup>2</sup>Department of Physics and Energy and Materials & Surface Science Institute, University of Limerick, V94 T9PX, Limerick, Ireland

The design of artificial scaffolds that can recreate the unique physico-mechanical features of specific cellular niches is of vital importance for tissue engineering applications. Anisotropic biomechanical properties of tendon tissues are attributed to the high degree of alignment of collagen fibrils, which provides topographical guidance for tenocytes and promote tissue organisation. However, an often overlooked physical property of collagen-rich musculoskeletal tissues is the inherent piezoelectric response to mechanical loading. The conversion of mechanical forces into electrical fields is thought to significantly modulate cell function through transmembrane voltage-gated receptors.

In this study, primary human tendon cells were subjected to dynamic tension on a piezoelectric fibrous scaffold developed from poly (vinylidene fluoride-co-trifluoroethylene) P(VDF-TrFE), a material capable of generating electrical charges under mechanical loading with physiological conditions. The sensitivity of the material was further modulated through the incorporation of piezoelectric Boron Nitride nanotubes. The nanomaterials were evaluated as regenerative scaffolds through the analysis of cellular proliferation and the expression of tendon-specific genes.

1. M.A. Fernandez-Yague, S. A. Abbah, L. McNamara, D. I. Zeugolis, A. Pandit, M.J.P. Biggs., *Advanced Drug Delivery Reviews* **84**, 1 (2015).
2. M.A. Fernandez-Yague, A. Larrañaga, O. Gladkovskaya, A. Stanley, G. Tadayyon, Y. Guo, J-R. Sarasua, S.A.M Tofail, D. Zeugolis, A. Pandit, M.J.P Biggs. *Bioconjugate Chemistry* **26**, 2025 (2015).

## Piezoelectric, pyroelectric and ferroelectric behavior of non-fibrous proteins

A. Stapleton<sup>1,2</sup>, M.R. Noor<sup>2,3</sup>, M. Ivanov<sup>4</sup>, J. Sweeney<sup>1</sup>, V. Casey<sup>1</sup>, C. Silien<sup>1,2</sup>, A.A. Gandhi<sup>1,2</sup>, T. Soulimane<sup>2,3</sup>, A.L. Khokin<sup>4</sup>, S.A.M. Tofail<sup>1,2</sup>

<sup>1</sup>*Department of Physics and Energy, University of Limerick, Limerick, Ireland*  
tofail.syed@ul.ie

<sup>2</sup>*Materials and Surface Science Institute, University of Limerick, Limerick, Ireland*

<sup>3</sup>*Chemical and Environmental Science Department, University of Limerick, Limerick, Ireland*

<sup>4</sup>*Department of Materials and Ceramic Engineering and CICECO, University of Aveiro, Aveiro, Portugal*

Similar to inorganic materials such as barium titanate, a number of biological materials such as peptides, proteins (e.g. collagen and elastin) have been found to exhibit interesting dielectric properties. Linear electromechanical coupling (piezoelectricity) and temperature-induced polarization changes (pyroelectricity) have been observed in many biological materials. A reversible spontaneous polarization such as ferroelectricity is rare but has been observed recently in elastin. Here we report that globular proteins such as lysozyme also exhibit piezoelectricity, pyroelectricity and ferroelectricity. Lysozyme is found abundantly in hen egg whites and its function is to protect against infection by breaking down bacterial cell walls. Lysozyme can be crystallized in different forms which are capable of exhibiting piezoelectricity in the most classical sense. In addition to piezoelectricity, we found that lysozyme can also show pyroelectricity perhaps due to the presence of defects that can lower its symmetry to a pyroelectric group. Ferroelectricity cannot be predicted from symmetry arguments only but its appearance in lysozyme indicates further to the lowering of symmetry from that has been determined by single crystal X-ray diffraction on near perfect single crystals.

Funding from Irish Research Council (IRC) Embark Postgraduate Scholarship 2012-2015 is acknowledged. CICECO and FCT are acknowledged via grant Pest-C/CTM/LA0011/013.

1. B. Jaffe, W.R. Cook, H. Jaffe, *Non-Metallic Solids* (Academic press), 3 (1971).
2. Kholkin, N. Amdursky, I. Bdkin, E. Gazit, G. Rosenman, *ACS Nano*, **4**, 610 (2010).
3. D. Denning, M.V. Paukshto, S. Habelitz, B.J. Rodriguez, *Journal of Biomedical Materials Research Part B: Applied Biomaterials*, **102**, 284 (2014).
4. Y. Liu, H-L. Cai, M. Zelisko, Y. Wang, J. Sun, F. Yan, F. Ma, P. Wang, Q.N. Chen, H. Zheng, *Proceedings of the National Academy of Sciences*, **111**, E2780 (2014).

**Decoding electroactive organic materials using solid state physics approach**

S. Guerin, S.A.M. Tofail, D. Thompson

*Department of Physics and Energy and Materials & Surface Science Institute, University of Limerick, V94 T9PX, Limerick, Ireland*  
*tofail.syed@ul.ie*

Piezoelectric materials exhibit the unique characteristic of becoming electrically charged when strained. Conversely, they deform in the presence of an electric field. Inorganic materials such as quartz, aluminium nitride and PZT demonstrate piezoelectricity due to their non-centrosymmetric crystal structures. Many organic materials including bone, tendon and DNA are also piezoelectric. The presence of piezoelectricity in biological materials invokes many questions e.g.:

Why are so many organic materials piezoelectric?

Can this property be used to regulate certain physiological functions?

Are these small, flexible materials the future of energy generation?

A solid state physics approach may help us in finding solutions to these queries using high performance computing combined with advanced experimental characterizations. Here we present a method to accurately calculate piezoelectric constants of both inorganic and organic materials using density functional perturbation theory within the Vienna Ab-initio Simulation Package (VASP). We have also calculated other properties such as dielectric and elastic constants that are relevant to the piezoelectric behavior. This approach will help us to pre-screen candidate biological materials for potential technical applications. Our computer simulations indicate that the crystal forms of amino acids, the basic building block of biological structures can have a surprisingly-large influence on their piezoelectric behavior. Further deconstruction is ongoing as regard to the contributions from molecular packing and single-molecule electronic structure.



## Synthesis of water suspension of metal oxide nanoparticles for nanotoxicological research

V.Ya. Shur, A.E. Tyurnina, D.K. Kuznetsov, E.A. Linker, E.D. Greshnyakov, A.A. Esin

*Institute of Natural Sciences, Ural Federal University, 620000 Ekaterinburg, Russia  
evgeny.greshnyakov@urfu.ru*

One of the modern research directions of toxicology is study of influence nanosize particles on biological objects. The stable suspensions of high concentration with model pure nanoparticles of given composition, sizes and shapes need to implement this research [1]. Suspension of pure metals and metal oxides can be produced by laser ablation of pure metal target in water. It was shown recently that variation of the technological parameters allowed to produce the particles of different shapes, such as: balls, rods, and wires.

The Yb fiber laser with 1062 nm wavelength and 100 ns pulse duration was used with the following beam settings: fluence 80 J/cm<sup>2</sup>, spot diameter 40 μm. Scanning electron microscope CrossBeam Workstation Auriga, Carl Zeiss, scanning probe microscope Ntegra-Aura, NT-MDT and particle size analyzer Zetasizer Nano ZS, Malvern were used for analysis of the target surface condition and parameters of nanoparticles (z - potential and sizes) after each step of the synthesis [2].

The synthesis of nanoparticles was performed in several stages: (1) surface treatment by laser beam scanning, (2) ablation of the target, (3) additional fragmentation, (4) drying to increase the concentration of the solution [2]. The subsequent heating of the suspension was used for self-organization and reshape of nanoparticles. We have produced the stable suspensions of Au, Ag, CuO, NiO, Fe<sub>2</sub>O<sub>3</sub>, PbO, ZnO and Mn<sub>3</sub>O<sub>4</sub> nanoparticles with concentration 0.5 g/l and narrow distribution function. The suspensions have been used for nanotoxicological research [3]. The influence of the nanoparticle shapes will be studied in near future.

The equipment of the Ural Center for Shared Use «Modern Nanotechnology», Ural Federal University has been used. The work was supported by Government of the Russian Federation (Act 211, Agreement 02.A03.21.0006)

1. B.A. Katsnelson, L.I. Privalova, M.P. Sutunkova, I.A. Minigalieva, V.B. Gurvich, V.Ya. Shur, O.H. Makeyev, I.E. Valamina, E.V. Grigoryeva, *Toxicol.*, **337**, 79 (2015).
2. A.E. Tyurnina, V.Ya. Shur, R.V. Kozin, D.K. Kuznetsov, E.A. Mingaliev, *Proc. of SPIE.*, **9065**, 90650D (2013).
3. I.A. Minigalieva, B.A. Katsnelson, L.I. Privalova, V.B. Gurvich, V.Ya. Shur, E.V. Shishkina, I.E. Varaksin, V.E. Panov, T.V. Slyshkina, E.V. Grigorieva, *Toxicol Lett.*, **238**, 371 (2015).

## Elastic and thermal properties of diphenylalanine nanotubes: a micro-Raman study

P.S. Zelenovskiy<sup>1</sup>, A.O. Davydov<sup>1</sup>, S.G. Vasilev<sup>1</sup>, V.V. Yuzhakov<sup>1</sup>,  
A.L. Kholkin<sup>2</sup>, V.Ya. Shur<sup>1</sup>

<sup>1</sup>*Institute of Natural Sciences, Ural Federal University, 620000, Ekaterinburg, Russia*

<sup>2</sup>*Physics Department & CICECO, University of Aveiro, 3810-193 Aveiro, Portugal*

Piezoelectric and pyroelectric micro- and nanotubes of diphenylalanine (C<sub>18</sub>H<sub>20</sub>N<sub>2</sub>O<sub>3</sub>, FF) are considered as an advanced material for developing new biocompatible sensors, coatings, generators etc. for medical equipment [1,2]. Understanding its elastic and thermal properties is important for any applications. The detailed study of these properties was not performed until now. In this work we demonstrate application of confocal Raman microscopy for analysis of elastic constants, Young's modulus and heat capacity of FF nanotubes. These physical properties are determined by lattice vibrations and can be analysed in context of a simple mechanical model of the nanotube.

Micro- and nanotubes of diphenylalanine were grown from FF peptide powder (Bachem, Germany) by conventional method [3]. Raman spectra were measured using confocal Raman microscope Alpha 300AR (WiTec GmbH, Germany). Direct measurements of Young's modulus were performed with nano-hardness tester NanosScan-4D (FSBI TISNCM, Russia).

Low frequency part (from 10 to 375 cm<sup>-1</sup>) of Raman spectrum at room temperature was used for determination of effective frequency of lattice vibrations of FF nanotubes and calculation of spring constants and effective elastic constants. Obtained elastic constants were used for evaluation of transversal Young's modulus, E<sub>T</sub> = 16 GPa, that is in line with experimental data and first principles calculations. Analysis of experimental and calculated data allowed to conclude crucial role of water inside the nanotube.

Effective spring constants derived from effective frequency of lattice vibrations were used for calculation of heat capacity of FF nanotubes. Obtained value is about 1617 J kg<sup>-1</sup> K<sup>-1</sup> and is close to 1871 J kg<sup>-1</sup> K<sup>-1</sup> determined by differential scanning calorimetry.

The equipment of the Ural Center for Shared Use «Modern Nanotechnology», Ural Federal University has been used. The research was made possible in part by RF President grant for young scientists (Contract 14.Y30.15.6554-MK) and by the Government of the Russian Federation (Act 211, Agreement 02.A03.21.0006).

1. A.S. Tayi, M. Matsumoto, *Nature Chem.* **7**, 281 (2015).
2. S. Horiuchi, Y. Tokura, *Nature Mater.* **7**, 357 (2008).
3. A.S. Nuravaeva, S.G. Vasilev et al., *Cryst. Growth Des.* **16**, 1472 (2016).

**Domain structure of single crystal  $\beta$  – glycine**

D.S. Vasileva<sup>1</sup>, S.G. Vasilev<sup>1</sup>, P.S. Zelenovskiy<sup>1</sup>, V.Ya. Shur<sup>1</sup>, A.L. Kholkin<sup>1,2</sup>

<sup>1</sup>*Institute of Natural Sciences, Ural Federal University, 620000 Ekaterinburg, Russia  
semen.vasilev@urfu.ru*

<sup>2</sup>*Physics Department & CICECO – Aveiro Institute of Materials, University of Aveiro,  
3810-193 Aveiro, Portugal*

Recent studies of the simplest amino acid glycine ( $\text{NH}_2\text{CH}_2\text{COOH}$ ) single crystals revealed that among three polymorphic phases  $\alpha$ ,  $\beta$  and  $\gamma$  formed at ambient conditions, only  $\beta$ -phase possesses both piezoelectric and ferroelectric properties [1]. However, sensitivity of  $\beta$ -glycine to humidity, temperature and mechanical stress is a great problem in producing the crystals large enough for research and applications [2,3]. It was shown recently by PFM that as-grown domain structure consists of domains extended along the polar axis with neutral and two types of charged domain visualized [4].

The faceted crystals with in-plane polar axis were grown from aqueous solution via drop drying on Pt/SiO/Si substrate in air with controlled relative humidity. The detail experimental study of the neutral and charged domain walls in  $\beta$ -glycine microcrystals using atomic force (AFM) and piezoresponse force microscopy (PFM) was realized by scanning probe microscopes Ntegra Aura (NT-MDT, Russia) and Asylum MFP 3D SA (Asylum Research, USA). The local polarization reversal by application of the conductive tip to nonpolar surface has been studied.

The different shape of tail-to-tail and head-to-head charged domain walls has been revealed and attributed to difference of conductivity along the walls. The shallow wells of 0.2-1 nm-depth and about 150 nm-width were revealed along the charged walls. The formation of these features was attributed to selective etching by water layer appeared at the surface in humid air. In contrast the pits appeared at neutral domain walls are due to deformation of the crystal lattice in the vicinity of the wall.

The equipment of the Ural Center for Shared Use “Modern Nanotechnology”, Ural Federal University has been used. The research was made possible by the President of Russian Federation grant for young scientists (Contract 14.Y30.15.6554-MK).

- 1 A. Heredia, V. Meunier, et al., *Adv. Funct. Mater.* **22**, 2996 (2012).
- 2 D. Isakov, D. Petukhova, et al., *Cryst. Growth Des.* **14**, 4138 (2014).
- 3 Q. Jiang, A.G. Shtukenberg, et al., *Cryst. Growth Des.* **15**, 2568 (2015).
- 4 V.S. Bystrov, E. Seyedhosseini, et al., *Ferroelectrics* 496(1), **28** (2016).

## Piezoelectric properties of thin films and microcrystals derived from carboranyl-(*S*)-glutamine and carboranyl-(*S*)-asparagine

A.S. Nuraeva<sup>1</sup>, P.S. Zelenovskiy<sup>1</sup>, D.A. Gruzdev<sup>2</sup>, V.P. Krasnov<sup>2</sup>,  
A.L. Kholkin<sup>1</sup>, V.Ya. Shur<sup>1</sup>

<sup>1</sup>*Institute of Natural Sciences, Ural Federal University, 620000 Ekaterinburg, Russia*  
*alla.nuraeva@urfu.ru*

<sup>2</sup>*Postovsky Institute of Organic Synthesis UB RAS, 620990 Ekaterinburg, Russia*

Organic ferroelectrics and piezoelectrics are considered as promising materials in current chemical physics. The films derived from organic compounds are flexible, biocompatible and environmental friendly. Amino acids and their derivatives are well recognized organic piezoelectrics [1, 2]. Recently, we have shown that crystals of valine derivative bearing 1,2-dicarba-*closo*-dodecaborane (carborane) moiety demonstrate pronounce piezoelectric properties [3].

In this work, thin films and microcrystals of carboranyl-derivatives of (*S*)-glutamine (**1**) and (*S*)-asparagine (**2**) were obtained and their morphology and piezoelectric properties were studied (Fig. 1). Films of compounds **1** and **2** were prepared by evaporation of droplets of solutions in H<sub>2</sub>O/HFP mixtures on Pt/SiO/Si substrates. Morphology of the films was studied using optical and atomic force microscopy. Values of piezoelectric response were determined using piezoresponse force microscopy (PFM). It has been established that the film of compound **1** contains microcrystals organized in dendritic framework. Piezoelectric response of films of compound **1** was up to 115 pC/N (superior than that of LiNbO<sub>3</sub>). Compound **2** forms thin films of multi-layered structure. Piezoelectric response of films **2** was substantially lower than that of films **1**.

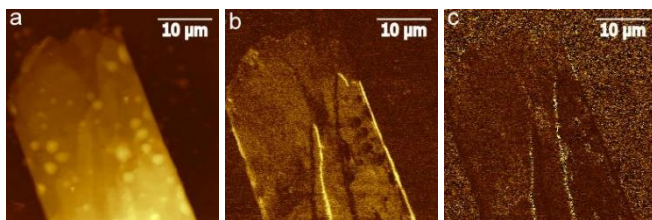


Figure 1. PFM images of films of compound **1**: (a) topography, vertical (b) amplitude, and (c) phase signals.

The equipment of Ural Center for Shared Use “Modern Nanotechnology” UrFU has been used. The work was financially supported by Russian Foundation for Basic Research (grant 16-33-60122).

1. S. Vasilev, P. Zelenovskiy, D. Vasileva, A. Nuraeva, V. Shur, A. Kholkin, *J. Phys. Chem. Solids* **93**, 68 (2016).
2. V.V. Lemanov, *Ferroelectrics* **238**, 211 (2000).
3. A. Nuraeva, D. Vasileva, S. Vasilev, P. Zelenovskiy, D. Gruzdev, V. Krasnov, V. Olshevskaya, V. Kalinin, V. Shur, *Ferroelectrics* **496**, 1 (2016).

## Polarization reversal and domain kinetics in PMN-30PT single crystals

V. Ya. Shur<sup>1</sup>, E.D. Greshnyakov<sup>1</sup>, A.D. Ushakov<sup>1</sup>, E.M. Vaskina<sup>1</sup>,  
A.R. Akhmatkhanov<sup>1</sup>, X. Wei<sup>2</sup>, Z. Xu<sup>2</sup>, Z. Li<sup>2</sup>, S. Wang<sup>2</sup>, Y. Zhuang<sup>2</sup>, Q. Hu<sup>2</sup>

<sup>1</sup>*Institute of Natural Sciences, Ural Federal University, 620000, Ekaterinburg, Russia  
 andrey.akhmatkhanov@urfu.ru*

<sup>2</sup>*International Center for Dielectric Research, Xian Jiaotong University, 710000, Xi'an, China*

The polarization process and kinetics of the domain structure have been studied in relaxor ferroelectric  $(1-x)\text{Pb}(\text{Mg}_{1/3}\text{Nb}_{2/3})\text{O}_3-x\text{PbTiO}_3$  (PMN-PT) single crystals with  $x = 0.3$  (rhombohedral phase) grown by modified Bridgeman method. The studied samples representing  $40 \times 40\text{-mm}^2$ -area  $0.5\text{-mm}$ -thick (001) cut plates. The static domain structure was visualized using complementary high-resolution methods of scanning electron microscopy (SEM), piezoelectric force microscopy (PFM), and Raman confocal microscopy (RCM). It was demonstrated that the silica polishing of the PMN-PT sample results in slight selective etching of the domain structure.

It was shown that the domain structure in as-grown samples consists of the laminar domains with typical width  $2\text{-}5\ \mu\text{m}$ . The poling of the sample was realized by cooling from  $240^\circ\text{C}$  down to RT at cooling rate  $0.8^\circ\text{C}/\text{min}$  under the field  $100\ \text{V}/\text{mm}$  applied in [001] direction. The silver paint electrodes were used. The annealing time at temperature  $240^\circ\text{C}$  was equal to 30 min. It was shown by high-resolution methods that the poling of the sample resulted in partial decay of the as-grown domain structure and decrease of the domain width down to about 200 nm.

The polarization reversal after poling was realized by rectangular field pulses with amplitude ranged from 85 to  $170\ \text{V}/\text{mm}$  using liquid electrodes (saturated aqueous solution of LiCl). It was shown, that the domain structure kinetics in PMN-PT can be visualized by optical microscopy during polarization reversal. *In situ* visualization allowed to reveal the main stages of the domain structure evolution. It was shown that the polarization reversal process in PMN-PT represents growth of the bunch of needle-like domains from the electrode edges. The switching current data was analyzed using modified Kolmogorov-Avrami approach (K-A). It was shown that the field dependence of the extracted characteristic time follows the activation law with activation field equal to  $(1030 \pm 50)\ \text{V}/\text{mm}$ .

The equipment of the Ural Center for Shared Use “Modern Nanotechnology”, Ural Federal University was used. The work was supported by Government of the Russian Federation (act 211, agreement 02.A03.21.0006). VYS acknowledges financial support within the State Task from the Ministry of Education and Science of Russian Federation (Project No. 1366.2014/236).